



SCHOOL of
GRADUATE STUDIES
EAST TENNESSEE STATE UNIVERSITY

East Tennessee State University
Digital Commons @ East
Tennessee State University

Electronic Theses and Dissertations

Student Works

5-2016

Synthesis of Diazonium (Perfluoroalkyl) Arylsulfonimide Monomers from Perfluoro (3-Oxapent-4-ene) Sulfonyl Fluoride for Proton Exchange Membrane Fuel Cell

Faisal Ibrahim

East Tennessee State University

Follow this and additional works at: <https://dc.etsu.edu/etd>

 Part of the [Organic Chemistry Commons](#)

Recommended Citation

Ibrahim, Faisal, "Synthesis of Diazonium (Perfluoroalkyl) Arylsulfonimide Monomers from Perfluoro (3-Oxapent-4-ene) Sulfonyl Fluoride for Proton Exchange Membrane Fuel Cell" (2016). *Electronic Theses and Dissertations*. Paper 3034. <https://dc.etsu.edu/etd/3034>

This Dissertation - Open Access is brought to you for free and open access by the Student Works at Digital Commons @ East Tennessee State University. It has been accepted for inclusion in Electronic Theses and Dissertations by an authorized administrator of Digital Commons @ East Tennessee State University. For more information, please contact digilib@etsu.edu.

Synthesis of Diazonium (Perfluoroalkyl) Arylsulfonimide Monomers from Perfluoro (3-Oxapent-4-ene) Sulfonyl Fluoride for Proton Exchange Membrane Fuel Cell

A thesis
presented to
the faculty of the Department of Chemistry
East Tennessee State University

In partial fulfilment
of the requirements for the degree
Masters of Science in Chemistry

by
Faisal Ibrahim
May 2016

Dr. Hua Mei, Chair
Dr. Ismail O. Kady
Dr. Aleksey Vasiliev

Keywords: Diazonium, Nafion, perfluoro(3-oxapent-4-ene) sulfonyl fluoride, proton exchange membrane fuel cells, perfluoroalkyl arylsulfonimide monomers

ABSTRACT

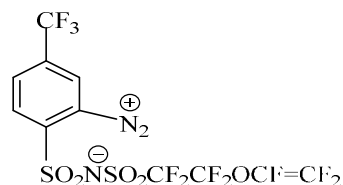
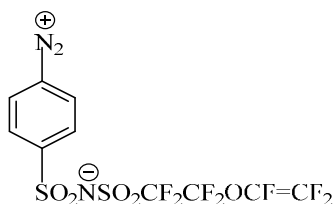
Synthesis of Diazonium (Perfluoroalkyl) Arylsulfonimide Monomers from Perfluoro (3-Oxapent-4-ene) Sulfonyl Fluoride for Proton Exchange Membrane Fuel Cell

by

Faisal Ibrahim

Two diazonium perfluoroalkyl arylsulfonimide (PFSI) zwitterionic monomers, 4-diazonium perfluoro(3-oxapent-4-ene)benzenesulfonimide (**I**) and 4-(trifluoromethyl)-2-diazonium perfluoro(3-oxapent-4-ene)benzenesulfonimide (**II**) have been synthesized from perfluoro(3-oxapent-4-ene) sulfonyl fluoride (POPF) for proton exchange membrane fuel cells. PFSI polymers are proposed as new electrolytes due to their better thermal stability, inertness to electrochemical conditions, and lower susceptibility to oxidative degradation and dehydration. For a better integration between the electrode and the electrolyte, the PFSI polymers are expected to be grafted onto the carbon electrode via the diazonium moiety.

All the reaction intermediates and the final product were characterized with ^1H NMR, ^{19}F NMR and IR spectroscopies.



DEDICATION

I dedicate this research work to my late parents: my dad; Mr. Ibrahim and mom; Rahanatu Muhammed for their care and support. My siblings; Murtala Muhammed Ibrahim and Rukaya Ibrahim for their unconditional love, continuous support and encouragement. My wife; Ramatu Umar Labaran, for her love, affection and devotion through all the trying times in the course of my studies.

ACKNOWLEDGEMENTS

In the name of the **ALLAH**, the most gracious and the ever merciful. Thanks be to **ALLAH** for His abundant grace and protection throughout the course of this work.

I would like to thank my advisor, Dr. Hua Mei, for her advice, guidance and support. Her momentous contribution to the success of this work is immeasurable, and I say thank you.

A special thank you to Drs. Ismail O. Kady and Aleksey Vasiliev for serving as committee members and providing valuable and insightful contributions to this work. Dr. Reza Moheseni deserve a special mention for his enormous support with the instrumentation.

I would also like to thank Dr. Scott Kirkby for assisting with the Spartan calculation and editing my manuscript.

I also recognize the diverse support of my colleagues and friends: Isaac Addo, Abdulmajeed Alayyaf and Grace Abban. Thank you for making the laboratory an exciting place to work.

My appreciation also goes to the Bridges (Mr. and Mrs Tim, Ms. Angelica, Austin and Gloria) for their unflinching support throughout my stay in Johnson City Tennessee

Finally, I would like to thank the ETSU Department of Chemistry for giving me the opportunity to pursue my Masters of Science degree. I am grateful to the faculty, staff, and graduate students of the Department of Chemistry for their assistance and support throughout my stay at ETSU.

TABLE OF CONTENTS

	Page
ABSTRACT	2
DEDICATION	3
ACKNOWLEDGEMENTS	4
LIST OF TABLES	10
LIST OF FIGURES	11
LIST OF SCHEMES.....	12
LIST OF ABBREVIATIONS	13
1. INTRODUCTION	16
Preface.....	16
Fuel Cells	16
Proton Exchange Membrane Fuel Cells	19
Polymer Electrolyte Membrane	23
POPF Polymer	29
Proposed MEA System.....	30
Diazonium PFSI Zwitterions Monomers	31
2. RESULTS AND DISCUSSION	35

Ammonolysis Reaction	36
Bromination Reaction	37
Coupling Reaction	38
Debromination Reaction	40
<i>N</i> -deacetylation Reaction	43
Reduction Reaction	45
Diazotization Reaction	47
3. EXPERIMENTAL	50
General Considerations	50
NMR Spectroscopy	50
Infra-red Spectroscopy	50
Gas Chromatography-Mass Spectrometer	51
Thin Layer Chromatography	51
Glass Vacuum System	51
Purification of Solvents and Experimental Practice	52
Synthesis of Benzenesulfonyl amide (2a-b)	52
Synthesis of FSO ₂ CF ₂ CF ₂ OCFBrCF ₂ Br (4)	53
Synthesis of CH ₃ CONHPhSO ₂ N(M)SO ₂ CF ₂ CF ₂ OCFBrCF ₂ Br	54
Synthesis of 4-CF ₃ -2-NO ₂ -PhSO ₂ N(M)SO ₂ CF ₂ CF ₂ OCFBrCF ₂ Br	54
Synthesis of 4-NH ₂ PhSO ₂ N(M)SO ₂ CF ₂ CF ₂ OCFBrCF ₂ Br (6a)	55
Synthesis of 4-NH ₂ PhSO ₂ N(M)SO ₂ CF ₂ CF ₂ OCF=CF ₂ (7a)	56

Synthesis of 4-CF ₃ -2-NO ₂ -PhSO ₂ N(M)SO ₂ CF ₂ CF ₂ OCF=CF ₂ (6b)	57
Synthesis of 4-CF ₃ -2-NH ₂ -PhSO ₂ N(M)SO ₂ CF ₂ CF ₂ OCF=CF ₂ (7b)	58
Synthesis of 4-N ₂ ⁺ PhSO ₂ N ⁻ SO ₂ CF ₂ CF ₂ OCF=CF ₂ (8a).....	59
Synthesis of 4-CF ₃ -2-N ₂ ⁺ PhSO ₂ N ⁻ SO ₂ CF ₂ CF ₂ OCF=CF ₂ (8b)	59
4. CONCLUSION.....	60
REFERENCES	62
APPENDICES	69
Appendix A1: GC-MS Chromatogram of Compound 2a	69
Appendix A1: GC-MS Chromatogram of Compound 2b	70
Appendix B1: 19F NMR spectrum of compound 3 , 400MHZ, CD ₃ CN	71
Appendix B2: 19F NMR spectrum of compound 4 , 400MHZ, CD ₃ CN	72
Appendix B3: 19F NMR spectrum of compound 5a , 400MHZ, Acetone-d ₆	73
Appendix B4: Expanded 19F NMR spectrum of compound 5a , 400MHZ, Acetone-d ₆	74
Appendix B5: ¹⁹ FNMR spectrum of compound 6a , 400MHZ, Acetone-d ₆	75
Appendix B6: Expanded ¹⁹ FNMR spectrum of compound 6a , 400MHZ, Acetone-d ₆	76
Appendix B7: ¹⁹ FNMR spectrum of compound 7a , 400MHZ, Acetone-d ₆	77
Appendix B8: Expanded ¹⁹ FNMR spectrum of compound 7a , 400MHZ, Acetone-d ₆	78
Appendix B9: ¹⁹ FNMR spectrum of compound 8a , 400MHZ, CD ₃ CN	79
Appendix B10: Expanded ¹⁹ FNMR spectrum of compound 8a , 400MHZ, CD ₃ CN	80
Appendix C1: ¹⁹ FNMR spectrum of compound 2b , 400MHZ, Acetone-d ₆	81
Appendix C2: ¹⁹ FNMR spectrum of compound 5b , 400MHZ, Acetone-d ₆	82

Appendix C3: Expanded ^{19}F NMR spectrum of compound 5b , 400MHz, Acetone- d_6	83
Appendix C4: ^{19}F NMR spectrum of compound 6b , 400MHz, Acetone- d_6	84
Appendix C5: Expanded ^{19}F NMR spectrum of compound 6b , 400MHz, Acetone- d_6	85
Appendix C6: ^{19}F NMR spectrum of compound 7b , 400MHz, Acetone- d_6	86
Appendix C7: Expanded ^{19}F NMR spectrum of compound 7b , 400MHz, Acetone- d_6	87
Appendix C8: ^{19}F NMR spectrum of compound 8b , 400MHz, CD_3CN	88
Appendix C9: Expanded ^{19}F NMR spectrum of compound 8b , 400MHz, CD_3CN	89
Appendix D1: ^1H NMR spectrum of compound 2a , 400MHz, CD_3CN	90
Appendix D2: Expanded ^1H NMR spectrum of compound 2a , 400MHz, CD_3CN	91
Appendix D3: ^1H NMR spectrum of compound 5a , 400MHz, Acetone, d_6	92
Appendix D4: Expanded ^1H NMR spectrum of compound 5a , 400MHz, Acetone, d_6	93
Appendix D5: ^1H NMR spectrum of compound 6a , 400MHz, CD_3CN	94
Appendix D6: Expanded ^1H NMR spectrum of compound 6a , 400MHz, CD_3CN	95
Appendix D7: ^1H NMR spectrum of compound 7a , 400MHz, CD_3CN	96
Appendix D8: Expanded ^1H NMR spectrum of compound 7a , 400MHz, CD_3CN	97
Appendix D9: ^1H NMR spectrum of compound 8a , 400MHz, CD_3CN	98
Appendix D10: Expanded ^1H NMR spectrum of compound 8a , 400MHz, CD_3CN	99
Appendix E1: ^1H NMR spectrum of compound 2b , 400MHz, CD_3CN	100
Appendix E2: Expanded ^1H NMR spectrum of compound 2b , 400MHz, CD_3CN	101
Appendix E3: ^{19}F NMR spectrum of compound 5b , 400MHz, CD_3CN	102
Appendix E4: Expanded ^{19}F NMR spectrum of compound 5b , 400MHz, CD_3CN	103
Appendix E5: ^1H NMR spectrum of compound 6b , 400MHz, CD_3CN	104

Appendix E6: Expanded ¹ HNMR spectrum of compound 6b , 400MHz, CD ₃ CN.....	105
Appendix E7: ¹ HNMR spectrum of compound 7b , 400MHz, CD ₃ CN.....	106
Appendix E8: Expanded ¹ HNMR spectrum of compound 7b , 400MHz, CD ₃ CN.....	107
Appendix E9: ¹ HNMR spectrum of compound 8b , 400MHz, CD ₃ CN.....	108
Appendix E10: Expanded ¹ HNMR spectrum of compound 8b , 400MHz, CD ₃ CN.....	109
Appendix F1: FT-IR Spectrum of Compound 2a	110
Appendix F2: FT-IR Spectrum of Compound 5a	111
Appendix F3: FT-IR Spectrum of Compound 6a	112
Appendix F4: FT-IR Spectrum of Compound 7a	113
Appendix F4: FT-IR Spectrum of Compound 8a	114
Appendix G1: FT-IR Spectrum of Compound 2b	115
Appendix G2: FT-IR Spectrum of Compound 5b	116
Appendix G3: FT-IR Spectrum of Compound 6b	117
Appendix G4: FT-IR Spectrum of Compound 7b	118
Appendix G5: FT-IR Spectrum of Compound 8b	119
VITA.....	120

LIST OF TABLES

Table	Page
1. Classifications of fuel cell.....	17
2. Fuel cell types	18
3. Categories of Membranes	27
4. Results for debromination of the Coupling Products.....	41

LIST OF FIGURES

Figure	Page
1. The Structure of PEMFC	20
2. Expanded view of the Cathode part of the MEA Structure	21
3. A Dense MEA in PEMFCs	23
4. Chemical Structure of the Sulfonic Form of Nafion [®]	24
5. Proton transport via (a) Free solution diffusion and (b) Proton hops mechanism (Grotthussmechanism)	25
6. Chemical Structure of the Sulfonic Form of POPF Polymer.....	29
7. A Porous Carbon-Catalyst-Electrodes System in the PEMFCs.....	31
8. Structure of First Diazonium PFSI Monomers	31
9. The hydrolysis by-product from coupling reaction	39
10. 2-(trifluoromethyl)-4-sulfamonylacetanilide	45
11. Byproducts Associated with the Reduction Reaction	47
12. Structure of 2-nitro-4-(trifluoromethyl) benzene sulfonylamide	49
13. The line diagram of a dual-manifolds glass vacuum line	51

LIST OF SCHEMES

Scheme	Page
1. The reaction occurring in a PEM Fuel Cell.....	20
2. Proton hopping mechanism.....	25
3. Delocalization of Perfluoroalkyl Sulfonyl Group.	32
4. Electrochemical reduction of an aryl diazonium salt.....	33
5. Example of Amino Acid at the isoelectric point.....	34
6. Overall Synthetic Scheme for Diazonium PFSI Arylsulfonimide Monomers.....	35
7. Ammonolysis Reaction.....	36
8. The hydrolysis reaction during Ammonolysis.....	37
9. Bromination of Perfluoro(3-oxapent-4-ene) Sulfonylfluoride Monomer.....	37
10. Comparison of Coupling Reactions.....	39
11. Acidification of the Crude Coupling Products.....	39
12. Debromination of Cinnamic Acid.....	40
13. Debromination Reaction.....	42
14. The <i>N</i> -deacetylation reaction of the coupled product.....	43
15. The mechanism for the acid catalyzed <i>N</i> -deacetylation.....	44
16. The resonance structure of the PFSI monomer 8a.....	45
17. Reduction of the coupling product.....	45
18. The Intermediates of the Reduction of Aryl Nitro Compounds.....	46
19. Mechanism for Reduction of Aromatic Nitro Compounds.....	47
20. Diazotization of 1° Aromatic Amines mechanism.....	48
21. Synthesis of the diazonium compound.....	48

LIST OF ABBREVIATIONS

POPF	Perfluoro (3-Oxapent-4-ene) Sulfonyl Fluoride
AFC	Alkaline Fuel Cell
DMFC	Direct Methanol Fuel Cell
EW	Equivalent weight
FDZ	Functional Diazonium Zwitterion
FTIR	Fourier Transform Infra Red
GDL	Gas Diffusion Layer
Hz	Hertz
IEC	Ion Exchange Capacity
MCFC	Molten Carbonate Fuel Cell
MEA	Membrane Electrode Assembly
NMR	Nuclear Magnetic Resonance
DIEA	N, N-Diisopropylethylamine
PAFC	Phosphonic Acid Fuel Cell
PEMFC	Polymer Electrolyte Membrane Fuel Cell

PFSA	Perfluorosulfonic acid
PFSI	Perfluorosulfonylimide
ppm	Parts per million
PTFE	Polytetrafluoroethylene
SOFC	Solid Oxide Fuel Cell
TMS	Tetramethylsilane
UV	Ultra Violet
GE	General Electric Company
GFCs	Gas Flow Channels
CL	Catalyst Layer
TPB	Triple-Phase Boundary
HOR	Hydrogen Oxidation Reaction
ORR	Oxygen Reduction Reaction
MHQ	N-methyl-6-hydroxyquinolinium
PFCA	Perfluorocarboxylic Acid
PTFE-g-TFS	Sulfoated Trifluorostyrene Grafted Poly(tetrafluoroethylene)

PVDF-g-PSSA	Styrene-Grated Sulfonated Poly(vinylidene fluoride)
NPI	Naphthalenic Polyimide
BAM3G	Ballard Advance Material of third Generation Membrane
SPEEK	Sulfonated Poly(ether ether ketone)
SPPBP	Sulfonated poly(4-phenoxybenzoyl-1,4-phenylene)
SPEEK/PBI	Sulfonated Poly(ether ether ketone)/Polybenzimidazole
SPEEK/PEI	Sulfonated Poly(ether ether ketone)/Poly(ethyleneimine)
SPSU /PEI	Sulfonated Polysulfone/Poly(ethyleneimine)
PtC	Platinum Catalyst
TLC	Thin Layer Chromatography

CHAPTER 1

INTRODUCTION

Preface

This research aims at synthesizing two analogues of diazonium perfluoroalkyl(aryl) sulfonimide (PFSI) monomers from perfluoro(3-Oxapent-4-ene) sulfonyl fluoride (POPF) monomer for proton exchange membrane fuel cells (PEMFCs). The first is prepared from 4-nitrobenzene sulfonyl chloride and the POPF monomer and the other from 2-nitro-4-(trifluoromethyl) benzene sulfonyl chloride and the POPF monomer.

The background and motivation for this research are discussed in the introduction. Short overview of the fuel cells and their development are first elaborated. And then, the definition of zwitterions and the comparison with recently reported diazonium PFSI zwitterionic monomers are illustrated.

Fuel Cells

Fuel cells are electrochemical devices that convert chemical energy of the reactants directly into electricity and heat with high efficiency.¹ The efficiency of the fuel cell may range from 60% to 80% depending on the application, with more than 90% reduction in major pollutants²⁻⁴ compared to fossil fuel powered by internal combustion engines. The fuel cell does not need to be recharged as long as there is a constant supply of the appropriate fuel. Not only hydrogen gas is used as fuel but also hydrocarbons like natural gas and alcohol (methanol) are employed for different kinds of fuel cells.⁵

The development of different kind of fuel cells has received tremendous interest, in the last few decades. In general, a fuel cell is comprised of two electrodes with the electrolyte

situated between them.⁶ The electrodes are generally permeable to hydrogen and oxygen. Metals like platinum and palladium are often used as catalyst to hasten the reaction.⁶

Fuel cells are designed for a wide range of applications, such as transportation, stationary combined power and heat supply of portable electronic equipment.^{3, 4}

Fuel cells may be classified into two major categories based on operating temperatures as shown in Table 1 below:

Table 1: Classifications of fuel cell

FUEL CELL CATEGORIES	
LOW TEMPERATURE, °C	HIGH TEMPERATURE, °C
Alkaline Fuel Cell (AFC)	Carbonate Fuel Cell or Molten Carbonate Fuel Cell (CFC or MCFC)
Phosphoric Acid Fuel Cell (PAFC)	Solid Oxide Fuel Cell (SOFC)
Proton Exchange Membrane Fuel Cell (PEMFC)	

These five categories of fuel cells are also classified according to the electrolyte as listed in Table 2. The electrolyte employed depends on the nature of the electrochemical reaction, the operating temperature and the applications.

Table 2: Fuel cell types⁶

Fuel Cells	Electrolytes	Fuel Used	Oxidant Used	Operating Temperatures
Proton Exchange Membrane Fuel Cell (PEMFC)	H ⁺ conducting membrane	H ₂	Air, O ₂	~80 °C
Direct Methanol Fuel Cell (DMFC)	H ⁺ conducting membrane	CH ₃ OH	Air, O ₂	80-130 °C
Alkaline Fuel Cell (AFC)	KOH	H ₂	O ₂	~100 °C
Phosphoric Acid Fuel Cell (PAFC)	Concentrated H ₃ PO ₄	Natural gas, H ₂	Air, O ₂	~200 °C
Molten Carbonate Fuel Cell (MCFC)	Molten K ₂ CO ₃	Natural gas, H ₂	Air, O ₂	~650 °C
Solid Oxide Fuel Cell (SOFC)	ZrO ₂	Natural gas, H ₂	Air, O ₂	800-1000 °C

Polymer electrolyte membrane fuel cells (also referred to as proton exchange membrane fuel cells, PEMFCs) is the focus of this research. The PEMFCs have several advantages, such as excellent electrical efficiency, clean and silent operation. In contrast to the PEMFCs, another kind of widely studied fuel cell, direct methanol fuel cells (DMFC) use pure liquid methanol

instead of the hydrogen gas as fuel. The DMFCs produce CO₂ (a pollutant) and also suffers from high rates of methanol-crossover⁷ which reduces cell performance and lowers fuel efficiency.⁸

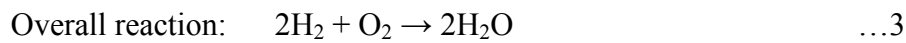
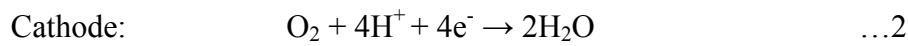
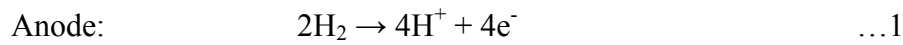
Proton Exchange Membrane Fuel Cells

PEMFCs' development began in the 1950s by General Electric Company (GE) although the first one was invented in 1839 by Sir William Robert Grove.⁹ No practical applications for PEMFCs were found until the 1960's when they were used as the power source for the Gemini space mission. PEMFC technology has attracted considerable attention from the early 1970s when Nafion[®] membrane was adopted¹⁰ as a membrane material. As environment friendly energy sources, PEMFCs are proposed to be used mainly for transportation although other applications such as distributed/stationary and portable power generation have been explored. PEMFCs also have advantages, such as relatively low operating temperature, excellent power density, longer life span and quick start up.¹¹

The reaction occurring in PEMFCs is a reversible oxidation-reduction reaction that alternate when switching from charge to discharge.¹² In PEMFCs, hydrogen and oxygen gas from air are channeled through the anode and the cathode gas flow channels (GFCs) respectively. And then, these gases are transported through the gas diffusion layers (GDLs) to reach the catalyst layers (CLs). At the anode's CL, the H₂ is oxidized into protons and electrons with the protons migrating through the proton conducting polymer membrane to the CL at the cathode. The electrons produced at the CL in the anode are transported to the cathode current collector via an external circuit. At the cathode, the electrons combine with the protons and reduced O₂ to form water. The membrane does not allow the passage of the electrons as it is electrically non-conducting. The water is expelled out of the cathode CL through the GDL and eventually out of the cathode GFC.

For PEMFCs, there are many factors which affect performance. For example, high temperature can boost the operation because it can enhance the membrane's proton conductivity. As the exothermic reactions occur in the PEMFCs, external heat is not required. On the contrary, a water-cooling system is needed to remove the excess heat.¹³ Another example is that, a relatively pure hydrogen source is required for the fuel.¹⁴ Otherwise, the performance of the PEMFC will be diminished by tainting the electrodes and membrane with contaminants like CO, CO₂.^{15, 16}

The reaction is shown in scheme 1 below:



Scheme 1: The reaction occurring in a PEM Fuel Cell

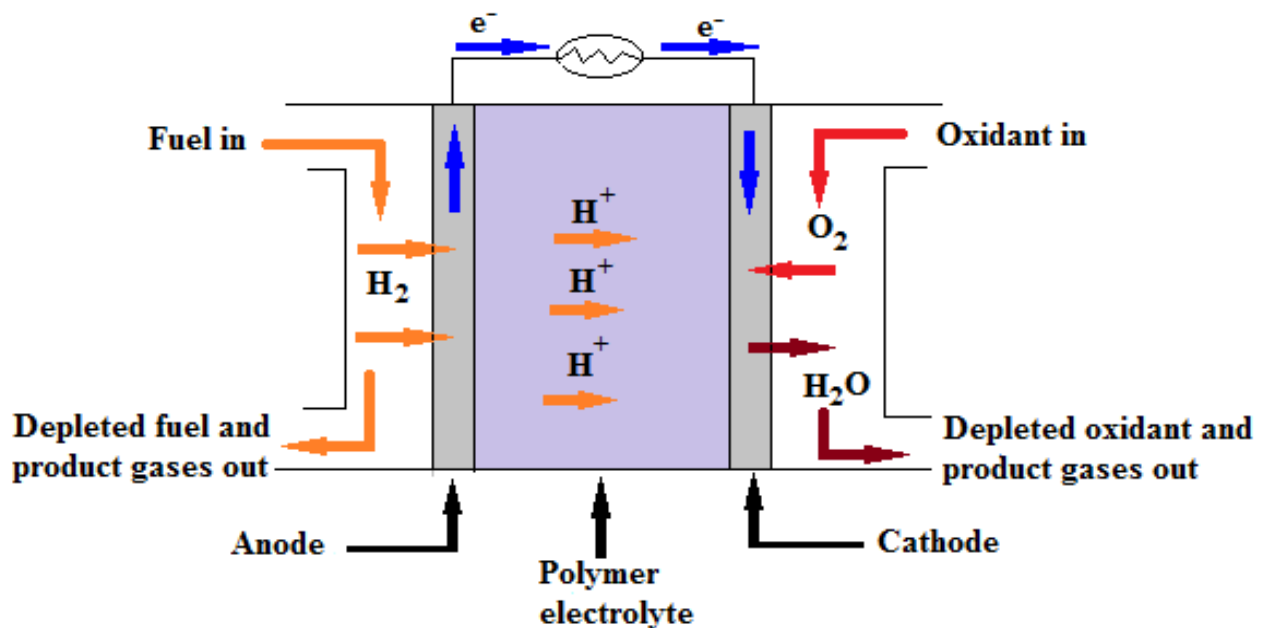


Figure 1: The Structure of PEMFC (modified from Thampan¹⁷ - used with permission)

There are three key components in the typical PEMFCs and they are the membrane-electrode assembly (MEA) and two bipolar (flow field or separator) plates. The MEA consists of two dispersed CLs, two GDLs, and a membrane which allows protons to crossover between the electrodes to complete the overall reaction.

As the ‘engine’ of the PEMFC, the MEA plays a foremost role in determining cell performance. The basic MEA configuration includes the proton exchange membrane (PEM) sandwiched between two GDLs. The membrane serves as the vehicle for transportation of protons from the anode to the CL through the GDL.

Overall, the critical requirements of membrane include: (1) high protonic conductivity, (2) low gas permeability, (3) low electronic conductivity, (4) good chemical stability and mechanical properties^{18, 19}.

Figure 2 shows the cathode section of the MEA which comprise the electrolyte membrane and the carbon electrodes. The electrochemical reaction in the cell takes place at the triple-phase boundary (TPB), where the protons, the electrons and the reactant (product) gases meet in the MEA.

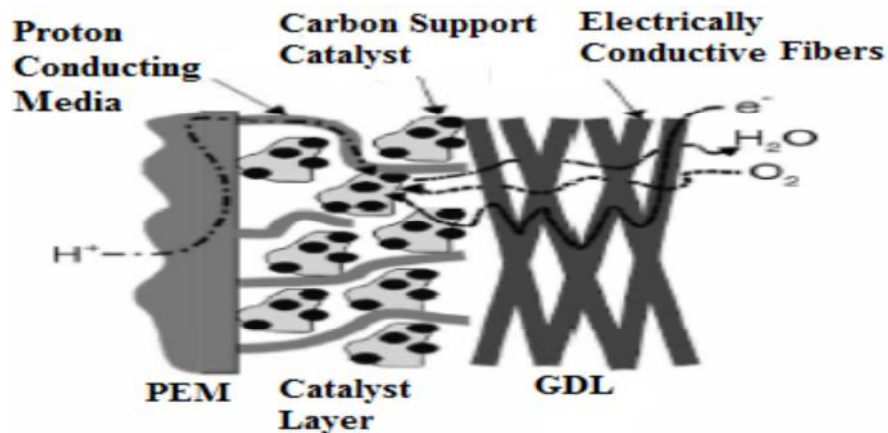


Figure 2: Expanded view of the cathode of the MEA structure.¹⁸ Used with permission

The CLs, as other components of the MEA, are directly adjacent to the membrane on each side. They are also referred as the active layers. The CL is the site for the half-cell reaction in a PEMFC. The hydrophobic/hydrophilic properties of CL also can have an impact on the efficiency of the PEMFC. The small amount of polymer electrolyte membrane is usually required in the CLs since the hydrophobic nature of the carbon retards the transport of the protons to the reaction sites. On the other hand, an excessively hydrophilic CL will shelter the carbon surface area and preclude the reactant/product gases from diffusing onto the catalyst.²⁰ The accumulation of water at the cathode can lead to the swelling of the CL, and finally cause the cell to become inoperable. Therefore, for optimal performance of the PEMFC, a balance between the hydrophobic carbon powder and hydrophilic fluorinated polymer resin is required for the CL.

The CLs are usually fabricated by mixing the catalyst with the membrane and applying the paste to the GDL. However, according to Thompson et al., up to 50% of the catalyst particles in such electrodes may be inactive.²¹ The catalyst utilization in an MEA is controlled by two important factors: (1) the catalyst activity, and (2) the proton transport resistance in the CLs.²² The catalyst activity depends on the surface area of the catalyst particles while the proton transport resistance depends on the protons transport pathway in the CLs and the ratio of the catalyst particles in contact with the sulfonic acid groups.²²

Platinum or platinum alloys are the commonly used catalysts for both the hydrogen oxidation reaction (HOR) and the oxygen reduction reaction (ORR) in PEMFCs. Figure 3 shows the conventional MEA with the catalyst randomly deposited on the dense electrode.

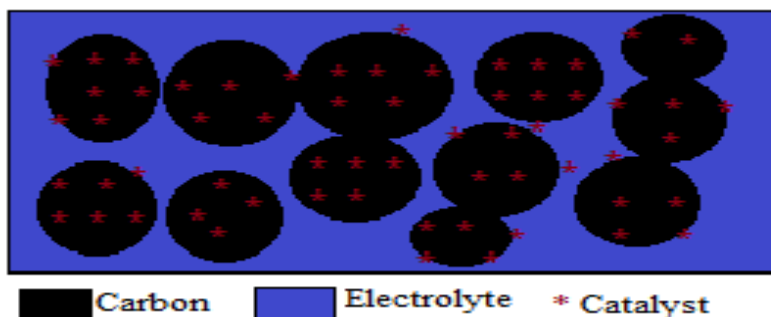


Figure 3: A Dense MEA in PEMFCs (modified from Creager²³-used with permission)

The third component of MEA structure is the bipolar plates, which have four basic functions: (1) to dispense the fuel and oxidant, (2) to expedite water management, (3) to separate the individual cells, and (4) to transport current away.

The detailed configurations and modifications of the MEA components are discussed as follows.

Polymer Electrolyte Membrane

It is generally known that, the perfluorosulfonic acid (PFSA) polymers are the most commonly used membrane materials for PEMFCs.²⁴ With the characteristic polytetrafluoroethylene (PTFE) backbone, PFSA polymers exhibit great stability in both oxidative and reductive conditions.²⁵ PFSA polymers also have high proton conductivity of 0.10 S/cm under fully hydrated conditions.⁴ PFSA polymers are generally made of two basic parts: (1) a perfluorinated main chain and (2) ion clusters comprising sulfonic acid ions. The membrane must be hydrated to enhance the proton conductivity by moving protons between the sulfonic acid sites.

Nafion[®], a perfluorosulfonic acid (PFSA) ionomer, is the most well studied and used polymer membrane in PEMFCs due to its desirable characteristics including low gas and liquid permeability, and good chemical and mechanical stability at low temperatures¹⁸.

Nafion[®] polymers permit the entry of water vapor which makes it a better ionic conductor (greater than 0.1 S cm⁻¹ at 80 °C).²⁶ It also has a low electric constant.²⁷

Nafion[®] polymers are fabricated via copolymerization of tetrafluoroethylene (TFE) with sulfonic acid (-SO₃⁻H⁺) containing perfluoroalkyl (-vinyl ether chains).²⁸ Nafion[®] polymers are commercially available in the sulfonic acid form (-SO₃⁻H⁺) as illustrated in Figure 4.

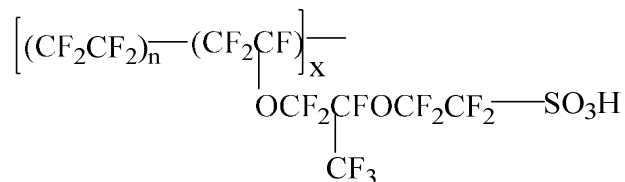


Figure 4: Chemical Structure of the Sulfonic Form of Nafion[®]²⁸

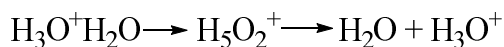
The perfluorinated alkyl backbones in Nafion[®] polymers are principally made of polytetrafluoroethylene (PTFE) or Teflon[®] and are responsible for Nafion's good chemical and thermal stability, significant mechanical strength and hydrophobicity.

Nafion[®] polymers have desired proton conductivity as very strong solid acids. For example, Nafion[®] 117 has pKa of -6^{29, 30} which is comparable to the “super” photoacid, N-methyl-6-hydroxyquinolinium (MHQ) with an excited-state pKa* ≈ -7.³¹ This acidity is not only attributed to the strong electron withdrawing perfluoroalkyl group but also the weak conjugate base as it has stabilized resonance structure.^{29, 30}

The proton conductivity of Nafion[®] polymers is dependent on the dissociation of protons from the -SO₃H pendant in the presence of water.²⁷ At the anode, the protons form hydronium complexes (H₃O⁺) and detach from the sulfonic acid pendant. This allows the protons to move easily from the anode to the cathode. The transfer of protons in the membrane follows two processes. The first is free solution diffusion (Figure 5(a)) and the other is proton hopping via the Grotthuss mechanism (Figure 5(b)), where protons “hop” from one water molecule to another by

the formation and breakage of hydrogen bonds as shown in Scheme 2 below.³² This successive proton hopping step leads to an effective proton transport through the water. In the free solution diffusion, the proton and associated water of hydration all diffuse through water phase.

The proton transport through a hydrated ion exchange membrane occurs via both of the two processes mentioned above.



Scheme 2: Proton hopping mechanism

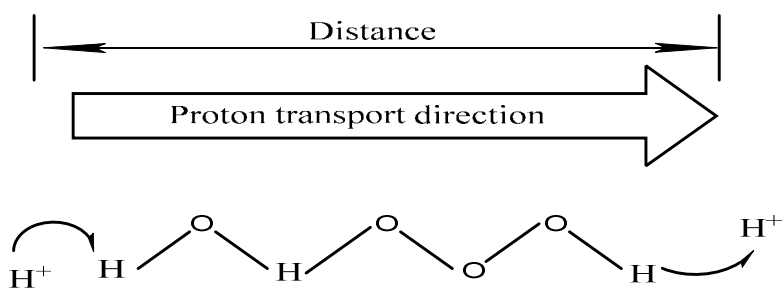
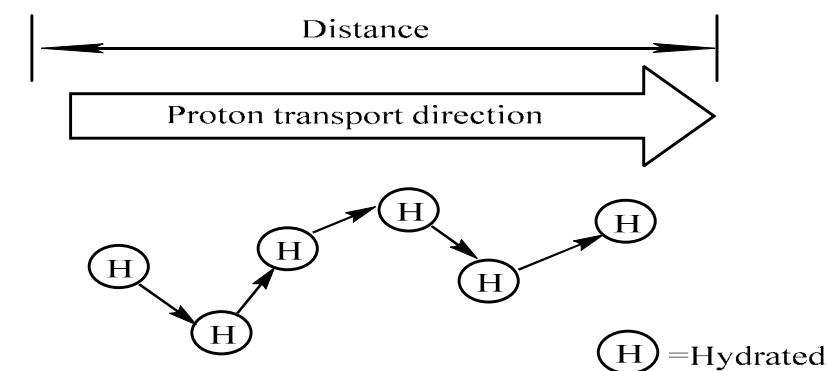


Figure 5: Proton transport via (a) Free solution diffusion and (b) Proton hops mechanism

(Grotthuss mechanism).³³

Other types of commercially available PFSA membranes include POPF, Flemion[®] (AsahiGlass), Aciplex[®] (Asahi Kasei), Celtec-P (BASF), Gore-Select (Gore) and Aquivion[®].

Notwithstanding the desirable features of Nafion[®] for PEM fuel cell, there are certain disadvantages of such polymers that limit the performance of PEM fuel cell. First, Nafion[®] polymers like to form large rod-shaped micelles which preclude their tight contact with the microporous carbon electrode. Thus, the membrane will be washed out after a long time of operation¹¹ and subsequently leads to poor ion conductivity and diminished performance. Moreover, when the temperature increases, the sulfonic acid group (-SO₃H) degrades into anhydride (-SO₂OSO₂-). Additionally, the integration between the electrolytes and carbon electrode also deteriorates in the highly acidic and oxidizing conditions.³⁴ This compromises the physical integrity between the fluoropolymer and the carbon support, resulting in a reduced life span.

Furthermore, the greatest barrier to commercialization of PEMFCs is the cost which is due to the expensive fabrication process of Nafion[®].³⁵ Last but not least, Nafion[®] polymers still cause environmental concerns since they emit toxic fumes at high temperature and are not biodegradable.^{36, 37}

According to the literature²⁴, the five other categories of polymers are designed as alternatives to the conventional PFSA polymer membrane for PEMFCs. A short summary are listed in Table 3.

Table 3: Categories of membranes^{24, 38}

Membrane Category	Structure	Example	Physical properties
Perfluorinated polymer	1. Fluorinated backbone like PTFE 2. Fluorocarbon side chain 3. Ionic clusters consisting of sulfonic acid ions attached to the side chains	1. PFCA 2. PFSA 3. PFSI	Membranes are strong and stable in both oxidative and reductive environments
Partially perfluorinated polymer	1. Fluorocarbon base 2. Hydrocarbon or aromatic side chain grafted onto the backbone, which can be modified	1. PTFE-g-TFS 2. PVDF-g-PSSA	Membranes are relatively strong in comparison to pf, but degrade fast
Non-perfluorinated hydrocarbon polymer	Hydrocarbon base, typically modified with polar groups	1. NPI 2. BAM3G	1. Membrane possess good mechanical strength 2. Poor chemical and thermal stability

Table 3 (continued)

Non-fluorinated aromatic	Aromatic base, typically modified with polar sulfonic groups	1. SPEEK 2. SPPBP	1. Good mechanical strength 2. Chemically and thermally stable even at elevated temperatures
Acid-base blend (Others)	Incorporation of acid component, into alkaline polymer base	1. SPEEK/PBI 2. SPEEK/PEI 3. SPSU /PEI	1. Stable in oxidizing, reducing and acidic environments 2. High thermal stability

POPF Polymer

To circumvent the limitations associated with Nafion[®], another PFSA copolymer, POPF (Figure 6), also caught the attention because of their better application efficiency.³⁹ The POPF polymers have the following advantages over the Nafion[®] polymers: (1) lower equivalent weights (EWs), (2) high water affinity, (3) high proton conductivity, and (4) relative stability at high temperatures (above 80°C).

With short side chains (*i.e.* $-\text{O}(\text{CF}_2)_4\text{SO}_3\text{H}$), POPF polymers contain more ionic groups than Nafion[®] and thus, higher proton conductivity can be offered by POPF polymers if the same equivalent weight (EW) polymers are prepared.

According to the literature, ionomers with low EWs are fully hydrated even at temperatures above 100 °C.⁴⁰ Therefore, ionomers with low EWs (typically 625 and 850 g/eq), such as POPF polymers, have high ionic conductivity (greater than 0.13 S/cm) and are well-suited for low humidity or high temperature fuel cell applications.⁴¹ They are thus, preferred for better application efficiency.

Despite the advantages of POPF polymer mentioned above, the high water affinity poses a threat to its physical integrity. The high water affinity may result in the accumulation of too much water at the cathode, leading to the swelling of the CL. This will render the cell unusable.

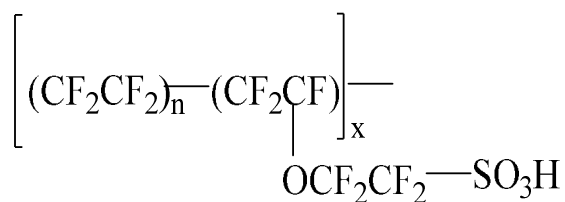


Figure 6: Chemical Structure of the Sulfonic Form of POPF Polymer

Proposed MEA System

As the key components in a fuel cell, the design and fabrication of MEA directly contribute to the overall performance and cost of the PEMFC. One of the principal contributors to the high cost of PEMFC is the Pt catalyst. Thus, raising the efficiency and utilization of the Pt catalyst is one of the central concerns for the cost reduction and the commercialization of the PEMFCs.⁴² For example, the reported catalyst utilization efficiency is as low as 10-20%.⁴³

One of the proposed modifications is to place the catalyst within close proximity of the membrane. Another one is to design thin electrolyte film. Yang et al.⁴⁴ reported improved fuel cell performances of their modified MEAs than the conventional MEA. Instead of using Pt-black (Pt content 100 wt. % Pt), they fabricated Pt-C-80 (Pt content 80 wt. %) thin layers at the boundaries between the PtC-40 layer and the GDL, the PEM and the Pt-C- 40 layer and reducing the Pt-C-40 loading. Also, a modified 7-layer and 9-layer MEAs with even a thinner CL has been reported by Yu et al.²² with better fuel cell performance. The modified 7-layer and 9-layer MEAs was made with thin Pt black CLs located either at the edge between Pt-CL and GDL or/and at the boundary between membrane and Pt-CL. However, the desired result is not obtained so far.

As the result, the investigation of MEA is focus on the first kind of modification. In our lab, a new MEA system, chemically grafting the electrolyte onto the pores of the electrode, is proposed to replace the traditional carbon electrode (Figure 7).²³ This is believed to raise the catalyst utilization and catalysis activity by forming a better bonding between the electrode and electrolyte; thus considerably improving the stability, conductivity, and catalyst usage of PEM fuel cells.

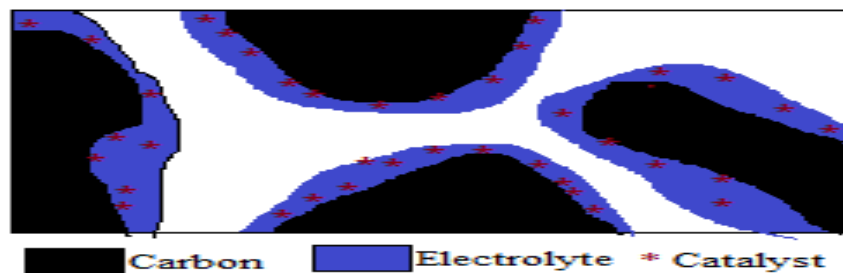


Figure 7: A Porous Carbon-Catalyst-Electrodes System in the PEMFCs (modified from Creager²³-used with permission)

Diazonium PFSI Zwitterion Monomers

For the new porous MEA system, in which the PFSI polymers are proposed to be chemically grafted onto the electrode, the diazonium pendant will be established as a ‘dais’ to impart covalent bonding between the PFSI polymer and the carbon support. Another critical improvement is to develop various PFSI monomers for polymerization to use as the electrolytes, which is expected to improve the membrane’s resistance to extreme conditions.

A series of novel functional diazonium PFSI zwitterions and monomers had been prepared in Dr. Mei’s group.¹¹ Figure 8 shows two diazonium PFSI monomers which have recently been prepared from Nafion[®] monomer.

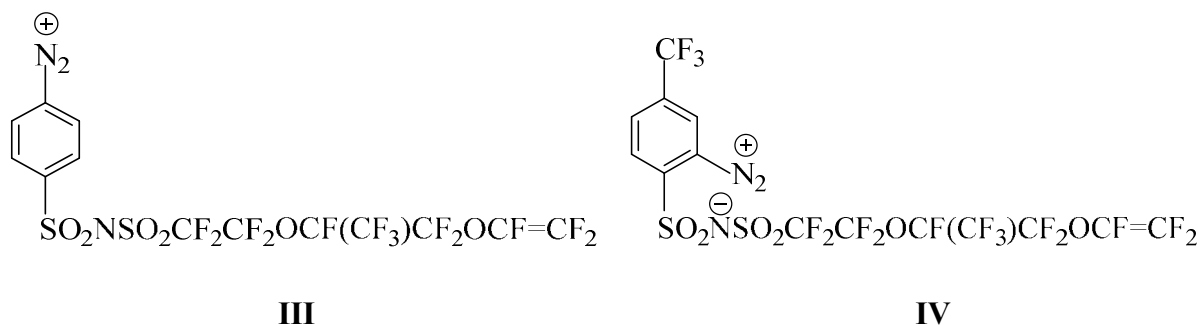
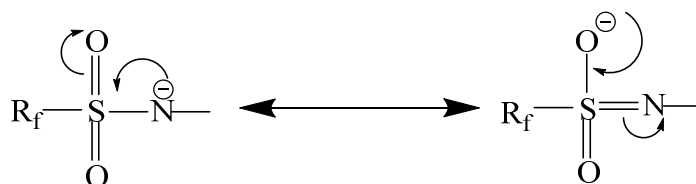


Figure 8: Structure of First Diazonium PFSI Monomers

The proposed monomers are expected to involve at least three major fragments: an aryl diazonium zwitterion, a perfluoroalkyl(aryl) sulfonamide pendant, and a perfluorovinyl ether or other polymerizable units. The perfluorovinyl ether groups, provides the avenue for copolymerization with tetrafluorovinly ether.

The perfluoroalkyl(aryl) sulfonamide pendants are expected to provide better ionic conductivity (higher than 0.1 Scm^{-1} at 80°C), greater thermal stability in acidic form, lower susceptibility to oxidative degradation and dehydration, and inertness to electrochemical conditions¹³, compared to Nafion. There are several factors which may be attributed to these phenomena. For example the delocalization of charge over the O-S-N skeleton and its stabilized conjugate base, $(\text{R}_f\text{SO}_2)_2\text{N}^-$ of the acid as shown in Scheme 3, increase the acidity of the PFSI monomer.

The perfluoroalkyl backbone is not only responsible for the excellent chemical and thermal stability of the polymer, but also increases the acidity of the polymer.

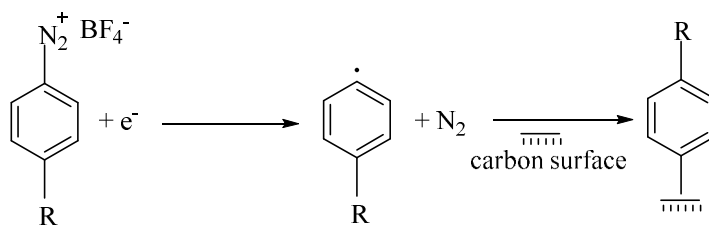


Scheme 3: Delocalization of perfluoroalkyl sulfonyl group⁴⁵

Bis[(perfluoroalkyl)-sulfonyl]imide acids are referred to as superacid. The simplest member, $(\text{CF}_3\text{SO}_2)_2\text{NH}$ has a pK_a of 7.8 in acetic acid compared to 10.2 for HNO_3 . Koppel et al. and later Zhang et al. measured the acidity, in the gas phase, of $(\text{C}_4\text{F}_9\text{SO})_2\text{NH}$ ⁴⁶⁻⁴⁸ which is considered as the strongest acid among neutral acids. The acids $(\text{R}_f\text{SO}_2)_2\text{NH}$, $(\text{R}_f \neq \text{CF}_3)$ ^{49,50} were found to be the very strong acids, based on earlier work done by Meussdoerffer and DesMarteau et al.^{51,52} The gas phase acidity of $(\text{C}_4\text{F}_9\text{SO})_2\text{NH}$ is believed to be affected by key substituent

effects: (1) the substituent/ π -electron-acceptor interaction (R effect), (2) correctly oriented dipolar interaction (F effect), and (3) polarizable substituent/anion interaction (P effect) which favorably stabilizes the strong electron-pair donor anion forms as against the corresponding weaker π -donor conjugate acid forms.

The diazonium moiety is used to chemically attach the substituted aromatic compound to carbon materials, and has been reported by Delamar et al.⁴⁹ The dediazotization is usually catalyzed by metal salts and metals. The reaction is proposed to give an aryl radical that covalently attaches to the carbon surface, as shown in Scheme 4.



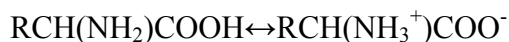
Scheme 4: Electrochemical reduction of an aryl diazonium salt.^{49, 51, 53-55}

The dediazotization procedure is either initiated by electrochemical reduction or thermal decomposition as shown in Scheme 4. It is achieved by the facile loss of the diazonium group- N_2^+ .^{56, 57}

The stable covalent carbon-carbon bond can increase the integration between the carbon electrode and the electrolyte. There have been successful examples of grafting of the simple diazonium perfluoroalkylsulfonimide (PFSI) compound, $p\text{-N}_2^+\text{PhSO}_2\text{N}^-\text{SO}_2\text{CF}_3$ onto the glass carbon electrode⁵⁸ via thermo- or electrochemical reaction.

Since the diazonium moiety is necessary for such a design, the stability of the diazonium compound is a major concern. Therefore, functional diazonium zwitterions (FDZs) and monomers containing perfluoroalkyl sulfonimide group were prepared for this purpose. As both anionic and cationic substituent groups are contained in the same molecule, the zwitterionic

compounds possess an overall neutral charge.⁵⁹ A typical example is the zwitterionic amino acid which has both an amino and a carboxylic acid functional group at the iso-electric point.



Scheme 5: Example of Amino Acid at the isoelectric point

With the experience of the previous works, two analogues of diazonium PFSI monomers were designed from POPF monomer as the research targets. One is 4-diazonium perfluoro(3-oxapent-4-ene) benzenesulfonimide (**I**) zwitterionic monomer and the other one is 4-(trifluoromethyl)-2-diazonium perfluoro(3-oxapent-4-ene) benzenesulfonimide (**II**) zwitterionic monomer(Figure 1).

It is hypothesized that, the acidity of the monomer **II** will be higher compared to monomer **I** due to the presence of CF_3 on the ring. The electron withdrawing CF_3 group is believed to increase the acidity of **II** through inductive effect. Therefore the proton conductivity of **II** is expected to be relatively higher.

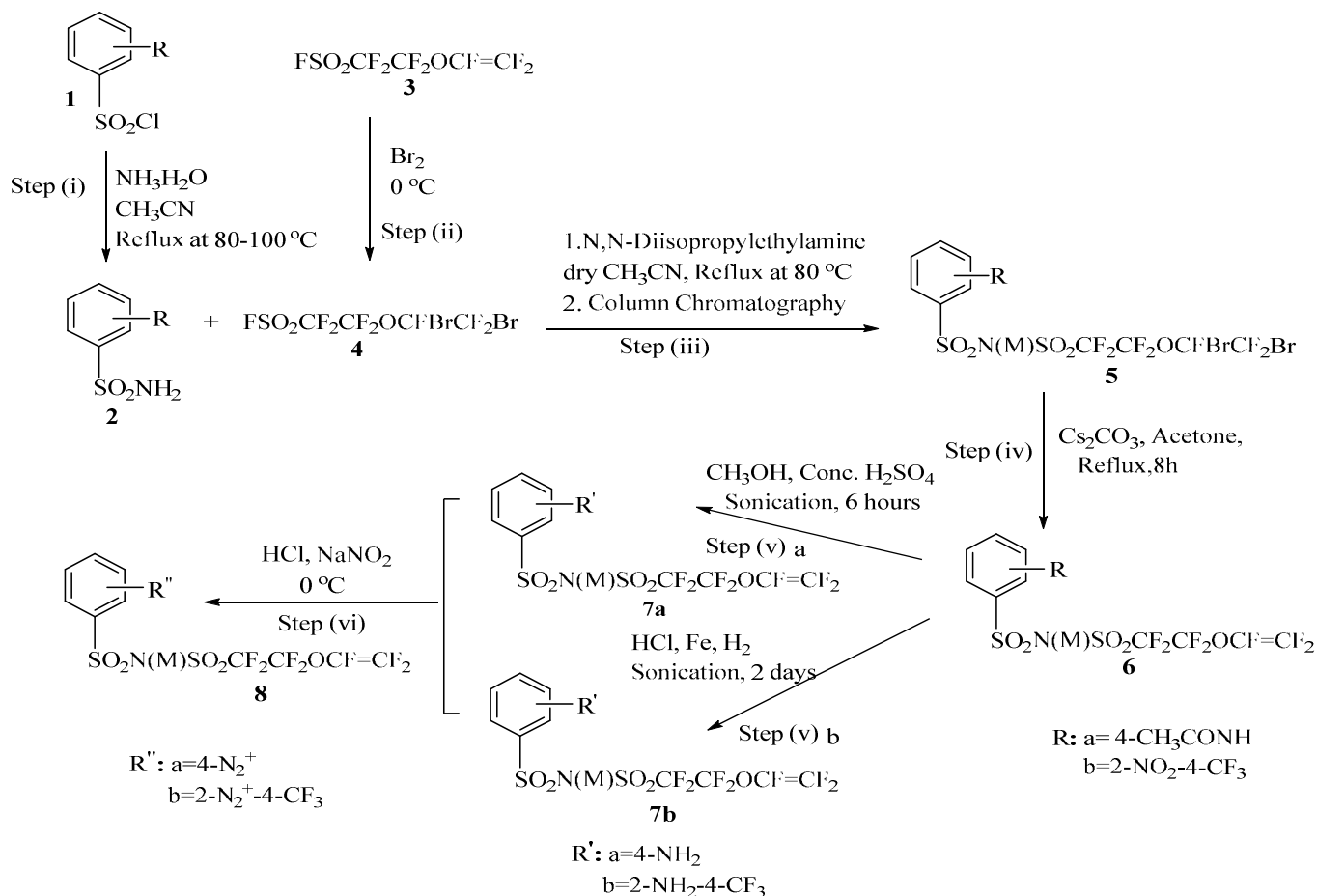
The synthesis methods will be compared first. Then, the reactivity and stability of the monomers **I** and **II** will be compared with those of an already synthesized Nafion[®] based diazonium PFSI monomers **III** and **IV** (Figure 8)^{60,61}, for further polymerization as polymer membranes in PEMFC.

CHAPTER 2

RESULTS AND DISCUSSION

Basically, there are two routes to prepare the analogues of diazonium PFSI monomers. The first kind employs the acetamide protected aromatic sulfonylchloride (such as **1a** in Scheme 6) while another, uses nitro substituted aromatic sulfonyl chloride (such as **1b** in Scheme 6) after conversion to aromatic sulfonamide to couple with brominated POPF monomer. Except for the different ways to obtain the aromatic amine (Step (v)), the synthesis routes of these monomers are quite similar (Scheme 6).

Scheme 6 summarizes the designed routes to the target diazonium PFSI arylsulfonimide monomers-**8a-b**.



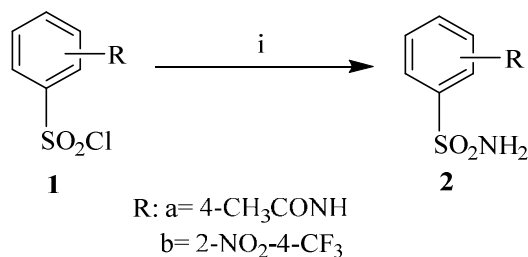
Scheme 6: Overall synthetic scheme for diazonium PFSI arylsulfonimide monomers

Compared with Nafion[®] monomer, the shorter perfluoroalkyl chain of the POPF monomer poses a great challenge in the synthesis procedure.

The reactions were monitored by TLC except bromination and diazotization. The synthesized intermediates and products were characterized by ¹H and ¹⁹F NMR and IR spectroscopies.

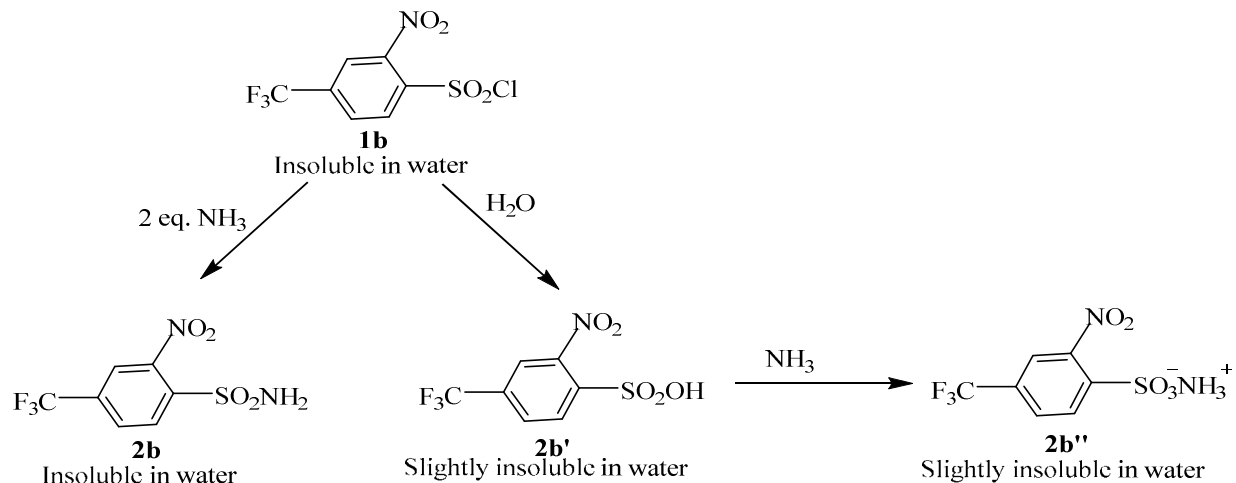
Ammonolysis Reaction

The synthesis of the aromatic amides **2a-b** was carried out by refluxing the substituted aromatic sulfonyl chlorides **1a-b**, in the presence of excess ammonium hydroxide and acetonitrile. These S_N2 reactions as shown in Scheme 7, involve the replacement of the Cl with the -NH₂ group.



Scheme 7: Ammonolysis reaction (i: ammonia water 28-30%, reflux at 100 °C overnight)

The ammonolysis reaction overrides the hydrolysis side reaction because NH₃ is a better nucleophile than H₂O. The hydrolysis by-product usually may be easily removed by vacuum filtration from water. However, for compound **1b**, because of the hydrophobic -CF₃ group on the benzene ring, the water solubility of the hydrolysis product **2b'** is reduced. Hence the purification of **2b** (Scheme 8) instead, was accomplished via column chromatography.

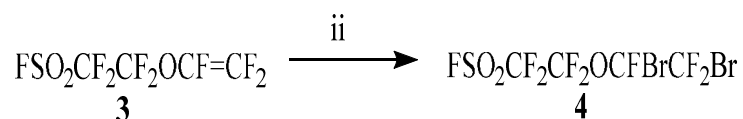


Scheme 8: The hydrolysis reaction during Ammonolysis

Bromination Reaction

As in the designed synthesis route (**Step ii, Scheme 6**), the double bond needs to be protected before the next coupling reaction. Because of the electron deficient perfluorovinyl ether moiety, the perfluorovinyl group of the monomer **3** is susceptible to base catalyzed nucleophilic attack in the presence of water at high temperature.

The protection of the double bond with bromine was achieved through a free radical reaction at low temperature. The brominated product **4** was purified by vacuum distillation at 70 °C. A lower percent yield was obtained compared to the Nafion monomer's bromination procedure. The lower boiling point may account for this result.



Scheme 9: Bromination of perfluoro(3-oxapent-4-ene) sulfonylfluoride monomer (ii: Br_2 , 0 °C at room temperature).

Coupling Reaction

It is critical to carry out the coupling reactions under extremely dry condition. Otherwise, the sulfonyl fluoride group ($-\text{SO}_2\text{F}$) in **4**, will be hydrolyzed to the sulfite ion ($-\text{SO}_3$) under the basic condition in step **iii** (**Scheme 6**), by reacting with weak base-catalyzed water. The hydrolyzed product may be removed later after recrystallization of the Cs salt of the product.

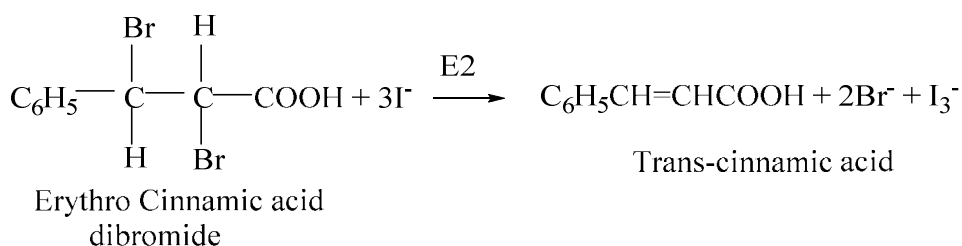
The nucleophilicity of the aromatic sulfonyl amide is enhanced when catalyzed by the organic base, diisopropyl ethylene amine (DIEA). To reduce the amount of hydrolysis product **5'** (**Figure 9**), extremely dry conditions and extra brominated POPF monomer **4** are necessary. The extra brominated POPF monomer is needed to compensate for the amount of POPF monomer consumed in the hydrolysis side reaction.

The preparation of **5a** is considerably faster than that of **5b**. Compared to the nitro substituted aromatic sulfonylamide **2b**, the acetamide substituted aromatic sulfonylamide **2a**, favors the typical $\text{S}_{\text{N}}2$ reaction. The inductive effect of the substituents on the aromatic ring account for this phenomenon.

The preparation of coupling product **5a-b** takes a longer reaction time compared to the similar coupling product **5a'-b'**. The major reason is that, the longer perfluoroalkyl chain of the brominated Nafion[®] monomer **4'**, implying the electron-deficient sulfonyl group might be easier to accept the nucleophilic attack (**Scheme 10**).

The debromination of the vic-dibromides of perfluorovinyl ether proceeded to provide **6a-b**. A lot of methods have been developed to debrominate the vicinal dibromides in versatile organic compounds. Among them, metals like magnesium, sodium, and zinc have been widely used as debrominating agents.⁶² Other debrominating agents include chromium sulfate ($\text{CrSO}_4 \cdot n\text{H}_2\text{O}$) in nitrogen atmosphere, sodium naphthalenide ($\text{Na}^+\text{C}_{10}\text{H}_8^-$)⁶³, and sodium hydrogen selenide (NaHS).

Another known debromination reagent is iodide ion/acetone.⁶⁴ According to Van Duin,⁶⁵ such reaction is a trans-stereospecific second order elimination (E2).



Scheme 12: Debromination of Cinnamic Acid

The debromination method of cinnamic acid with inorganic base, such as potassium iodide is shown in Scheme 12.

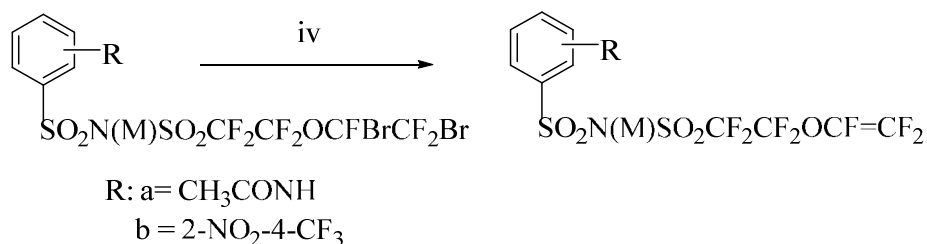
For **5b**, the rate of reaction toward elimination is faster than **5a**. The proposed reason is that, the more electron deficient the double bond, the faster such reaction runs.

The reaction conditions were tested to obtain **6a-b** and the conditions are summarized in Table 4.

Table 4: Results for debromination of the coupling products **5a-b**.

Entry	Base	n (Base): n (Dibromides)	Dibromide (mmoles)	Solvent	Time (hrs)	Condition	% Debromination	% Isolated
1 ^b	Na ₂ CO ₃	3.1 : 1	0.161	Acetone-water (1 : 2.7)	1	Sonication	7.4	71.4
2 ^b	Na ₂ CO ₃	12.4 : 1	0.161	Acetone-water (1 : 7.3)	1.5	Sonication	16	85.7
3 ^b	Na ₂ CO ₃	31.1: 1	0.161	Acetone-water (1 :18.2)	2.5	Sonication	17.1	85.7
4 ^b	Na ₂ CO ₃	62.1 :1	0.161	Acetone-water (1 : 16.1)	3	Sonication	18.2	78.6
5 ^b	Na ₂ CO ₃	62.1 : 1	0.161	Acetonitrile-water(1 :1.8)	3	Sonication	41.4	70.0
6 ^b	Na ₂ CO ₃	155.3 : 1	0.161	Acetonitrile-water(1:1.1)	5	Sonication	56.6	75.7
7 ^b	Na ₂ CO ₃	28.1 : 1	0.32	Acetone-water (1 : 1.8)	48	Sonication	100	85.7
8 ^a	Na ₂ CO ₃	20.8: 1	1.73	Acetone-water (1 : 1.8)	48	Sonication	100	87.8
9 ^a	NaOH	2.04 : 1	0.49	Acetone-water (1.3 : 1)	overnight	Reflux	67.8*	66.7
10 ^a	NaOH	2.6 : 1	0.464	Acetonitrile-water (2.3 : 1)	1.5	Sonication	28*	73.3
11 ^a	NaOH	1.3 : 1	2.35	Acetone-water (1 : 2.4)	7	Sonication	100*	90.8
12 ^b	NaOH	1.3 : 1	1.36	Acetone-water (1 : 2.4)	12	Sonication	100*	91.8
13 ^b	Cs ₂ CO ₃	20.8: 1	1.73	Acetone-water (1 : 1.8)	8	Reflux	100	86.3

*Contains unidentified impurity. ^a and ^b denote **5a** and **5b** respectively



Scheme 13: Debromination reaction (iv: Na_2CO_3 or Cs_2CO_3 , acetone, sonication at room temperature, or reflux at 80-100 °C).

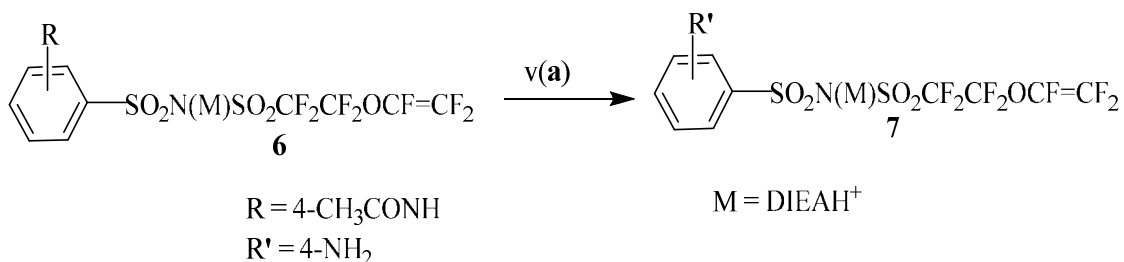
In summary, the optimal reaction conditions for the debromination of the **5a-b** were established with NaOH, Na_2CO_3 and Cs_2CO_3 in acetone/water under sonication or refluxing condition (entries 7, 8, 11-13 in Table 4). Among them, NaOH did promote the fast debromination, but resulted in unwanted side product (entries 9, 10-12 in Table 4). The mechanism is still under investigation. On the other hand, it is advantageous to use Cs_2CO_3 and Na_2CO_3 for practical reasons (entries 1-8 and 13 in Table 4). It is expected that the stronger base Cs_2CO_3 can accelerate the rate of reaction. The results encourage further study in optimizing reaction conditions. Owing to the low cost, the Na_2CO_3 facilitated reaction is the investigation focus. The initial trials involved either sonication or refluxation.

According to entries entries 1-8 in Table 4, the higher debromination percentage and isolated yield resulted from the increase in the reaction time or the concentration of the base.

Furthermore, acetonitrile, having a higher polarity index (5.8 compared to 5.1 for acetone) shows encouragingly high percentages of debromination, although there was no improvement in the yield (entries 4 and 5 in Table 4).

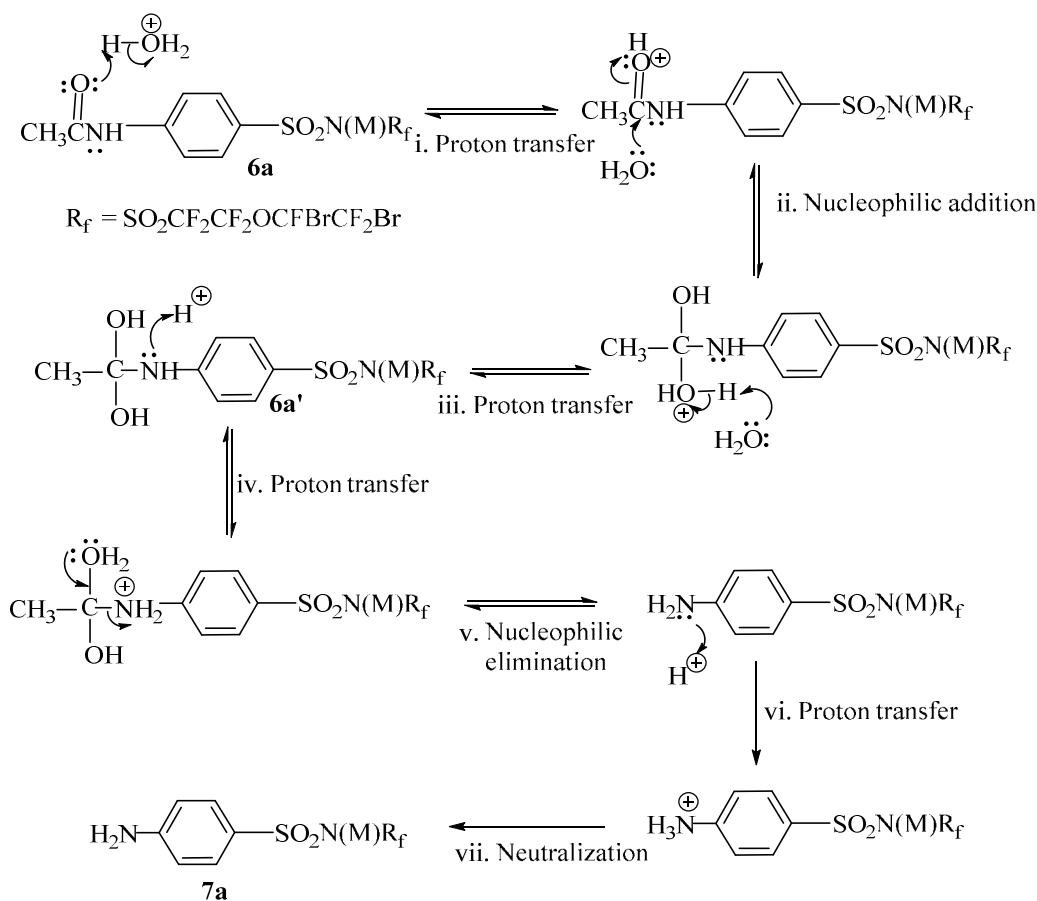
N-deacetylation Reaction

According to the literature,^{4,27} *N*-deacetylation, also called amide hydrolysis (a nucleophilic acyl substitution reaction) is accomplished by using strong acids or strong bases at high temperatures due to the lower reactivity of amides. The reaction occurs via an addition-elimination mechanism.



Scheme 14: The *N*-deacetylation reaction of the coupled product. (v: methanol, conc. H_2SO_4 , Sonication)

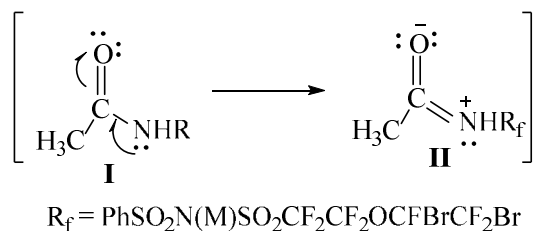
In previous research conducted in Dr. Mei's research group⁶⁶, *N*-deacetylation was reported to be effective in acidic media such as HCl (pKa = -6.0), H_2SO_4 (pKa = -9.0) and ClSO_3H (pKa = -6.6) under sonication or refluxing. The weakening of the C-N bond after the amide protonation, may be responsible for this phenomenon (Step 4, Scheme 15).



Scheme 15: The mechanism for the acid catalyzed *N*-deacetylation.⁶⁷

The carbonyl (C=O) of the amide **6a** is first protonated to become more electrophilic, making it more prone to a nucleophilic attack. Next, proton transfers follow in the subsequent Steps **iii** and **iv** after the addition of the water (H₂O) to form the tetrahedral adduct **6a'** (Scheme 15). The desired aromatic amine **7a** is obtained after neutralization of the protonated amine in Step 7.

To obtain the aromatic amine, the *N*-deacetylation of the PFSI aromatic acetamide (Step v(a) in Scheme 6), is more efficient than the reduction of the regular nitro substituted aromatic amide (Step v(b) in Scheme 6). The possible reason is that the PFSI aromatic acetamide is destabilized by the electron-withdrawing effect of the perfluoroalkyl chain in the resonance structure **II** (Scheme 16).



Scheme 16: The resonance structure of the PFSI monomer **8a**

Reduction Reaction

Due to the high cost of 4-(trifluoromethyl)-2-sulfamonylacetanilide **1'** (Figure 11), the aromatic nitro compound **6b** was converted to its corresponding aromatic amine **7b**, by reduction reaction. As the literature indicated⁶⁸ variety of reducing agents are used to accomplish this task. Examples of such reducing agents are: 1. Metal with acid, such as Fe/HCl or Fe/Acetic Acid, Zn/NaOH, Sn/HCl, Fe/ArOH; 2. catalytic hydrogenation using Raney Ni, H₂-Pd/C and H₂-PtO₂; 3. sodium polysulfide, NaBH₄/Pt-Ni, and so on.

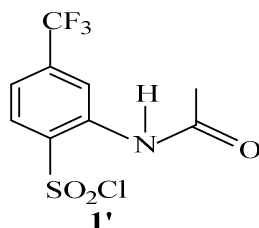
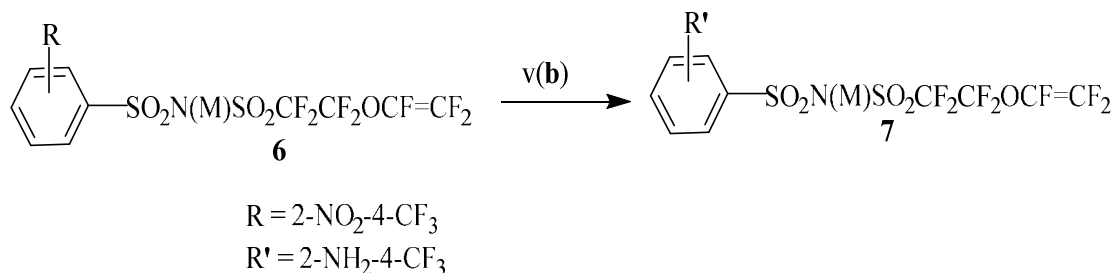


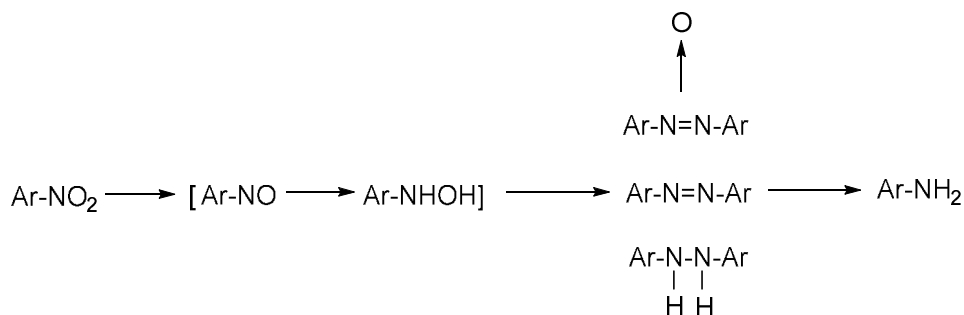
Figure 10: 4-(trifluoromethyl)-2-sulfamonylacetanilide



Scheme 17: Reduction of the coupling product (v(b): hydrogen gas, iron powder, sonication, HCl, dry CH₃OH, room temperature).

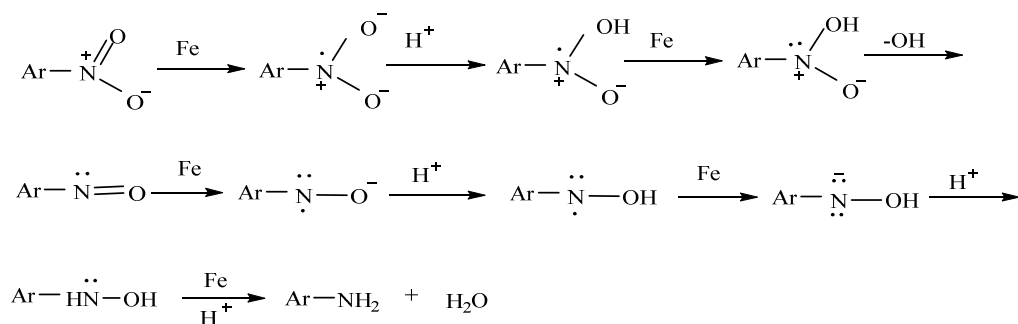
Fe/HCl/H₂ in ultra-sound sonicator at room temperature was employed based on a previous work in the Dr. Mei's research group⁶¹. To prevent the addition of perfluorovinyl ether by acid at high temperature, the reduction was performed at room temperature with sonication assistance. Nuchter et al.⁶⁹ reported that, ultrasound sonication is an alternative energy source for the initiation of organic reactions. Additionally, ultrasound also has the potential to accelerate chemical transformations, affect product distributions, improve yields and increase the catalytic activity of metal particles by factors as high as 10⁵.⁷⁰

It's been hypothesized that, the reduction of aryl nitro compounds proceed via the hydroxylamine, azoxy and azo compound intermediates to their corresponding aryl amines (Scheme 18).⁷¹ Therefore, the reaction time and the amount of partial reduced side product, could possibly be reduced by ultrasonic irradiation to accelerate the heterogeneous chemical reactions.



Scheme 18: The intermediates of the reduction of aryl nitro compounds.

Iron was chosen for this reaction because, in addition to being an inexpensive and readily available reagent, iron is very mild and selective for the nitro group. The reaction mechanism is shown in Scheme 19.⁷²



Scheme 19: Mechanism for Reduction of Aromatic Nitro Compounds

The other byproducts in the reduction reaction are shown in Figure 11.

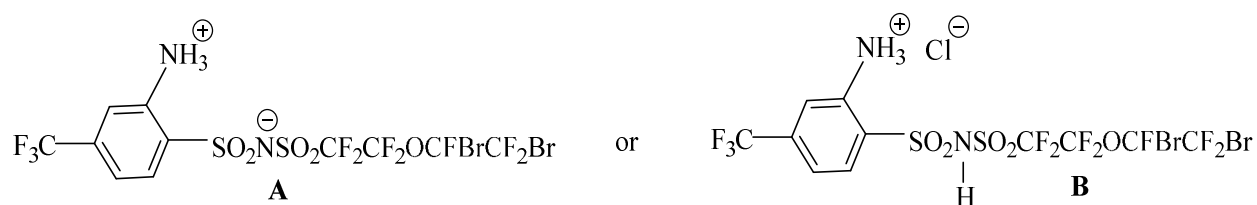


Figure 11: Byproducts Associated with the Reduction Reaction

Due to the acidic nature of the perfluorosulfonimide group, the aromatic amine **7b** can be protonated as the quaternary amine salts **A** and **B** (Figure 11). Both of them can be converted back to aromatic amine by neutralization with NaOH.

In reference to the previous synthetic design,⁶¹ a ratio of 5:1 iron powder to the coupling product was used to convert the nitroaromatic compound **6b** to its corresponding aminoaromatic **7b**. Higher equivalents of iron powder resulted in the formation of a green-colored iron chloride complex. On the other hand, lower equivalents of the iron powder only lead to incomplete reduction.

Diazotization Reaction

Diazotization reactions are employed to convert primary/aromatic amines to diazonium salts. The diazotization reactions are usually accomplished in aqueous media or organic solvents.⁷³ To prepare the diazonium salts, primary amines are generally reacted with nitrous

Contrary to the expected ^1H NMR spectrum of **2b**, **5b**, **6b** and **7b**, the experimental data obtained shows inconsistent chemical shift for the aryl protons. H_A (Figure 12) is anticipated to have the highest chemical shift since it is between two electron withdrawing groups. It however is between the two doublets (H_B and H_C , Figure 12).

After diazotization, all the protons' chemical shifts in the ^1H NMR spectrum of **8b** match the calculated data obtained from Spartan '14 mechanics program (DFT/6-31G *) (Spartan '14 (DFT/6-31G *): δ_A 8.26 (1H, s), δ_B 7.79 (1H, d), δ_C 8.07 (1H, d)). It will be a subject of further investigation why the differences of H_A 's chemical shift occurs between the calculated and the observed chemical shifts.

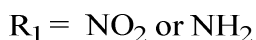
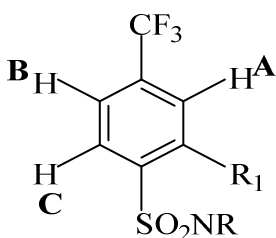


Figure 12: Structure of 2-nitro-4-(trifluoromethyl) benzene sulfonamide

CHAPTER 3

EXPERIMENTAL

General Considerations

NMR Spectroscopy

The ^1H and ^{19}F NMR spectra were measured on a Joel JNM-ECP 400 MHz FT NMR spectrometer. The chemical shifts are reported in parts per million (ppm) using the high-frequency position conversion, and the coupling constants are reported as a 'J' value in Hz. Tetramethylsilane (TMS) was used as a reference material for the ^1H NMR spectra while the ^{19}F NMR chemical shifts were referenced against a CFCl_3 external standard. The chemical shift of residual H in CD_3CN is 1.97 ppm with respect to TMS.

The splitting patterns of resonance were designated as singlet (s), doublet (d), triplet (t), quartet (q), and multiplet (m). The NMR spectra were measured using 1-2 mmol/L concentrations of the solutions (unless indicated otherwise) and small amounts of CFCl_3 gas in an appropriate deuterated solvent for ^{19}F NMR only.

Infra-red Spectroscopy

The infrared spectra were collected on a Shimadzu IR Prestige-2I FTIR spectrometer. The solid samples were prepared as fine powder and placed on the lens of the attenuated total internal reflectance (ATR) accessory. The IR spectra were collected from 4000 cm^{-1} to 450 cm^{-1} and quoted in wavenumbers (cm^{-1}) with intensity abbreviations of vs (very strong), s (strong), m (medium), w (weak), and vw (very weak).

Gas Chromatography-Mass Spectrometer

Gas Chromatography-Mass-Spectroscopy (GC-MS) spectra were recorded on a Shimadzu GCMS-QP2010 Plus GC system spectrometer. The samples were prepared by dissolving 1 mg of the solid samples in 1 mL of acetone.

Thin Layer Chromatography

Thin Layer Chromatography (TLC) was carried out using UV active silica gel plates in suitable solvents. The readout was carried out under UV lamp.

Glass Vacuum System

Volatile compounds were distilled, dried, purged, sublimed, and trapped using a glass vacuum line as seen in Figure 13.

This dynamic high-vacuum line is equipped with Teflon[®]. It comprise two manifolds; one manifold is for the vacuum and the other is for the nitrogen gas. A good vacuum of about 10^{-4} - 10^{-7} torr can be achieved.

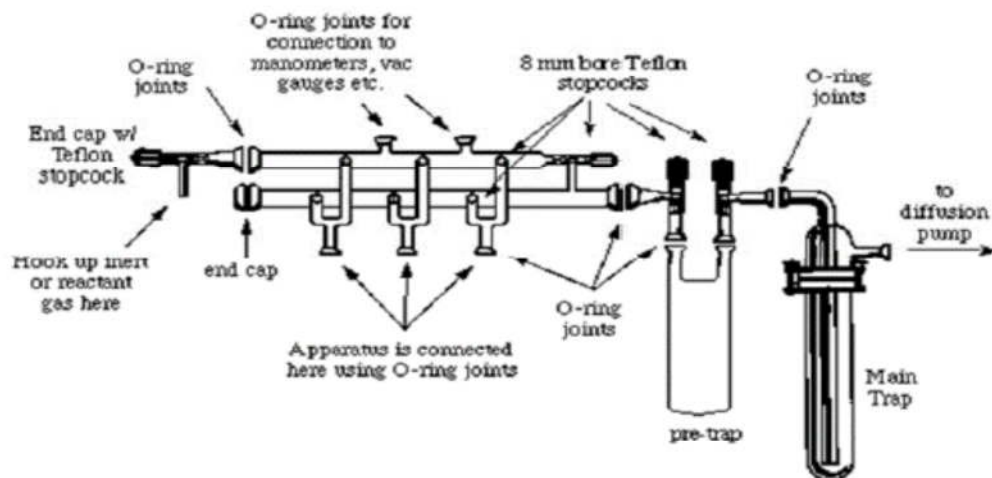


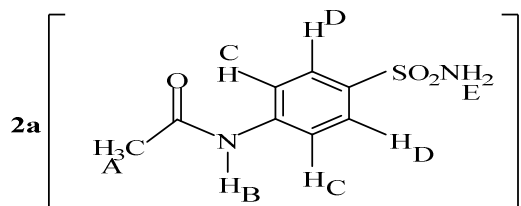
Figure 13: The line diagram of a dual-manifolds glass vacuum line. Used with permission.⁷⁵

Purification of Solvent and Experimental Practice

The starting materials: *N*-acetyl sulfanilyl chloride, *p*-nitro-*o*-trifluoromethyl benzene sulfonyl chloride, and POPF monomer (FSO₂CF₂CF₂OCF=CF₂) were bought from commercial sources and used as received unless otherwise specified. All the reactions were performed in glassware unless indicated otherwise. Air or moisture sensitive compounds were stored in a dry box under nitrogen gas. Solvents were dried using activated molecular sieves.

Synthesis of Benzenesulfonyl amide (2a-b)

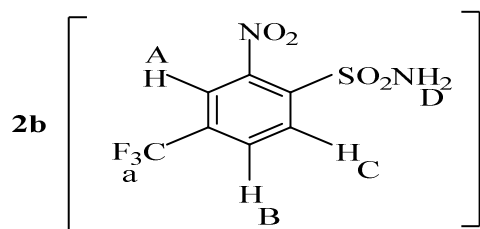
In a typical procedure, *N*-acetyl sulfanilyl chloride **1a** (10.0 g, 0.0428 mol) was dissolved in 60 mL of ammonia hydroxide (28-30%) and 40 mL of acetonitrile in a 100 mL round bottom flask. The solution was refluxed for 24 hrs at 90 °C and the solvent was removed by the rotary evaporator. The solid crude product was recrystallized from a water-methanol solution and then vacuum filtered. The pure product **2a** was obtained with a yield of 85.5 % after drying under vacuum for 2 hours. Compound **2b** was obtained by similar procedure with a 78.0 % yield.



¹H NMR (400 MHz; CD₃CN; ppm): δ_A 2.02 (3H, s), δ_B 8.58 (1H, s), δ_C 7.72 (2H, d), δ_D 7.66 (2H, d), J_{CD} = 8 Hz, and δ_E 5.53 (2H, s).

IR (ν_{max}/cm⁻¹): 3367.71 m (NH), 1656.85 m (C=O), 1593.20 m (NH) and 1317.38 s (S=O).

m/z: 43 (M⁺, 100%), 214, 172, 156, 108, 92, and 65



^{19}F NMR (400 MHz; CD_3CN ; ppm): δ_a -62.21 (3F, s).

^1H NMR (400 MHz; CD_3CN ; ppm): δ_A 8.22 (1H, s), δ_B 8.13 (1H, d), δ_C 8.29 (2H, d), $J_{BC} = 8$ Hz, δ_D 6.24 (2H, s).

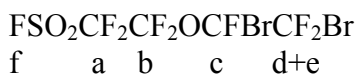
IR ($\nu_{\text{max}}/\text{cm}^{-1}$): 3296.35 (NH), 1521.84s and 1328.95s (NO), 1153.43s and 1184.29s (S=O).

m/z: 254 (M^+ , 100%), 206, 113, 75, 64, and 50

Synthesis of $\text{FSO}_2\text{CF}_2\text{CF}_2\text{OCFBrCF}_2\text{Br}$ (**4**)

In a typical procedure, POPF monomer $\text{FSO}_2\text{CF}_2\text{CF}_2\text{OCF}=\text{CF}_2$ **3** (3.0 g, 0.0107 mol) was added to a 25 mL round bottom flask containing a stir bar. The flask was put in an ice bath at 0 °C. Bromine (1.5 mL, 0.0293 mol) was then added slowly using a pressure equalizing funnel for about 2 hours. Persistence of a reddish color for 30 mins indicated that there was excess bromine. The excess bromine remained in the funnel and as the reaction was allowed to continue overnight in the presence of light, some bromine dissociated and was made available as $\text{Br}_2(\text{g})$ boosting the free radical reaction.

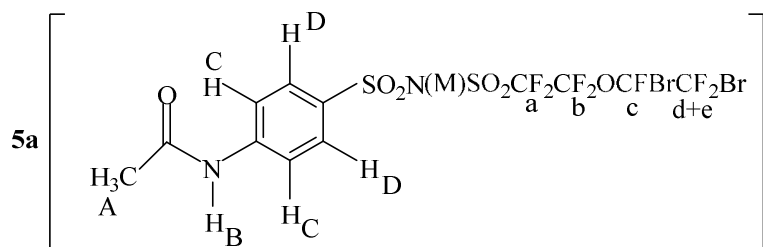
The excess bromine was removed by the addition of 5 % NaHSO_3 slowly until the reddish color disappeared. The product was separated by extraction with 3×5 mL DI water in a separatory funnel. The product was dried, using Na_2SO_4 after which it was distilled under dynamic vacuum. A percent yield of 70.5 % (3.32 g) of the product **4** was obtained.



^{19}F NMR (400 MHz; CD_3CN ; ppm): δ_a -111.38(2F, m), δ_b -63.81(2F, m), δ_c -72.15 (1F, m), δ_d -79.97 (1F, m), δ_e -83.45 (3F, qm), and δ_f 46.32 (1F, s)

Synthesis of $\text{CH}_3\text{CONHPhSO}_2\text{N}(\text{M})\text{SO}_2\text{CF}_2\text{CF}_2\text{OCFBrCF}_2\text{Br}$ (**5a-b**)

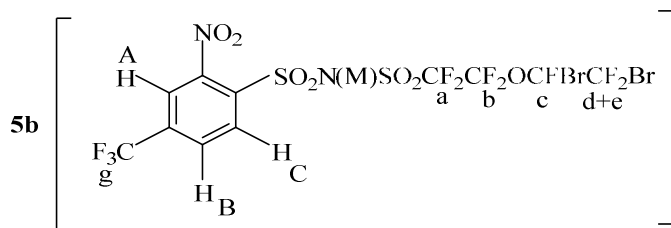
In a typical procedure, brominated POPF monomer **4** (1.5 g, 0.00341 mol) and the 4-sulfamonylacetanilide **2a** (0.72 g, 0.00334 mol) were added to a 100 mL three-necked round bottom flask equipped with a stir bar and two rubber septa in a dry box. Then 20 mL of dry acetonitrile and 5 mL of dry diisopropyl ethylamine (DIEA) were injected into the closed flask in the dry box. The solution was refluxed for 5 days at 90 ° C under nitrogen gas. The disappearance of the $-\text{SO}_2\text{F}$ peak in the ^{19}F NMR spectroscopy indicated the reaction was complete. All of the remaining volatile compounds were then removed by rotary evaporator, leaving the crude product, as the DIEAH^+ salt, and the inorganic impurities. The crude product was then run through a chromatography column with a 1:1 ratio of acetone to tert-butyl methyl ether to remove the extra starting material **2a-b**. Next, the hydrolysis by-product was removed by recrystallization with acetone/water. The purified product **5a** (1.85 g, 87.5 %) was obtained after removing the solvent and drying under vacuum for 24 hours. Compound **5b** (84.8 %) was obtained by similar procedure after purification using column chromatography.



^{19}F NMR (400 MHz; CD_3CN ; ppm): δ_a -116.81 (2F, m), δ_b -64.29 (2F, m), δ_c -72.03 (1F, m), δ_d -80.06 (1F, qm), and δ_e -84.78

^1H NMR (400 MHz; CD_3CN ; ppm): δ_{A} 2.09 (3H, s), δ_{B} 8.71 (1H, s), δ_{C} 7.66 (2H, d), and δ_{D} 7.79 (2H, d), $J_{\text{CD}} = 8$ Hz

IR ($\nu_{\text{max}}/\text{cm}^{-1}$): 3402.43 (NH), 1662.64 m (C=O), 1176.58 m and 1261.45 s (S=O), 1045.43 vs (CF_2).



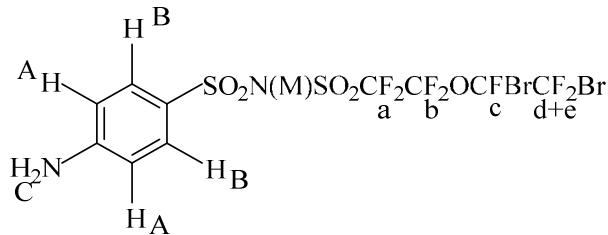
^{19}F NMR (400 MHz; CD_3CN ; ppm): δ_{a} -116.49 (2F, m), δ_{b} -84.04 (2F, m), δ_{c} -71.70 (1F, m), δ_{d} -79.79 (1F, m), δ_{e} -64.05 (2F, m), δ_{g} -63.24 (3F, s),

^1H NMR (400 MHz; CD_3CN ; ppm): δ_{A} 8.35 (1H, s), δ_{B} 8.26 (2H, d), δ_{C} 8.48 (2H, d), $J_{\text{BC}} = 8$ Hz

IR ($\nu_{\text{max}}/\text{cm}^{-1}$): 1541.12s and 1402.25m (NO), 1150.36vs (CF_2), 1049.28vs, 1095.92vs and 1319.31w (S=O).

Synthesis of 4-NH₂PhSO₂N(M)SO₂CF₂CF₂OCFBrCF₂Br (**6a**)

In a typical procedure, the coupled product **5a** (0.20 g, 0.0032 mol) was added into a 25 mL round bottom flask equipped with a stir bar. Then 4 mL of methanol and 2 mL of concentrated sulfuric acid (conc. H_2SO_4) were added to the flask. The pH of the resulting solution was measured as acidic, using a pH meter. The solution was allowed to react under sonication for 6 hours. Subsequently, the solution was neutralized with NaOH to pH 7 and the solvent was removed via rotary evaporator. Next the product was dried under vacuum overnight. The dried sample was re-dissolved in 5 mL of ethyl acetate, and then transferred into a 60 mL separatory funnel. The organic solution was washed with 3×5 mL of brine water. The solvent was removed and then dried under vacuum to give the pure product **6a** with 84.2 % yield.



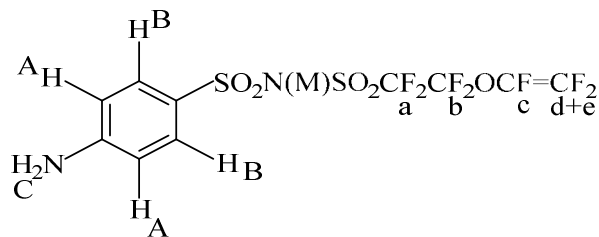
^{19}F NMR (400 MHz; CD_3CN ; ppm): δ_a -117.05 (2F, m), δ_b -64.22 (2F, m), δ_c -71.77 (1F, m), δ_d -80.08 (1F, m), δ_e -84.29 (1F, m)

^1H NMR (400 MHz; CD_3CN ; ppm): δ_A 7.56 (2H, s), δ_B 6.65 (2H, d), $J_{AB} = 8$ Hz, δ_C 4.66 (2H, s)

IR ($\nu_{\text{max}}/\text{cm}^{-1}$): 3369.64 (NH), 1300 m and 1315.45 s (S=O), 1143.79 vs (CF_2)

Synthesis of 4-NH₂PhSO₂N(M)SO₂CF₂CF₂OCF=CF₂ (**7a**)

In a typical procedure, the N-deacetylated product **6a** (0.10 g, 0.00017 mol) was added to a 25 mL round bottom flask equipped with a stir bar. Then 3 mL of acetone and 3 mL of 3.0 M Na_2CO_3 were added to it. The pH of the resulting solution was tested to be 8.83 using a pH meter. The solution was allowed to react under sonication for 2 days. Next the solvent was removed and dried under vacuum overnight. The dried sample was re-dissolved in 5 mL of ethyl acetate, and then transferred to a 60 mL separatory funnel. The organic solution was washed with 3×5 mL of brine water. The final product **7a** (0.063 g, 86.3 %) was isolated after removing the remaining solvent and drying under vacuum for 24 hours.



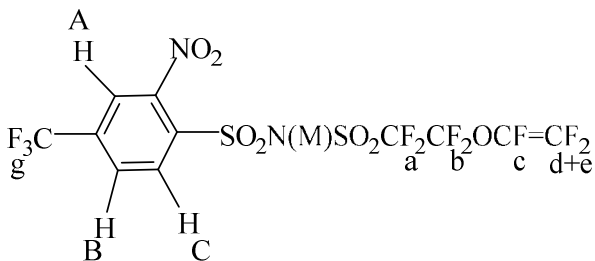
^{19}F NMR (400 MHz; CD_3CN ; ppm): δ_a -116.90 (2F, m), δ_b -83.71 (2F, m), δ_c -115.05 (1F, m), δ_d -123.19 (1F, m), δ_e -135.30 (2F, m)

^1H NMR (400 MHz; CD_3CN ; ppm): δ_A 7.48 (2H, s), δ_B 6.56 (2H, d), $J_{AB} = 8$ Hz, δ_C 4.55 (2H, s)

IR (vmax/cm-1): 3360.00m (NH), 1600.92 (C=C), 1259.52 s (S=O), 1014.56 vs (CF₂).

Synthesis of 4-CF₃-2-NO₂-PhSO₂N(M)SO₂CF₂CF₂OCF=CF (6b)

In a typical procedure, 0.5 g (0.00173 mol) of the coupled product **5b** was added to in a 50 ml round bottom flask equipped with a rubber septum. Then 10 mL of acetone and 12 ml of 3.0 M Cs₂CO₃ were added to the flask. The pH of the resulting solution was determined to be 10.76, using a pH meter. The solution was refluxed at 90 °C for 8 hours to complete the debromination. The excess solvent was then removed using rotate evaporate and the product dried under vacuum overnight. The dried product was re-dissolved in 5 ml ethyl acetate and then transferred into a 60 ml separatory funnel. The organic portion was extracted and washed with 3 x 5 ml brine water. The solvent was removed by rotary evaporator and dried under high vacuum overnight, to obtain the pure product **6b** with 92.8 % yield.



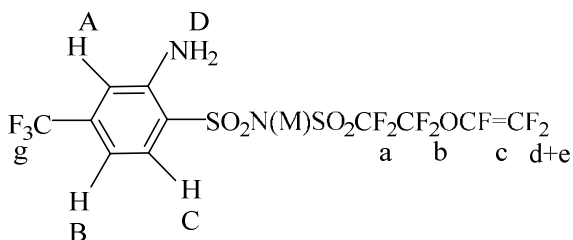
¹⁹F NMR (400 MHz; CD₃CN; ppm): δ_a -116.38 (2F, m), δ_b -83.30 (2F, m), δ_c -114.25 (1F, m), δ_d -122.63 (1F, m), δ_e -135.12 (2F, m), δ_g -63.17 (3F, s),

¹H NMR (400 MHz; CD₃CN; ppm): δ_A 7.93 (1H, s), δ_B 7.91 (2H, d), δ_C 8.24 (2H, d), J_{BC} = 8 Hz.

IR (vmax/cm-1): 1550.77s and 1367.53m (NO), 1124.50vs (CF₂), 1624.06 (C=C), 1076vs, 1280.73vs and 1321.24w (S=O).

Synthesis of 4-CF₃-2-NH₂-PhSO₂N(M)SO₂CF₂CF₂OCF=CF₂ (**7b**)

In a typical procedure, the debrominated product **7a** (0.18 g, 0.0034 mol) and iron powder (0.11 g, 0.00204 mol) were added to a 50 ml one-necked round bottom flask equipped with a stir bar. And then, 10 mL of methanol and 1 mL of 6.0 M HCl were subsequently added to the round bottom flask. The flask was equipped with a septum, a needle, and a H₂ gas filled balloon. The reaction was run at room temperature in an ultrasound sonicator for 2 days. TLC was used to monitor the reaction in 1.5:1 acetone to hexane, which revealed one spot with an R_f value of 0.07. The excess iron powder was removed out by vacuum filtration. The organic portion was extracted with 3x 10 mL of ethyl acetate from water. The final product **7b** (0.13 g, 76.5 %) was obtained after removing the remaining solvent and drying under vacuum for 24 hours.



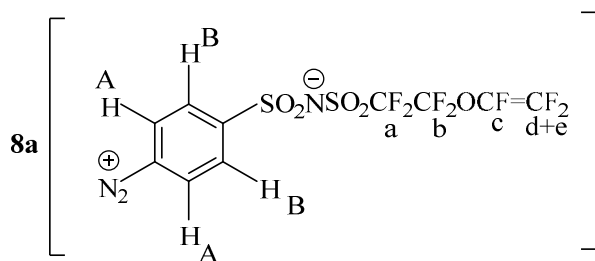
¹⁹F NMR (400 MHz; CD₃CN; ppm) δ_a -116.94 (2F, m), δ_b -83.72 (2F, m), δ_c -114.60 (1F, m), δ_d -123.14 (1F, m), δ_e -135.57 (1F, m), and δ_g -63.81 (3F, s)

¹H NMR (400 MHz; CD₃CN; ppm): δ_A 7.04 (1H, s), δ_B 6.88 (2H, d), δ_C 7.79 (2H, d), J_{BC} = 8 Hz, δ_D 5.56 (2H, s)

IR (ν_{max}/cm⁻¹): 3346m and 1633.71s (NH), 1259.57m and 1095.57vw (S=O), 1253.73s and 1050vs (CF₂).

Synthesis of 4-N₂⁺PhSO₂N⁻SO₂CF₂CF₂OCF=CF₂ (**8a-b**)

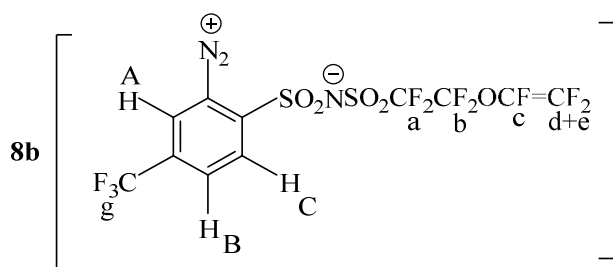
In a typical procedure, 0.10 g (0.000233 mol) of debromination product, 0.155 g (0.00223 mol) of NaNO₂, and 3 ml of 6.0 M HCl were added to a 50 ml round bottom flask equipped with a stir bar. The solution was stirred for 2 hours in an ice bath and then poured onto ice before vacuum filtration. The final purified product **8a** (0.075g, 72.8%) was obtained after drying under dynamic vacuum for 12 hours. Compound **8b** (74.4%) was obtained by a similar procedure.



¹⁹F NMR (400 MHz; CD₃CN; ppm): δ_a -116.77 (2F, m), δ_b -83.66 (2F, m), δ_c -114.91 (1F, m), δ_d -122.79 (1F, m), δ_e -135.30 (1F, m)

¹H NMR (400 MHz; CD₃CN; ppm): δ_A 8.51 (2H, d), δ_B 8.28 (2H, d), J_{BC} = 8 Hz

IR (ν_{max}/cm⁻¹): 2301.08w (N≡N), 1319.31s, and 1282.68w vs (S=O), 1012.63vs (CF₂)



¹⁹F NMR (400 MHz; CD₃CN; ppm): δ_a -116.35 (2F, m), δ_b -83.27 (2F, m), δ_c -113.60 (1F, m), δ_d -122.46 (1F, m), δ_e -135.84 (1F, m), δ_g -63.59 (3F, s)

¹H NMR (400 MHz; CD₃CN; ppm): δ_A 8.92 (1H, s), δ_B 8.53 (1H, d), δ_C 8.63 (1H, d), J_{BC} = 8 Hz.

IR (ν_{max}/cm⁻¹): 2301.08w (N≡N), 1319.31s, 1280.73w and 1078vs (S=O), 1124.50vs (CF₂)

CHAPTER 4

CONCLUSION

Two new PFSI diazonium zwitterions monomers, $\text{N}_2^+\text{PhSO}_2\text{N}^-\text{SO}_2\text{CF}_2\text{CF}_2\text{OCF}=\text{CF}_2$ **8a**, and $4\text{-CF}_3\text{-2-N}_2^+\text{-PhSO}_2\text{N}^-\text{SO}_2\text{CF}_2\text{CF}_2\text{OCF}=\text{CF}_2$ **8b**, were prepared and characterized. Except for the substituted aromatic amine (Step (v)), all the other steps, in the preparation of these two monomers followed similar routes as in previous synthesis with diazonium PFSI monomers from Nafion[®] monomer.

With respect to the preparation of compound $4\text{-CF}_3\text{-2-N}_2^+\text{-PhSO}_2\text{N}^-\text{SO}_2\text{CF}_2\text{CF}_2\text{OCF}=\text{CF}_2$, the ammonolysis reaction entails a cumbersome purification process due to the difficulty of removing the hydrolysis products, $4\text{-CF}_3\text{-2-NO}_2\text{-PhSO}_2\text{OH}$ by filtration from water. The purification was achieved through column chromatography.

The coupling reactions, in both cases, needed extensive purification processes to get rid of both the excess substituted benzene sulfonamide and the hydrolysis impurity, $(\text{CH}_3)_2\text{NHCHCH}_3\text{SO}_3\text{CF}_2\text{CF}_2\text{OCFBrCF}_2\text{Br}$ of the coupled products.

Because of the electron-withdrawing substituents (trifluoromethyl and nitro groups) on the benzene ring, the brominated perfluorovinyl ether moiety becomes more electron deficient than the acetamide substituted aromatic compound, accounting for the faster debromination of the first compound relative to the acetamide substituted aromatic compound.

In synthesizing the aromatic amine, the *N*-deacetylation procedure for the PFSI aromatic acetamide is better than the reduction reaction of the aromatic nitro compound since it takes relatively short time without any extensive purification process.

The diazotization process is much more facile for the trifluoromethyl substituted aromatic amine than the non-substituted aromatic amine because, the nucleophilicity of the

trifluoromethyl substituted compound is reduced by the partial withdrawal of electron pair into the nucleus.

Overall, the synthesis of 4-diazonium perfluoro(3-oxapent-4-ene)benzenesulfonimide was more efficient with a better total yield, [(27.9 % compared with 24.6 % for 2-diazonium-4-(trifluoromethyl)perfluoro(3-oxapent-4-ene)benzenesulfonimide)], purity, and reduced reaction time. It was less cumbersome and involved fewer extensive purification procedures.

REFERENCES

- [1] Spiegel, C. Designing and building fuel cells; McGraw-Hill, Two Penn Plaza, New York, **2007**; pp 3.
- [2] Papageorgopoulos D. DOE fuel cell technology program overview and introduction to the 2010 fuel cell pre-solicitation workshop in DOE fuel cell pre-solicitation workshop. Department of Energy, Lakewood, Colorado; **2010**.
- [3] Barbir F. PEM Fuel Cells: Theory and Practice. 1 st ed.; Elsevier Academic Press: New York, **2005**
- [4] Devanathan R. Recent developments in proton exchange membranes for fuel cells. Energy Environ Sci **2008**; 1:101–19.
- [5] Kim, J.; Kim, B.; Jung, B. Proton Conductivities and Methanol Permeabilities of Membranes Made from Partially Sulfonated Polystyrene-block-Poly(ethylene-ranbutylene)-block-Polystyrene Copolymers. J. Membr. Sci. **2002**, 207, 129-137.
- [6] Hickner, M.; Ghassemi, H.; Kim, Y.S.; Einsla, B.; McGrath, J.E. Alternative Polymer Systems for Proton Exchange Membranes (PEMs). Chem. Rev. **2004**, 104, 4587- 4612.
- [7] Ren, X.; Zelenay, P.; Thomas, S.; Davey, J.; and Gottesfeld, S. J. Power Sources, 86, 111-116, **2000**.
- [8] Bryan S.; Bender, P.G.; Davey, J.; Zelenay, P. Electrochemical and Electronic Materials and Devices, MST-11 Los Alamos National Laboratory, Los Alamos, NM 87545
- [9] Wand, G. Fuel cell history, Part One. www.ogniwa-paliwowe.info, **2006**.
- [10] Wang, Y.; Chen, K.S.; Mishler, J.; Cho, S.C.; Adroher, X.C. A review of polymer electrolyte membrane fuel cells: Technology, applications, and needs on fundamental research (2011). US DOE Publications. Paper 132.

- [11] Hua, Mei, Perfluoroalkyl (Aryl) Sulfonimide Zwitterions. Ph.D. Dissertation, Clemson University, Clemson, SC, **2006**.
- [12] Walter, Katie. The unitized regenerative fuel cell: Science and technology review, May **1997**, p. 13, <http://www.llnl.gov/str/Mitlit.html>.
- [13] Ryan Baker and JiuJun Zhang Institute for fuel cell innovation. National Research of Canada, 4250 Wesbrook Mall, Vancouver, British Columbia V6T 1W5, Canada, **2011**.
- [14] Steele, B.C.H., and Heinzl, Angelika. Materials for fuel-cell technologies: Nature, **2001** v. 414, p. 345–352.
- [15] Cheng, X.; Shi, Z.; Glass, N.; Zhang, L.; Song, D.; Liu, Z. S.; Wu, S.; Merida, W. A. A Review of PEM Hydrogen Fuel Cell. Journal of Power Sources. **2007**, 165, 739-756.
- [16] Schmittinger, W.; Vahidi, A.; A Review of the Main Parameters Influencing Longterm Performance and Durability of PEM Fuel Cells. Journal of Power Sources. **2008** v 180[1], p.1-14.
- [17] Thampan, T.; Malhotra, S.; Zhang, J.; Datta R. PEM Fuel Cell as a Membrane Reactor. Catal. Today, **2001**, 67[1-3], 15-32.
- [18] Litster, S.; Mclean, G. PEM Fuel Cell Electrodes. J. Power Source. **2004**, 130, 61.
- [19] Panchenko, A.; Dilger, H.; Moller, E.; Sixt, T.; Roduner, E. Insitu EPR investigation of Polymer Electrolyte Membrane Degradation in Fuel Cell Application. J. Power Sources **2004**, 127, 325-330, doi:10.1016/j.jpowsour.2003.09.047
- [20] Hogarth, W.H.J; da Costa, J.C.D; Lu, G.Q. J. Power Sources. **2005**, 142 223.
- [21] Thompson, S.D.; Jordan, L.R.; Forsyth, M. Platinum electrodeposition for polymer electrolyte membrane fuel cells. Electrochim. Acta, **2001**, 46, 1657-1663.
- [22] Yu, T.L.; Lin, H.; Su1, P.; and Wang, G. Structures of Membrane Electrode Assembly

Catalyst Layers, The Open Fuels & Energy Science Journal, **2012**, Volume 5

- [23] Creager, S. E. Proposal for DOE project, **2006**
- [24] Smitha, B.; Sridhar, S.; Khan, A. A. Solid Polymer Electrolyte Membrane for Fuel Cell. J. Membran. Sci. **2005**, 259, 10-26.
- [25] Moilanen, D. E., Spry, D. B., Fayer, M. D. Water Dynamics and Proton Transfer I Nafion Fuel Cell Membranes. Langmuir **2008**, 24 [8], 3690-3698
- [26] Fuel Cells, Types of Fuel Cells. <http://www.Fuelcells.Org/fuel/fctypes.html>, **2000**.
- [27] Chalkova E.; Fedkin, M. V.; Wesolowski, D. J.; Lvov, S. N. Effect of TiO₂ Surface Properties on Performance of Nafion-Based Composite Membranes in High Temperature and Low Relative Humidity PEM Fuel Cell. J. Electrochem. Soc. **2005**, 152, A1742.
- [28] Mauritz, K.A.; Moore, R.B. State of Understanding Nafion. Chem. Rev. **2004**, 104 4535-4585.
- [29] Hongxiang Teng. Review Overview of the Development of the Fluoropolymer Industry. Appl. Sci. **2012**, 2, 496-512; doi:10.3390/app2020496.
<http://www.mdpi.com/journal/applsci>
- [30] Olah, G. A.; Iyer, P. S.; Prakash, G. K. S. Perfluorinated Resinsulfonic Acid (Nafion- Hw) Catalysis on Synthesis. Synthesis **1986**, 7, 513
- [31] Gould, Elizabeth-Ann. The Photochemistry of “Super” Photoacid N-Methyl- 6-Hydroxyquinolinium and Other Novel Photoacids. Ph.D. Dissertation, Georgia Institute of Technology, Atlanta, GA, **2012**.
- [32] Tsushima, S., Teranishi, K., Hirai, S. Experimental elucidation of proton conducting mechanism in a polymer electrolyte membrane of fuel cell by nuclei labeling MRI. 210 ECS Meeting – Cancun, Mexico, October 29 ~ November 03, **2006**.

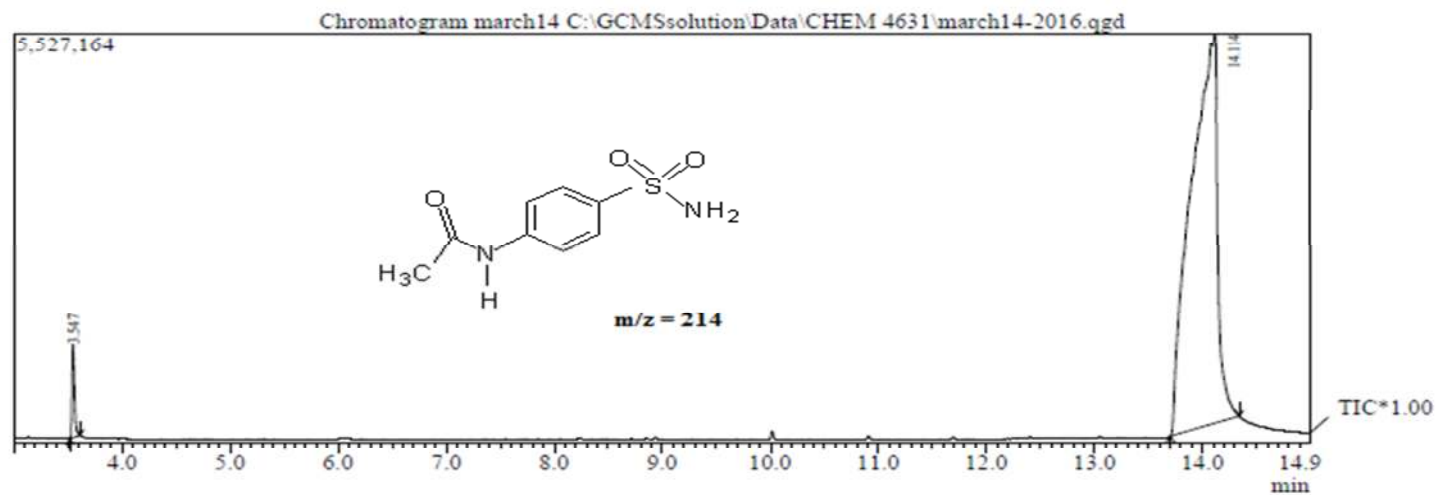
- [33] Nur Hidayati, Binti Othman. Synthesis, Characterization and Optimization of Sulfonated Polyether Ether Ketone Composite Membrane for Direct Methanol Fuel Cell. Ph.D. Dissertation, Universiti Teknologi, Malaysia, **2009**
- [34] Honma, I.; Nakajima, H.; Nishikawa, O.; Sugimoto, T.; Nomura, S. Family of High-Temperature Polymer-Electrolyte Membranes Synthesized From Amphiphilic Nanostructured Macromolecules, J. Electrochem. Soc., **2003**, 150, A616.
- [35] Savadogo, O. Emerging Membranes for Electrochemical Systems. I. Solid Polymer Membranes for Fuel Cell Systems. J. New Mater. Electrochem. Syst. **1998**, 1, 47.
- [36] DuPont. Safe Handling and Use of Perfluorosulfonic Acid Products. **2006**. 1 April 2008
http://www2.dupont.com/Fuel_Cells/en_US/assets/downloads/dfc301.pdf
- [37] DuPont. DuPont Nafion PFSA Membranes, 2006. 1 April **2008**
- [38] Smitha, B., Sridhar, S. and Khan A. A. Proton conducting Composite Membrane from Polysulfone and Heteropolyacid for Fuel Cell Application. Journal of Polymer Science. **2005** Part B, Polymer Physics, 43: 1538.
- [39] Atkins J R, Sides C R, Creager S E, Harris J L, Pennington W T, Thomas B H and DesMarteau DD. J. New Mater. Electrochem. Syst. **2003** 6.
- [40] Arcella, V.; Ghielmi, A.; Polastri, F.; Vaccarone, P. Fluorinated membranes, EP 1589062 A2, **2005**
- [41] Shen Wu, H.; Martin, C. W.; Chen, X. K. Low equivalent weight ionomer, US 7094851 B2, **2006**
- [42] Y.G. Chun, C.S. Kim, D.H. Peck, D.R. Shin, J. Power Sources 71 (**1998**) 174.
- [43] Wilson, M. S.; Gottesfeld, S. Thin-Film Catalyst Layers for Polymer Electrolyte Fuel Cell Electrodes. J. Appl. Electrochem. **1992**, 22, 1.

- [44] Yang, T.F.; Hourng L.W.; Yu, T.L.; Chi, P.H.; Su, A. High performance proton exchange membrane fuel cell electrode assemblies. *J. Power Sources*, **2010**, 195, 7350-7369.
- [45] Lee, D.; Hwang, S. Effect of loading and distributions of Nafion ionomer in the catalyst layer for PEMFCs. *Int. J. Hydrog. Energy* **2008**, 33, 2790–2794.
- [46] Gadallah, F. F.; Elofson, R. M. *J. Org. Chem.* **1969**, 34, 3335-3339.
- [47] Koppel, I. A.; Taft, R. W.; Anivia, F.; Zhu, S. Z.; Hu, L. Q.; Sun, K. S.; DesMarteau, D. D.; Yagupolskii, L. M.; Yagupolskii, Y. L.; Vlasoz, V. M.; Notario, R.; Maria, P. C. The Gas-Phase Acidities of Very Strong Neutral Bronsted Acids. *J. Am. Chem. Soc.* **1994**, 116, 3047
- [48] Zhang, M.; Sonoda, T.; Mishima, M.; Honda, T.; Leito, I.; Koppel, I. A.; Bonrath, W.; and Netscher, T. Gas-Phase Acidities of bis[(perfluoralkyl)]imides. Effects of the perfluoroalkyl group on acidity. *J.Phys.Org Chem.* **2014**, 27 676-679
- [49] Delamar, M.; De'sarmot, G.; Fagebaume, O.; Hitmi, R.; Pinsonc, J.; Save' ant, J.-M. *Carbon* 35 (6) (**1997**) 801–807; Brooksby, P.A.; Downard, A.J. *Langmuir* 20 (12) **2004** 5038 5045.
- [50] Foropoulos, J. Jr.; DesMarteau, D. D., *J. Am. Chem. Soc.*, 104, **1982**, 4260 and Foropoulos, J. Jr.; DesMarteau, D. D., *Inorg. Chem.*, 23, **1984**, 3720
- [51] Allongue, P.; Delamar, M.; Desbat, B.; Fagebaume, O.; Hitmi, R.; Pinson, J.; Save'ant, J.-M. *J. Am Chem. Soc.* **1997**, 119, 201-207.
- [52] Harzdorf, C.; Meussdoerffer, J.; Niederprum, H.; Wechsberg, M., *Justus Liebigs Ann.*
- [53] Ortiz, B.; Saby, C.; Champagne, G. Y.; Be'langer, D. J. *Electroanal. Chem.* **1998**, 455, 75-81.
- [54] Saby, C.; Ortiz, B.; Champagne, G. Y.; Be'langer, D. *Langmuir* **1997**, 13, 6805-6813.
- [55] Delamar, M.; Hitmi, R.; Pinson, J.; Save'ant, J. M. *J. Am. Chem. Soc.* **1992**, 114, 5883-

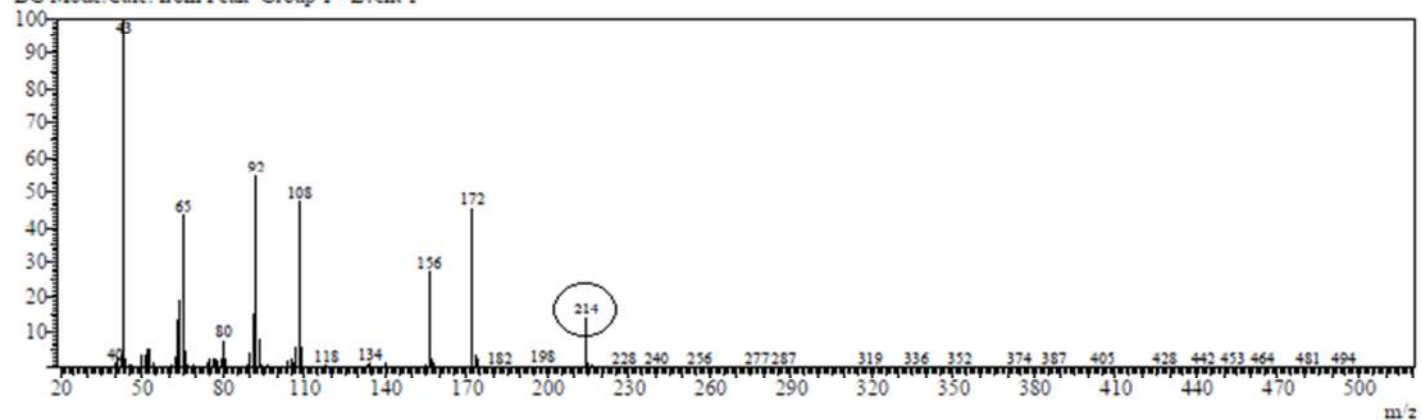
- [56] Hampden-Smith, M. J.; Atanassova, P.; Napolitano, P.; Bhatia, Rice, G.I.; Caruso, J.; Brewster, J.; Gurau, B. Modified Carbon Products, Their Use in Fluid/Gas Diffusion Layers and Similar Devices and Methods Relating to the Same WO2005/091416, **2005**
- [57] Creager, S.E.; Liu, B.; Mei, H. and DesMarteau, D. Electrochemical grafting of an arylfluorosulfonimide electrolyte onto glassy carbon. *Langmuir*, **2006**, 22(25), 10747-10753.
- [58] Mei, H.; D'Andrea, D.; Nguyen, T., Nworie, C. Synthesis of the Diazonium (perfluoroalkyl)benzenesulfonimide Monomer from Nafion Monomer for Proton Exchange Membrane. *Journal of Power Source*. **2014**, 248, 1177-1180
- [59] Cohn, E. J.; Edsall, J. T. *Proteins, Amino Acids and Peptides as Dipolar Ions*, Rheinhold,
- [60] Mei, H.; D'Andrea, D.; Nguyen, T., Nworie, C. Synthesis of the Diazonium (perfluoroalkyl) benzenesulfonimide Monomer from Nafion Monomer for Proton Exchange Membrane. *Journal of Power Source*. **2014**, 248, 1177-1180
- [61] Nworie, C. Synthesis of a 4-(Trifluoromethyl)-2-Diazonium Perfluoroalkyl Benzenesulfonimide (PFSI) Zwitterionic Monomer for Proton Exchange Membrane Fuel Cell. MS. Thesis, East Tennessee State University, Johnson City, TN, **2014**.
- [62] Pfeiffer, Z.: *Physik. Chem*; 48, 40 (**1904**)
- [63] Waldemer Adam and Josefina Arce, *J organic chem*. Vol. 37 No. 3, **1972**
- [64] Biilman, I. E.: *Rec, Trav. Chim*; 36, 313 (**1917**), 2.R. T. Dillon.: *J. Am. Chem. Soc*; 54, 952 (**1932**), 3. W. M. Schubert et al.: *ibid*; 77, 36 (**1955**).
- [65] Van Duin, C. F.: *Rec, Trav. Chim*; 43, 341 (**1924**); 45, 345 (**1926**); 47, 715 (**1928**)
- [66] Abban, G. Methodology Study of N-deacetylation of 4-acetamido

- perfluoroalkylbenzenesulfonimide. MS. Thesis, East Tennessee State University, Johnson City, TN, **2015**.
- [67] Karty J.; Organic Chemistry, Principles and Mechanism, 1st ed., W. W. Norton and Company, New York –London, **2014**, pp 1011-1027
- [68] Sir Derek Barton, F. R. S.; Davidollis, W. F. R. S., Comprehensive Organic Chemistry, **1979**.
- [69] Nuchter, M.; Ondruschka, B.; Jungnickel, A.; Muller, U. Organic processes initiated by nonclassical energy sources. J. Phys. Org. Chem. **2000**, 13, 579-586
- [70] Luche, J. L.; Bianc, C. Synthetic Organo Sonochemistry; Plenum Press: New York, **1998**.
- [71] Pasha, M. A.; Jayashankara, V. P. Reduction of aryl nitro compounds to azoarenes and/or arylamines by Al/NaOH in methanol under ultrasonic conditions. Ultrason. Sonochem. **2005**, 12, 433-435
- [72] Kumar, P. S.; Lokanatha Rai, K. M. Chemical Papers 66 (8) 772–778 (**2012**)
- [73] Patai, S. The Chemistry of Diazonium and Diazo Groups (II), John Wiley & Sons, Chichester, New York, Brisbane, Toronto, An Interscience Publication, **1978**, 647
- [74] Shaw, R. The Chemistry of Diazonium and Diazo Groups, Patai, S., Eds.; John Wiley & Sons: New York; **1978**; pp 199-164.
- [75] Toreki, R. The Glassware Gallery: Schlenk Lines and Vacuum Lines. <http://www.ilpi.com/inorganic/glassware/vacline.html> (accessed Mar 15, 2016).

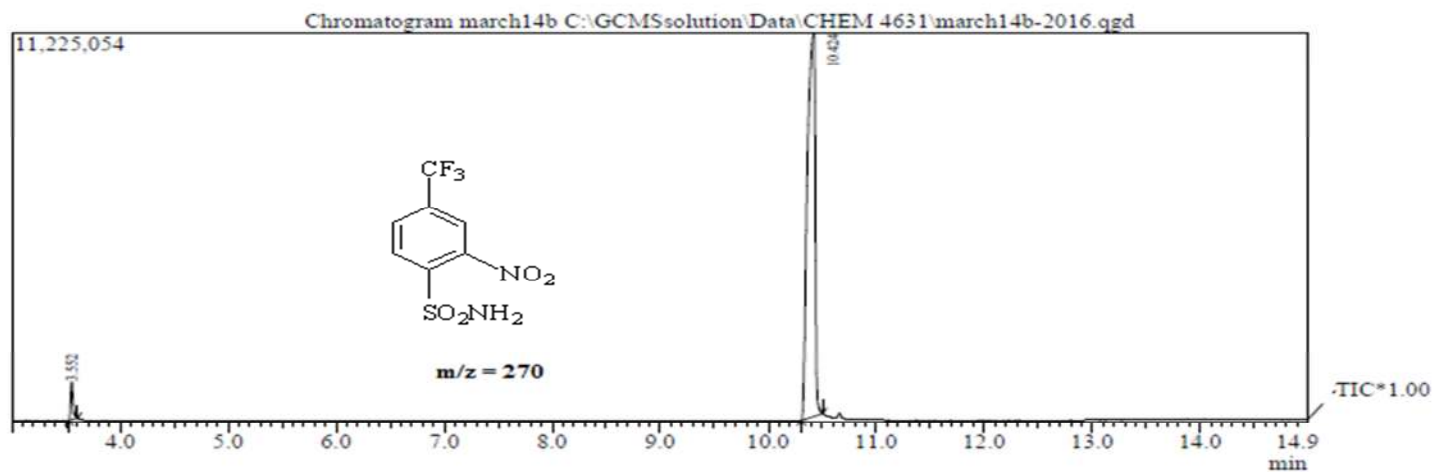
APPENDICES
APPENDIX A1: GC-MS Chromatogram of Compound 2a



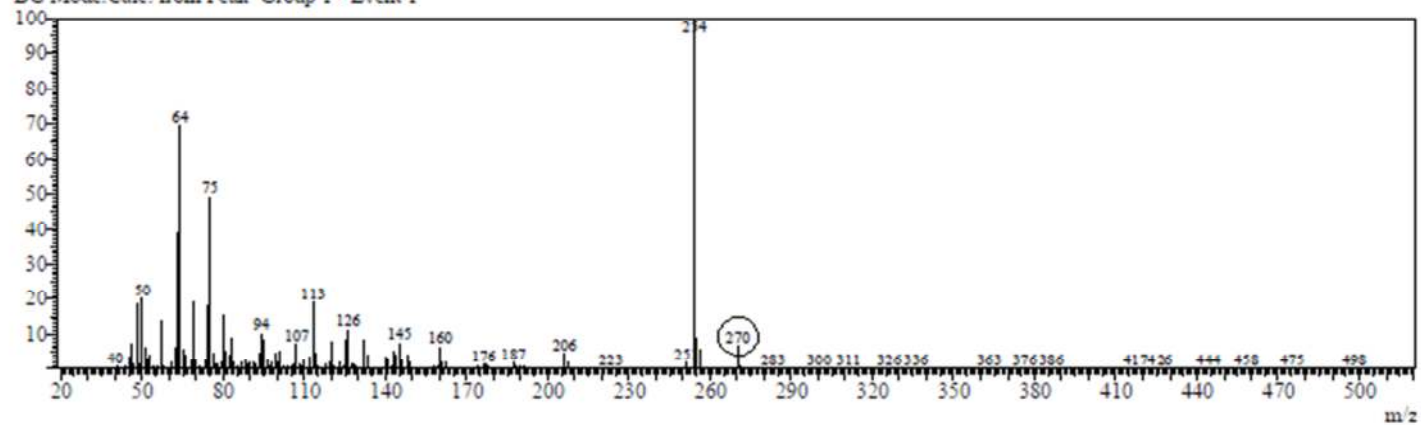
Line#:2 R.Time:14.1(Scan#:1589)
MassPeaks:263
RawMode:Averaged 14.1-14.1(1588-1590) BasePeak:43(1051061)
BG Mode:Calc. from Peak Group 1 - Event 1



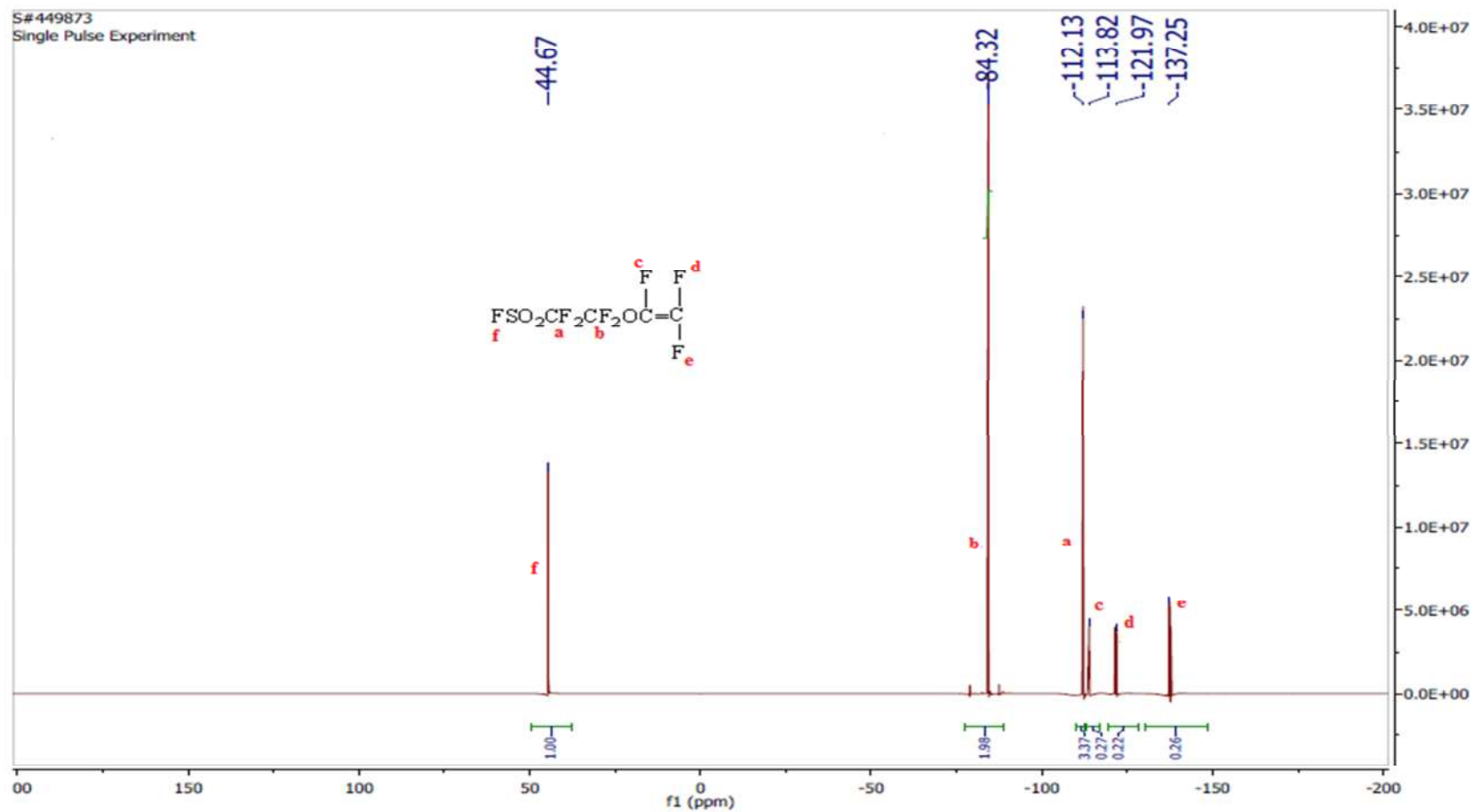
APPENDIX A2: GC-MS Chromatogram of Compound 2b



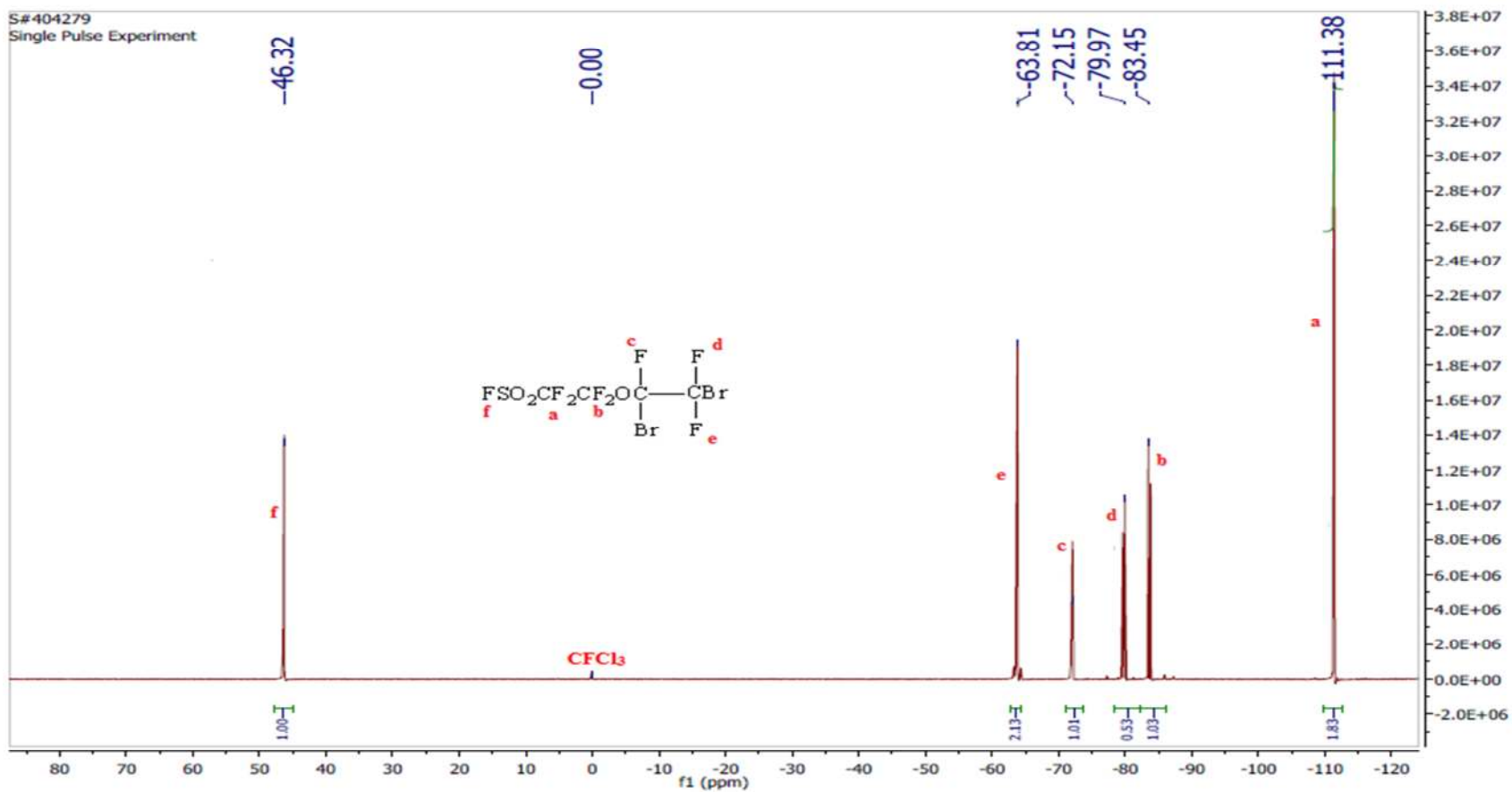
Line#:2 R.Time:10.4(Scan#:1062)
MassPeaks:324
RawMode:Averaged 10.4-10.4(1061-1063) BasePeak:254(1535186)
BG Mode:Calc. from Peak Group 1 - Event 1



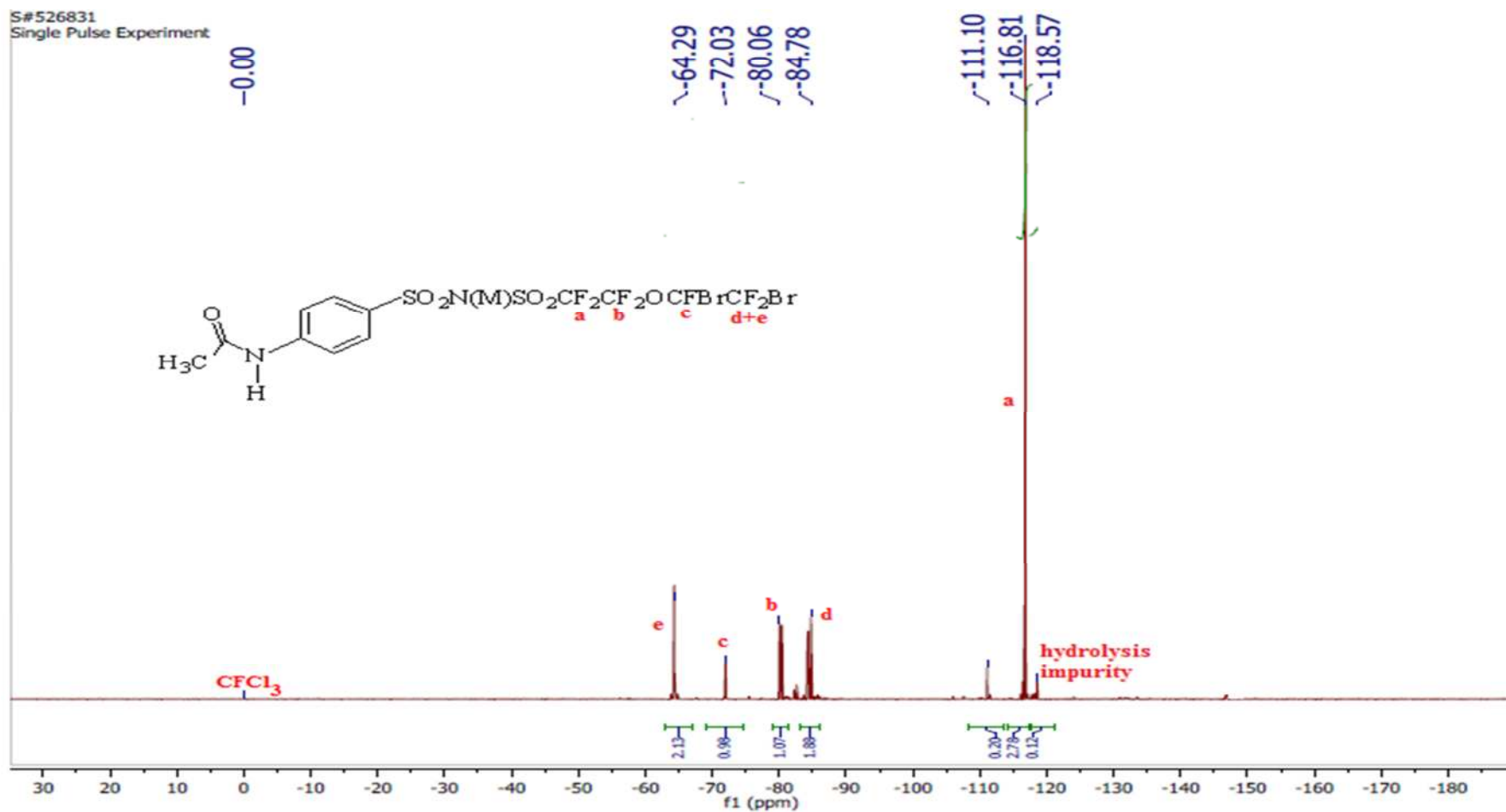
APPENDIX B1: ^{19}F NMR spectrum of compound **3**, 400MHz, CD_3CN



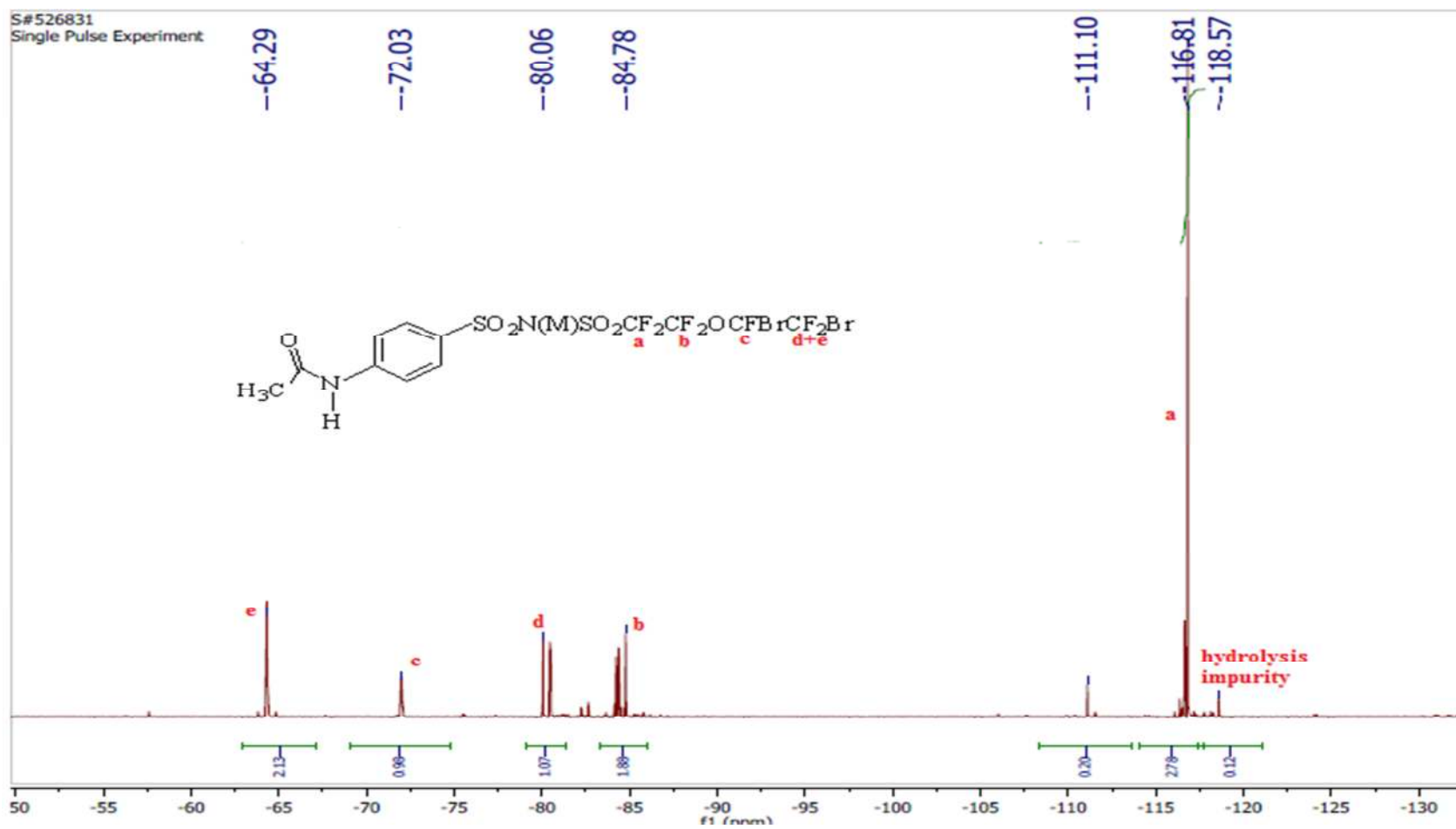
APPENDIX B2: ^{19}F NMR spectrum of compound 4, 400MHz, CD_3CN



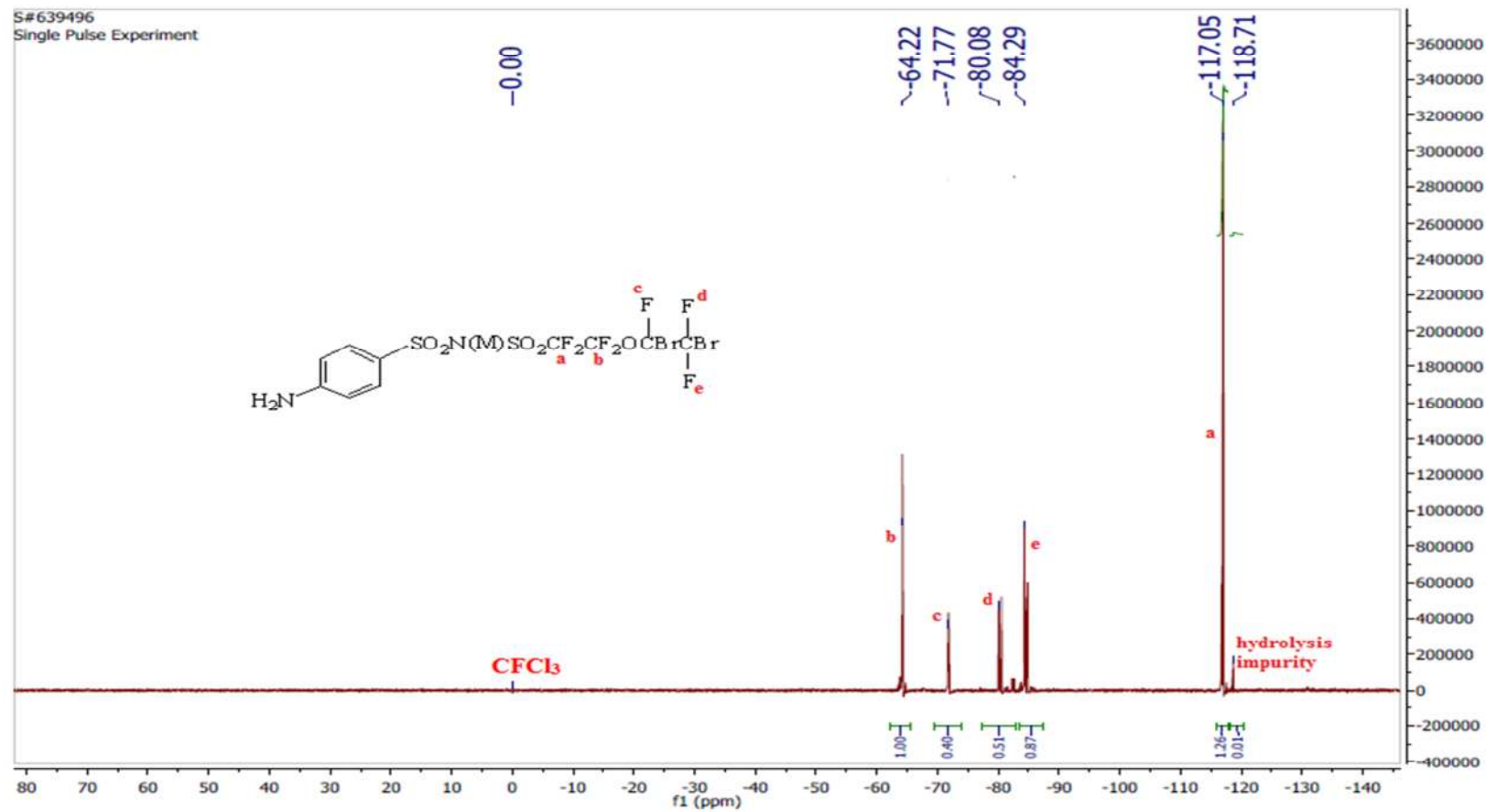
APPENDIX B3: ^{19}F NMR spectrum of compound **5a**, 400MHz, Acetone- d_6



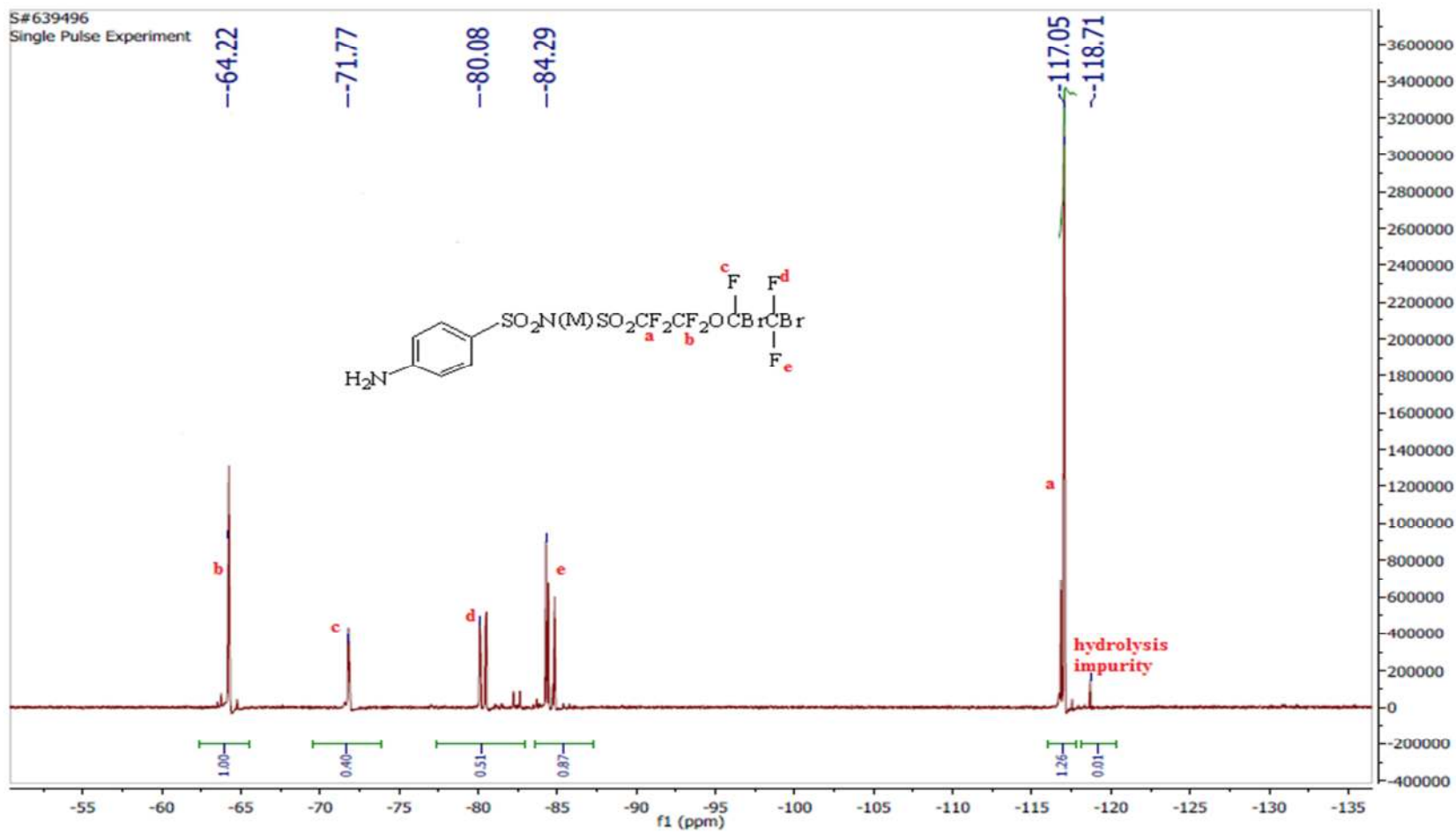
APPENDIX B4: Expanded ^{19}F NMR spectrum of compound **5a**, 400MHz, Acetone- d_6



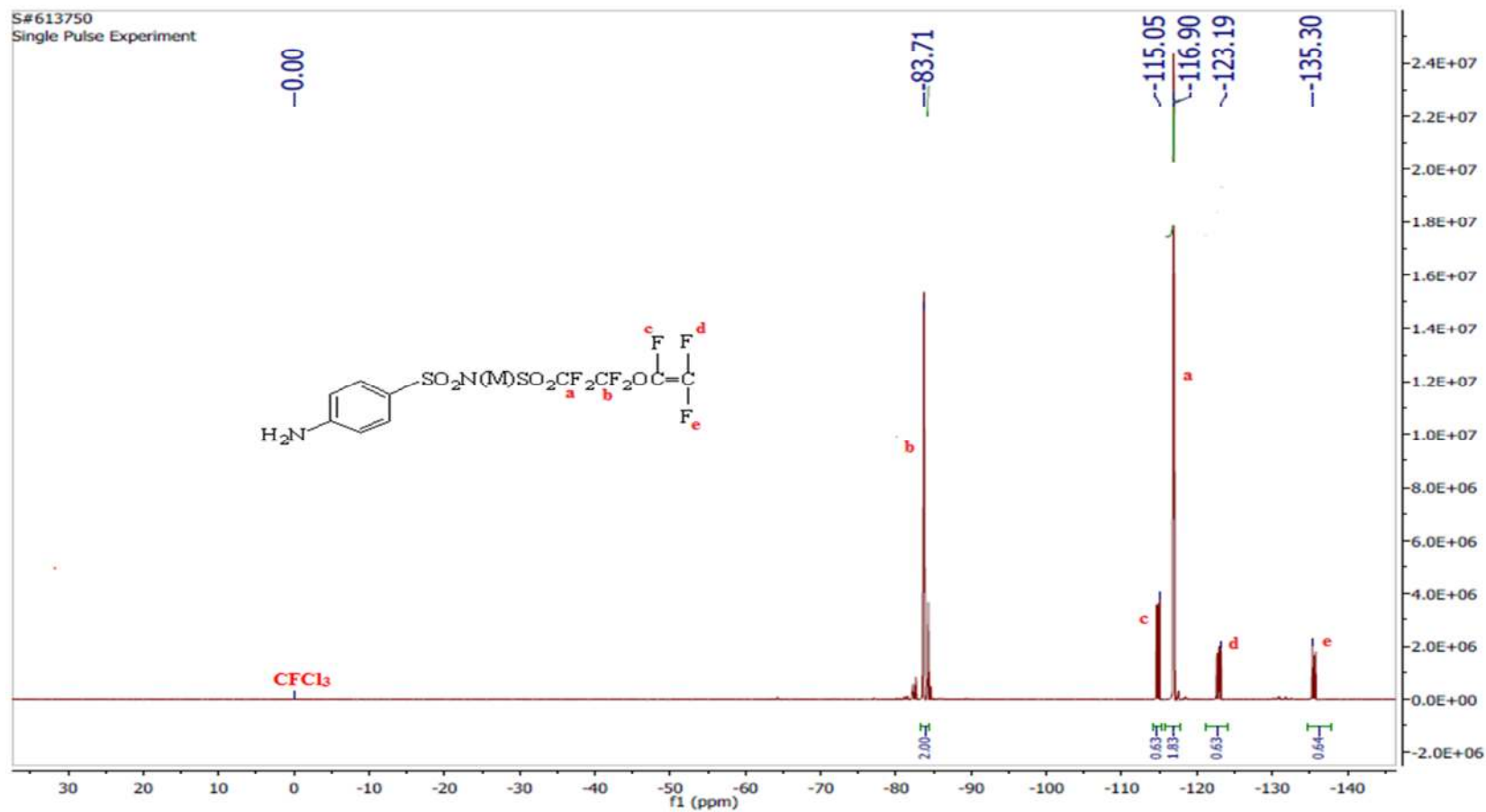
APPENDIX B5: ^{19}F NMR spectrum of compound **6a**, 400MHz, Acetone- d_6



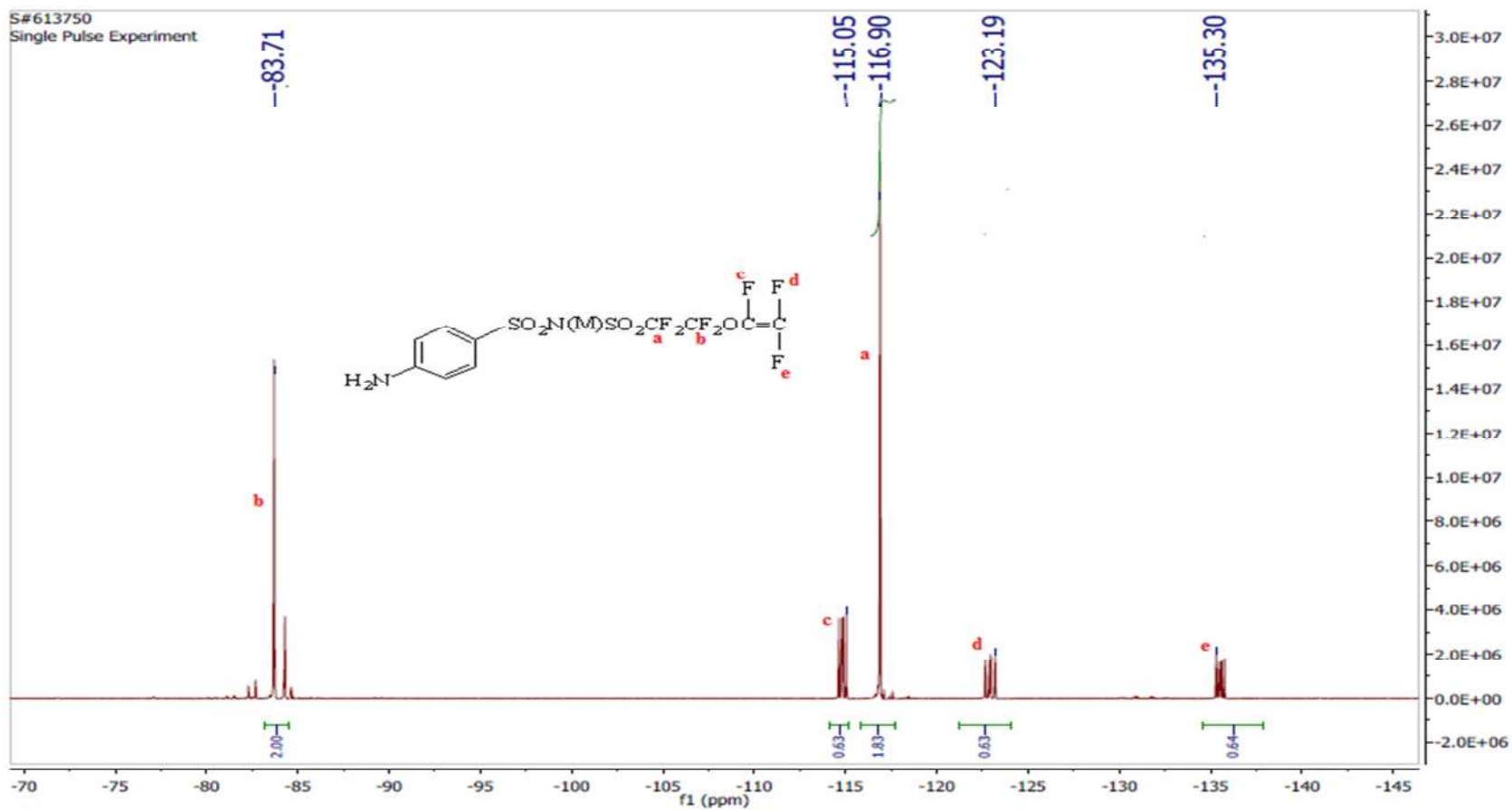
APPENDIX B6: Expanded ^{19}F NMR spectrum of compound **6a**, 400MHz, Acetone- d_6



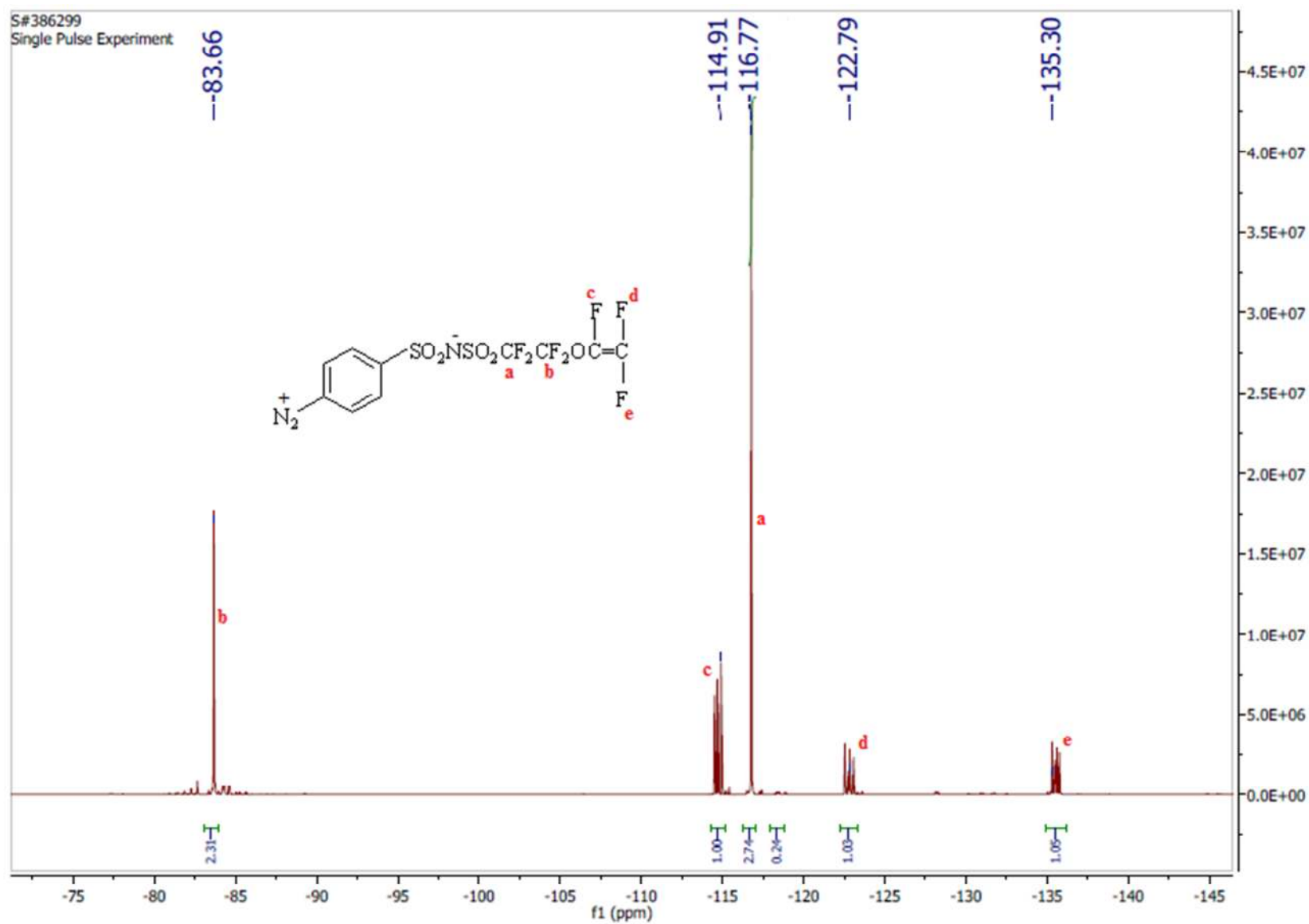
APPENDIX B7: ^{19}F NMR spectrum of compound **7a**, 400MHz, Acetone- d_6



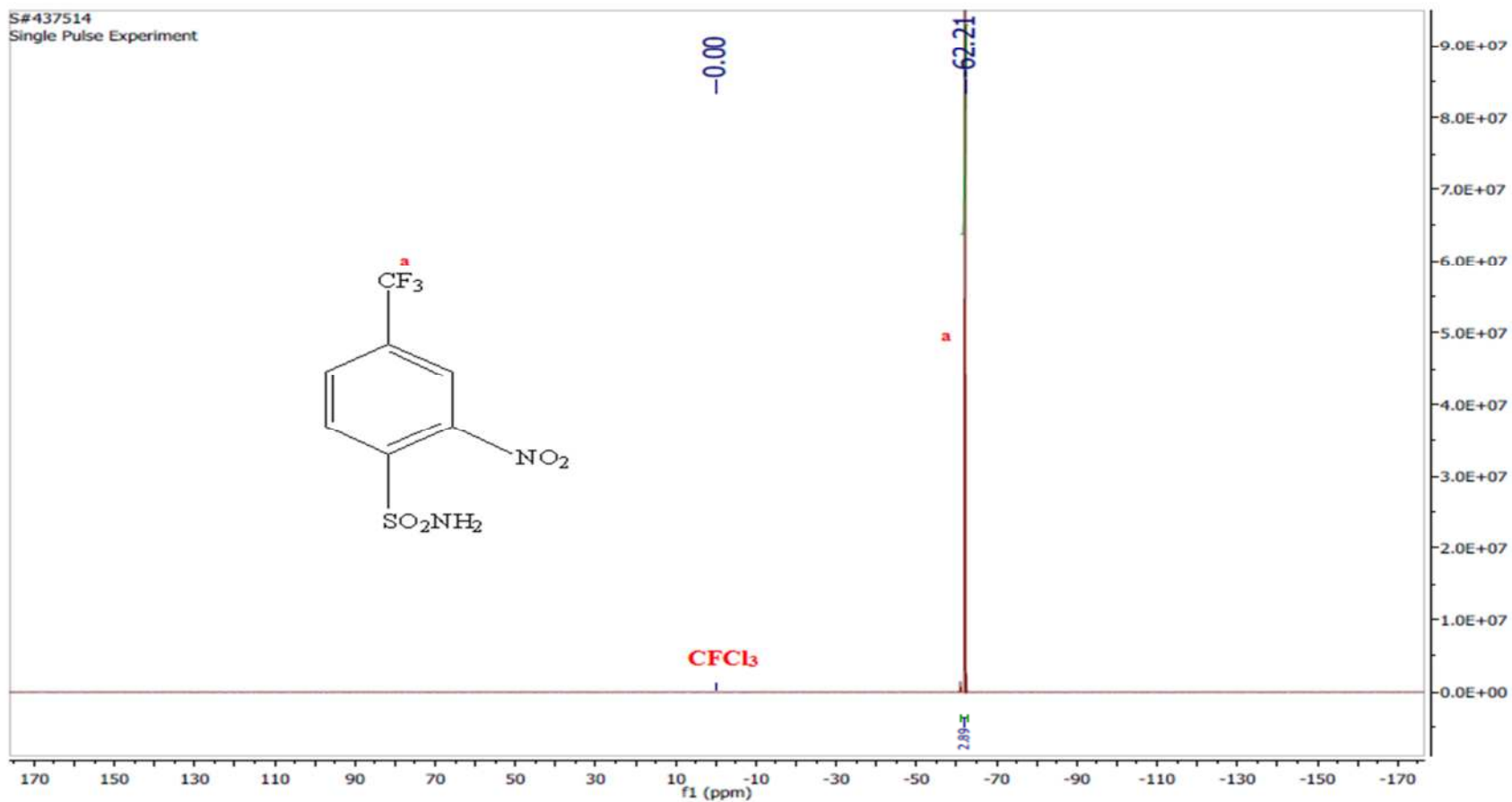
APPENDIX B8: Expanded ^{19}F NMR spectrum of compound **7a**, 400MHz, Acetone- d_6



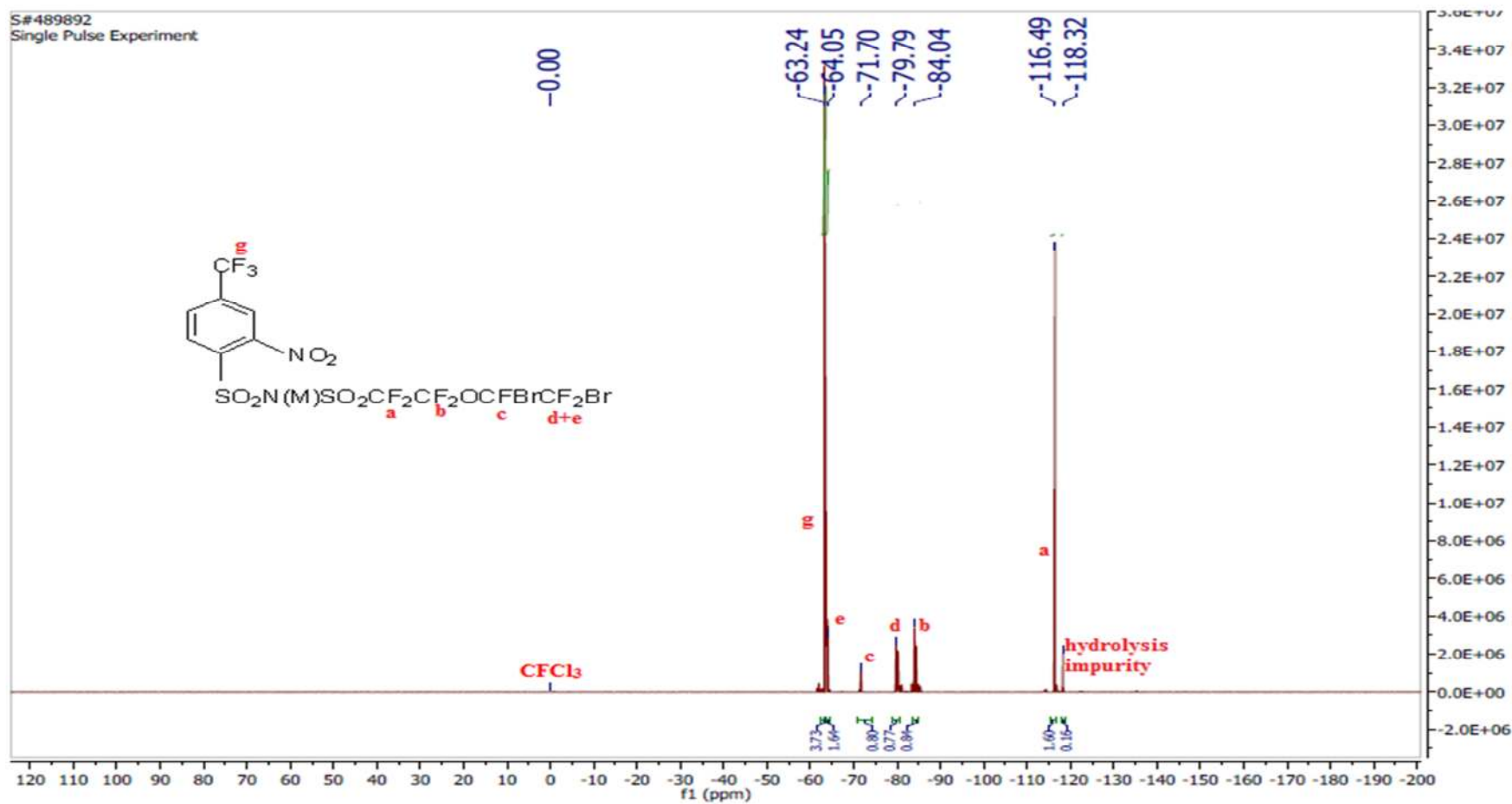
APPENDIX B10: Expanded ^{19}F NMR spectrum of compound **8a**, 400MHz, CD_3CN



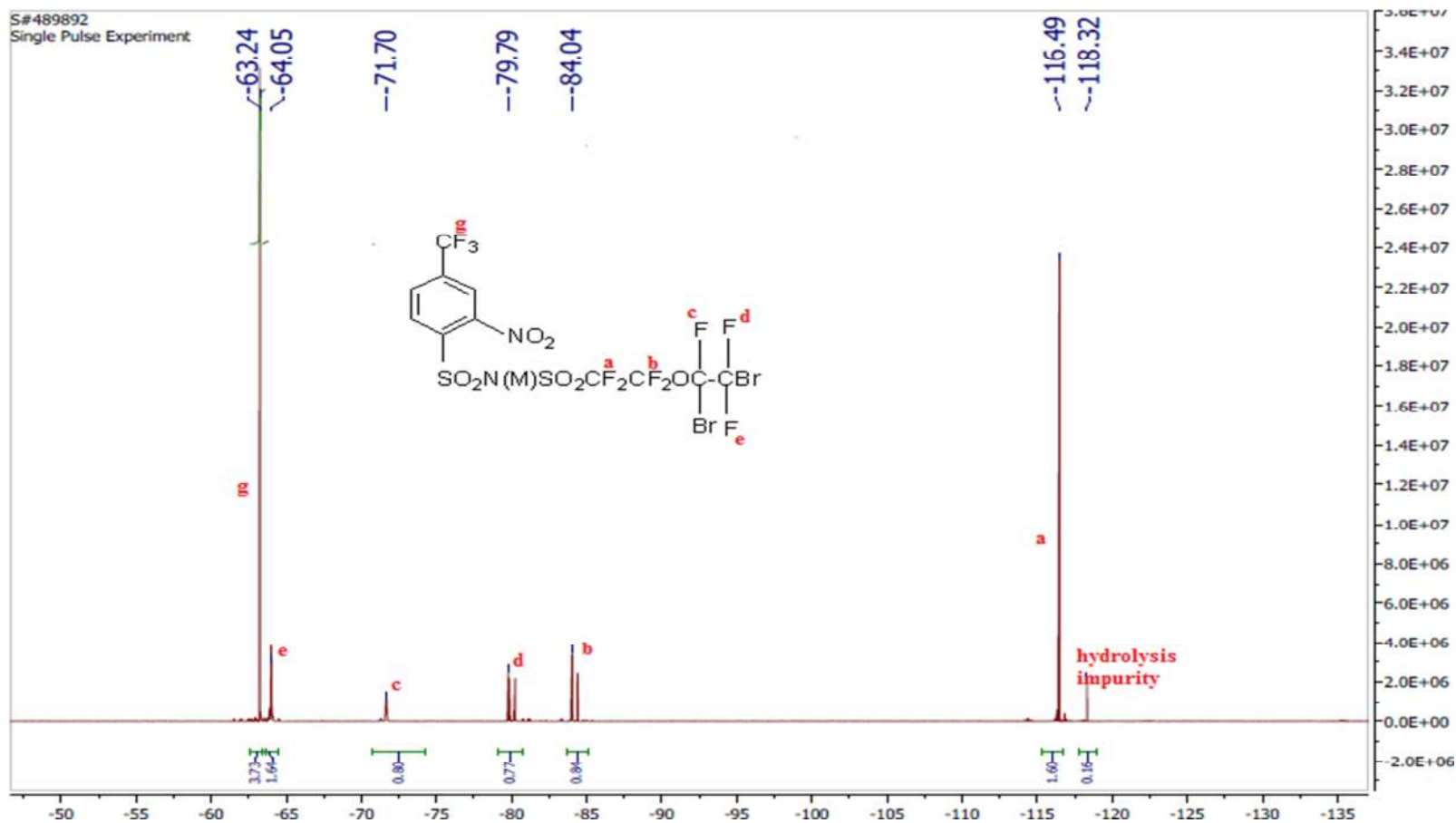
APPENDIX C1: ^{19}F NMR spectrum of compound **2b**, 400MHz, Acetone- d_6



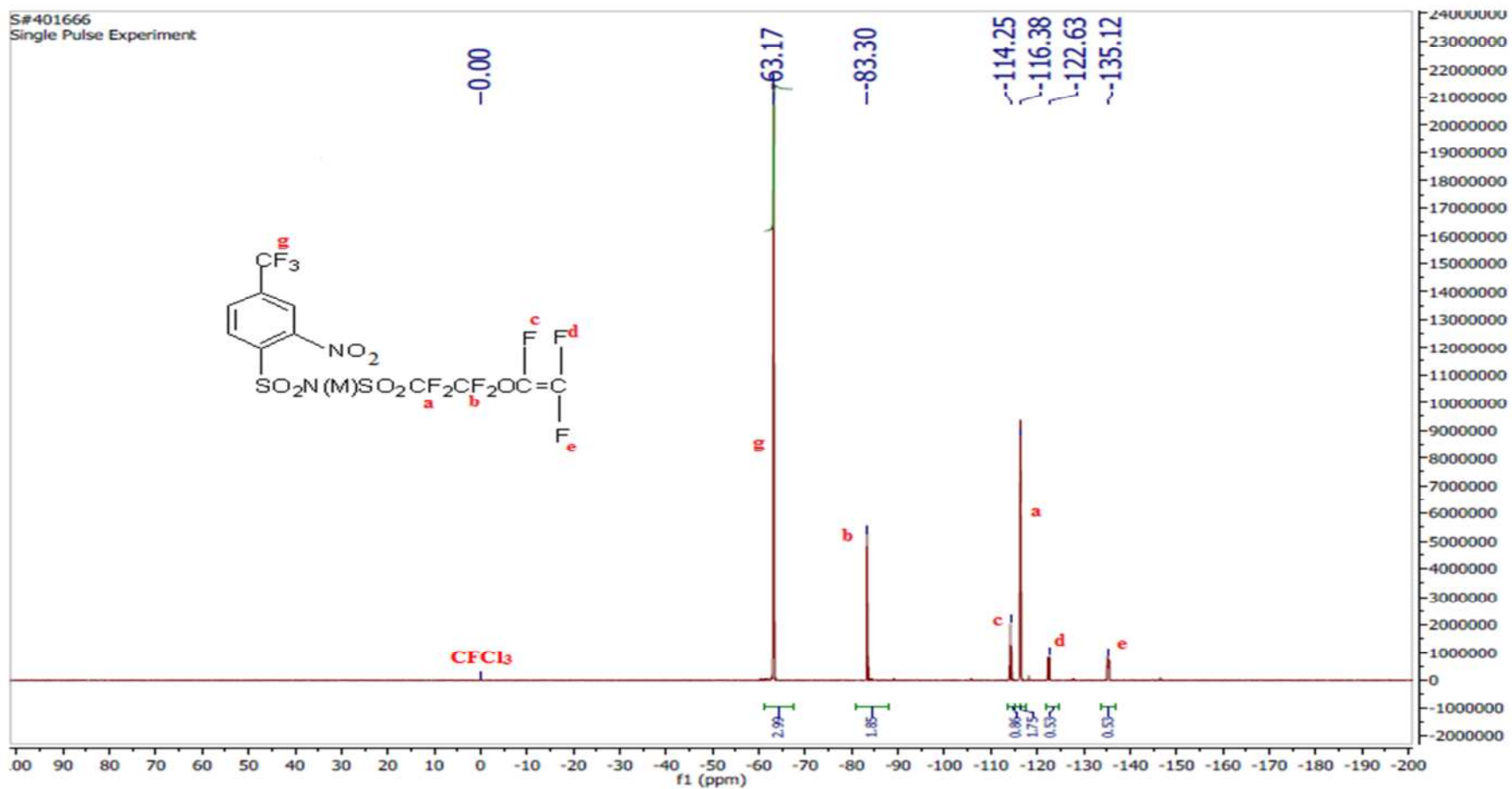
APPENDIX C2: ^{19}F NMR spectrum of compound **5b**, 400MHz, Acetone- d_6



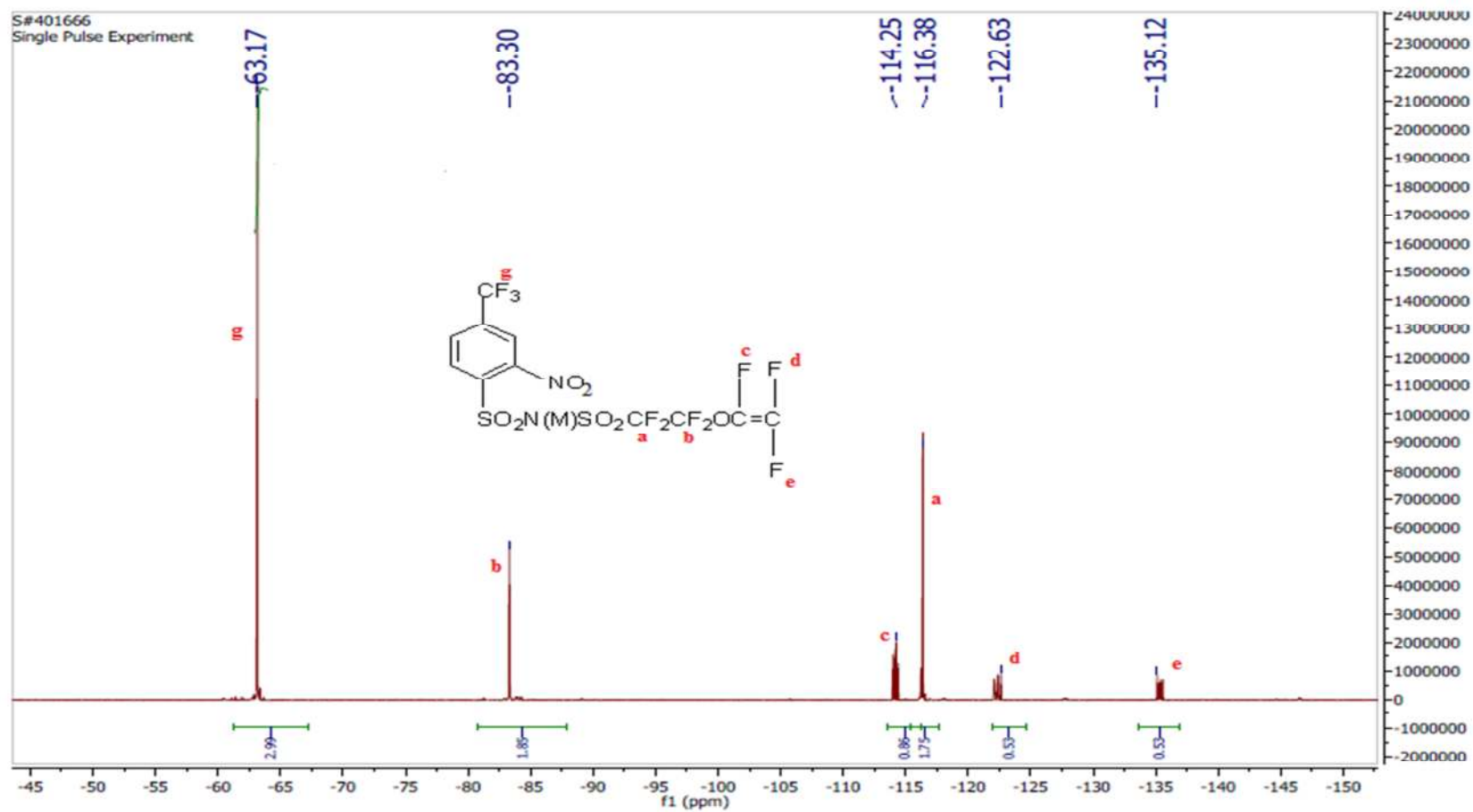
APPENDIX C3: Expanded ^{19}F NMR spectrum of compound **5b**, 400MHz, Acetone- d_6



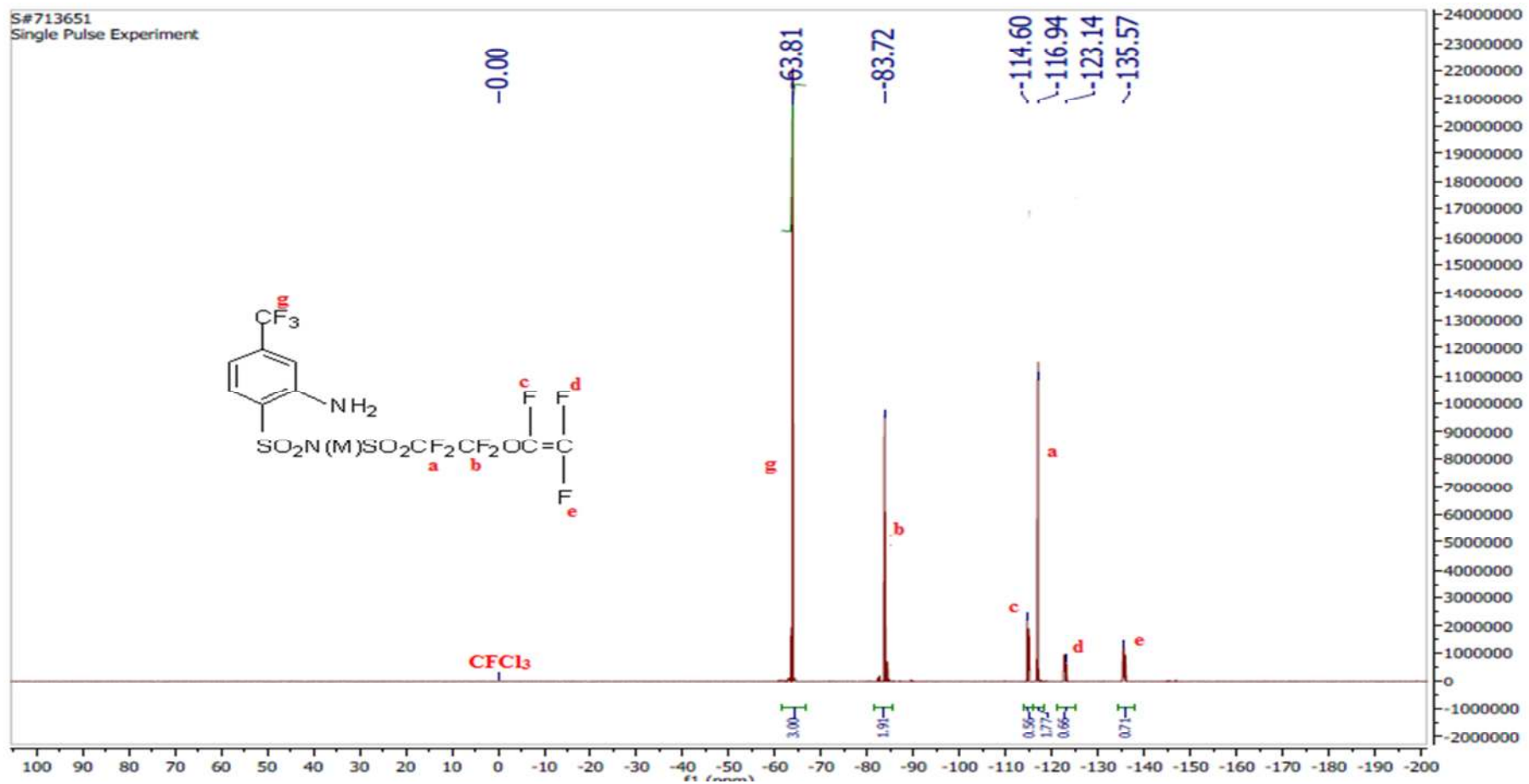
APPENDIX C4: ^{19}F NMR spectrum of compound **6b**, 400MHz, Acetone- d_6



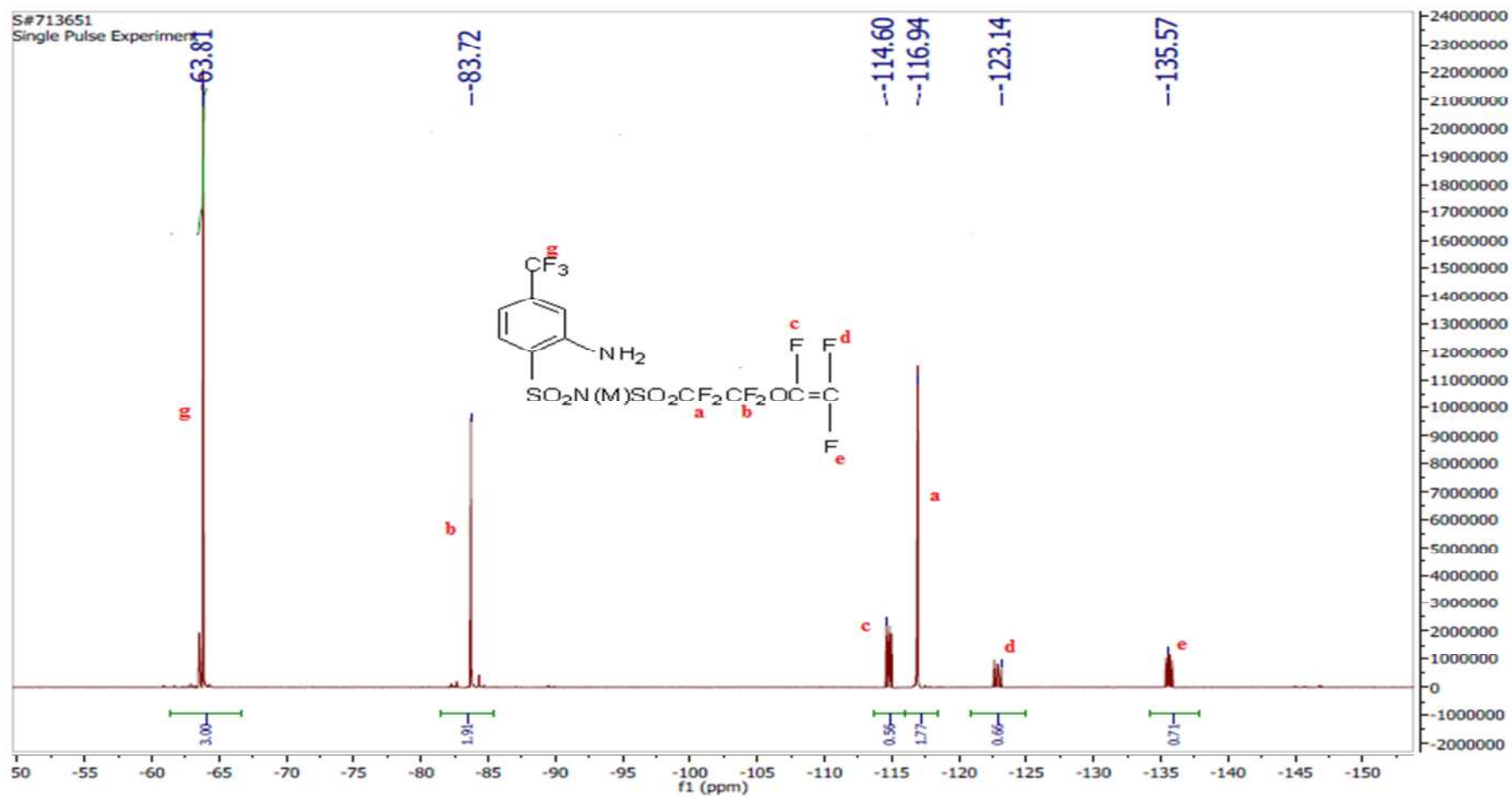
APPENDIX C5: Expanded ^{19}F NMR spectrum of compound **6b**, 400MHz, Acetone- d_6



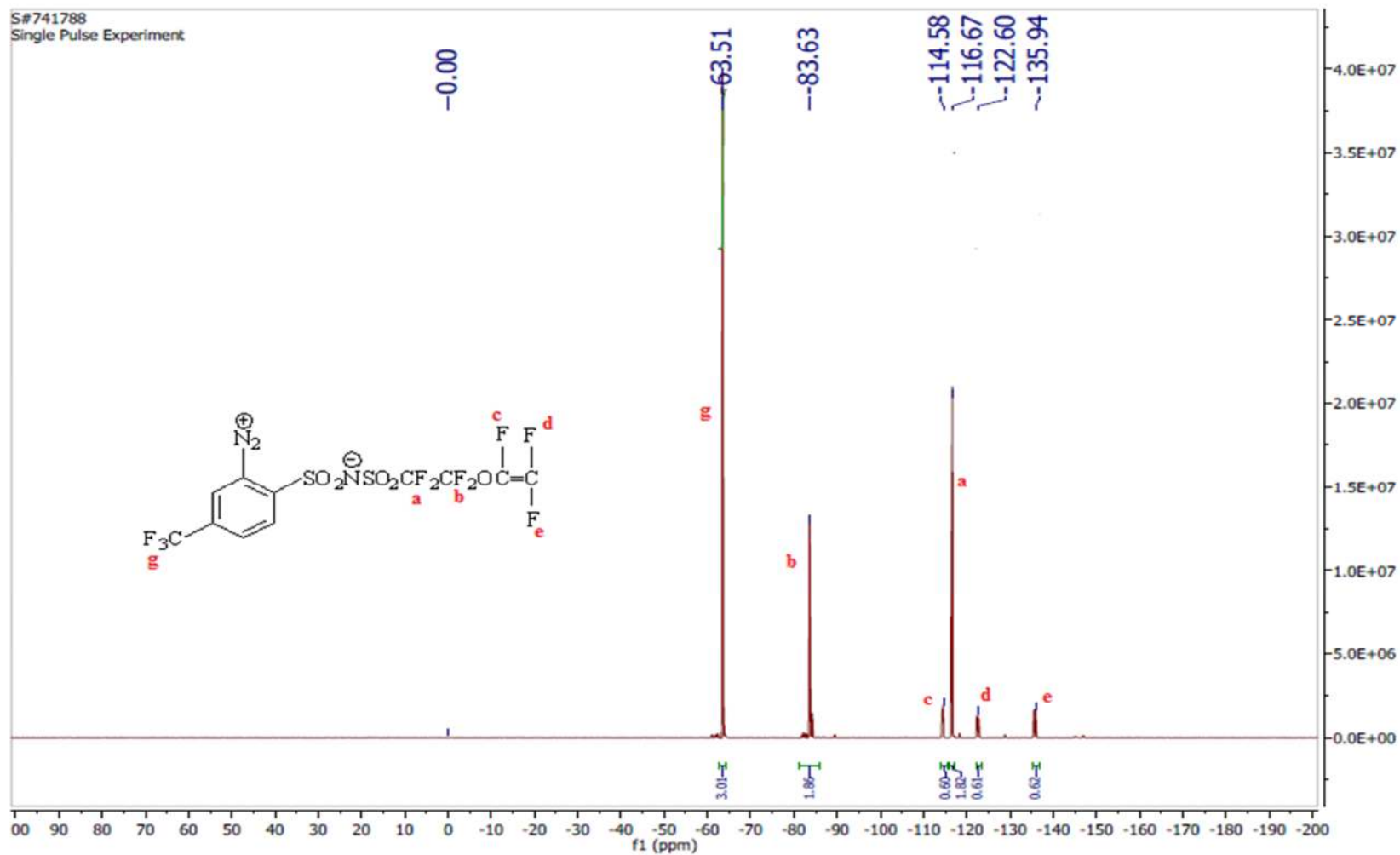
APPENDIX C6: ^{19}F NMR spectrum of compound **7b**, 400MHz, Acetone- d_6



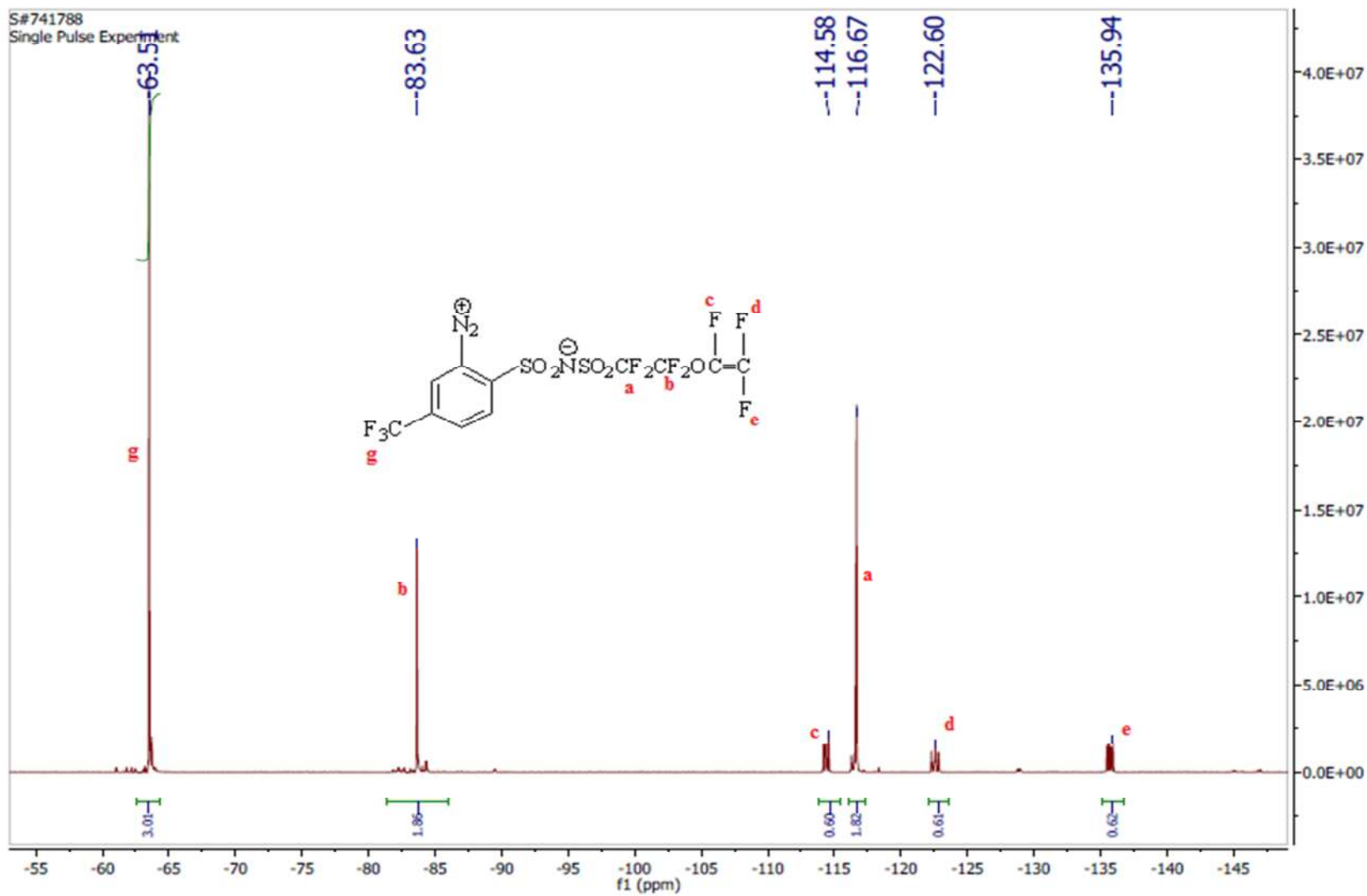
APPENDIX C7: Expanded ^{19}F NMR spectrum of compound **7b**, 400MHz, Acetone- d_6



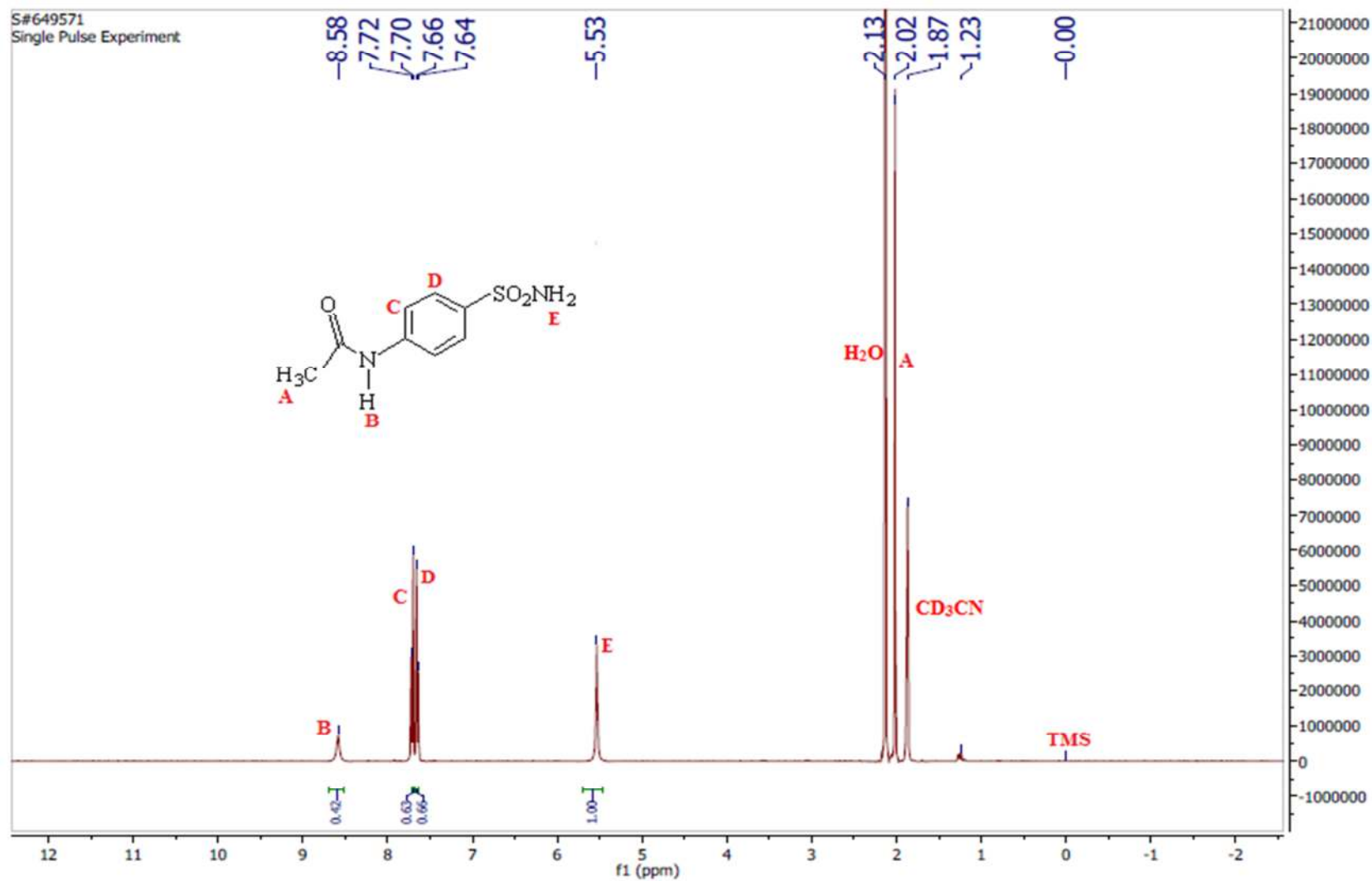
APPENDIX C8: ^{19}F NMR spectrum of compound **8b**, 400MHz, CD_3CN



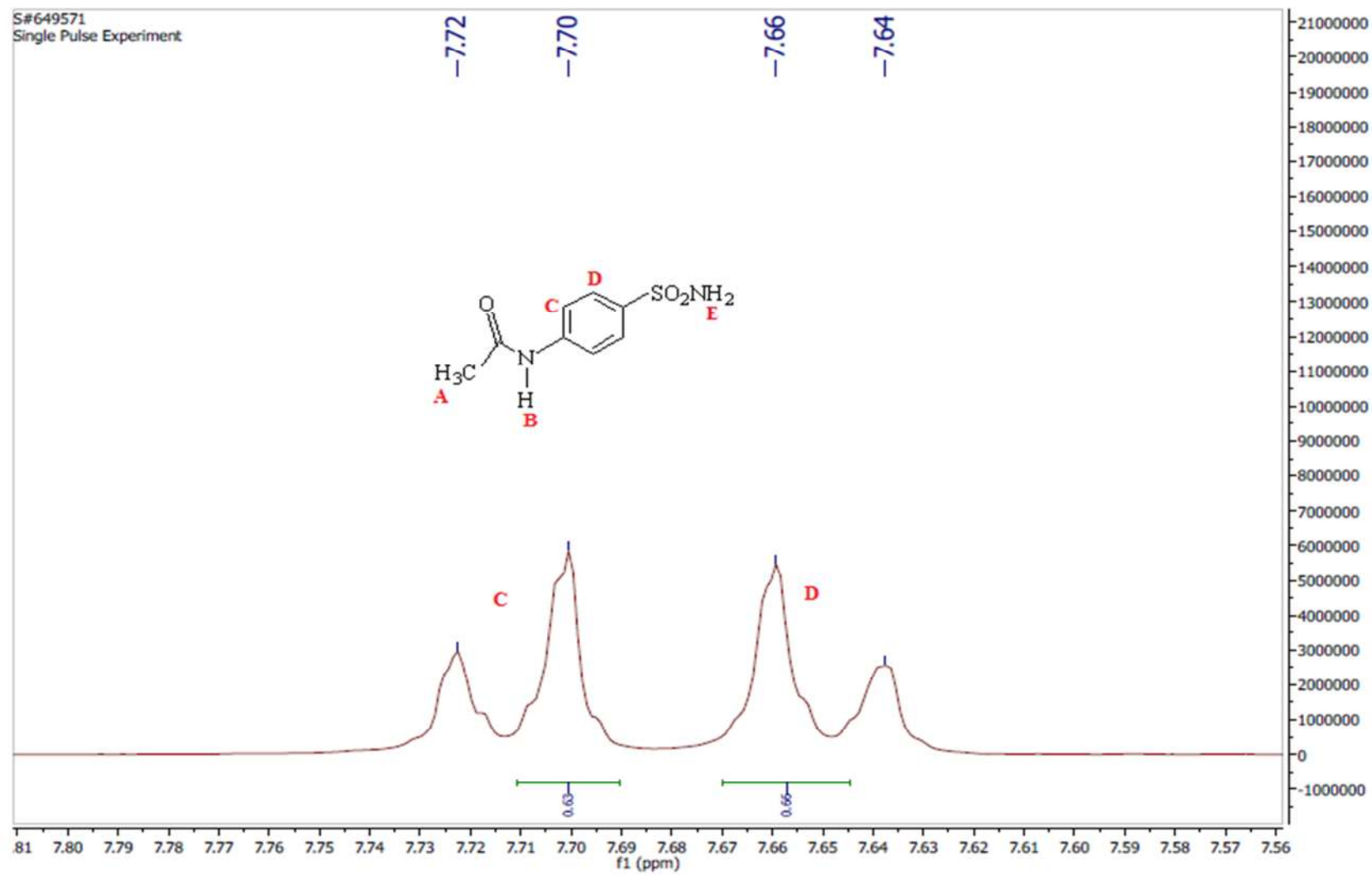
APPENDIX C9: Expanded ^{19}F NMR spectrum of compound **8b**, 400MHz, CD_3CN



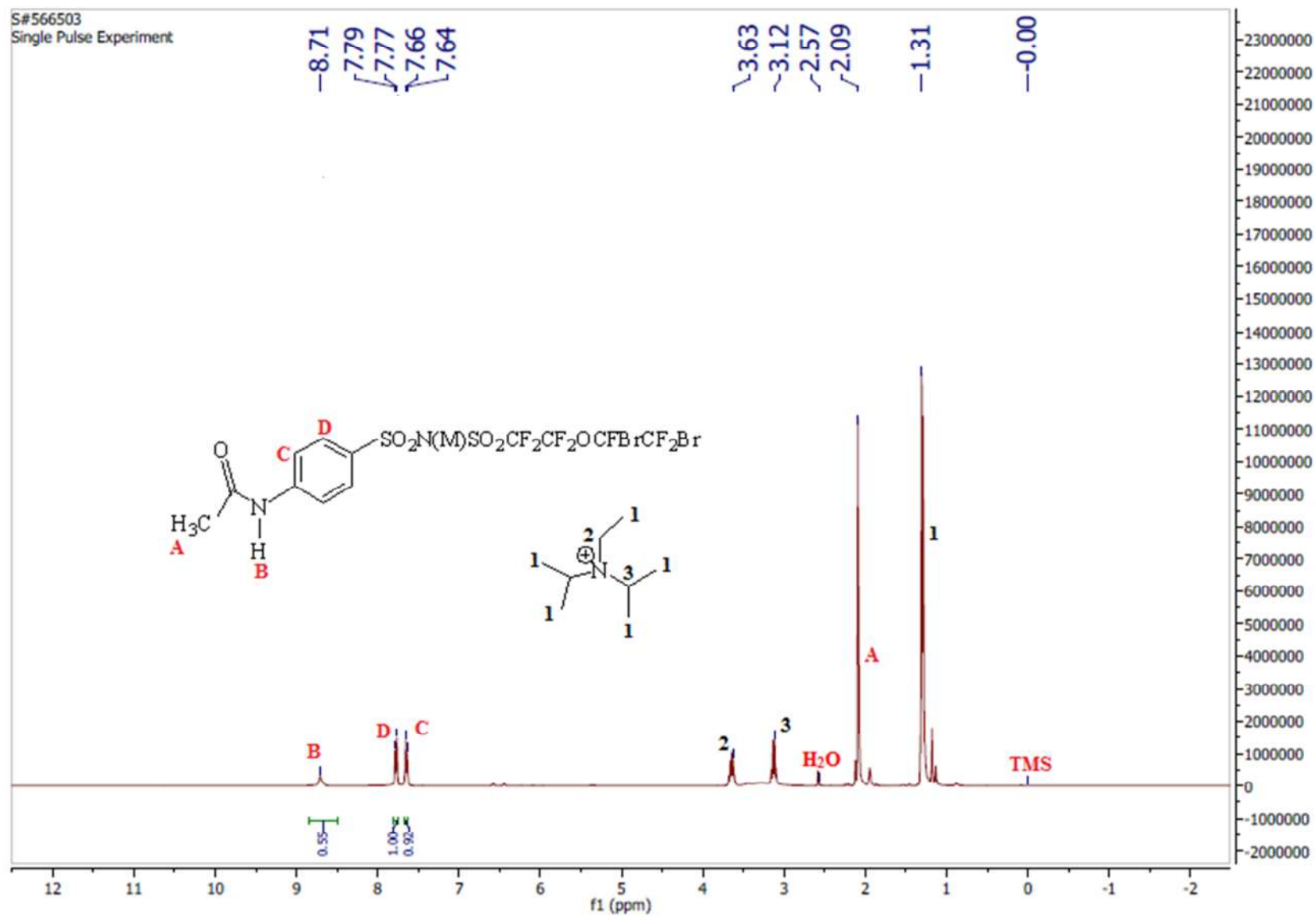
APPENDIX D1: ^1H NMR spectrum of compound **2a**, 400MHz, CD_3CN



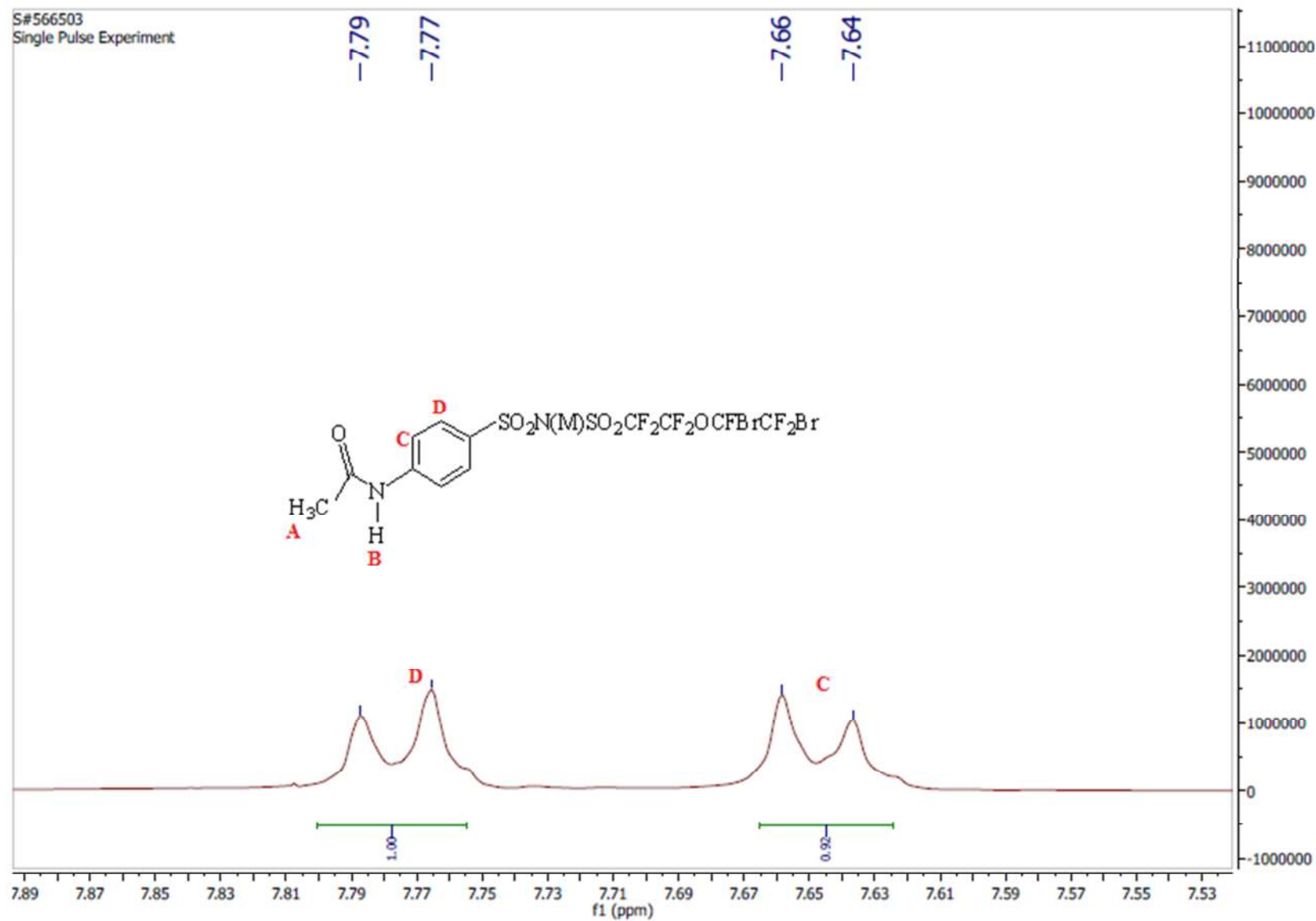
APPENDIX D2: Expanded ^1H NMR spectrum of compound **2a**, 400MHz, CD_3CN



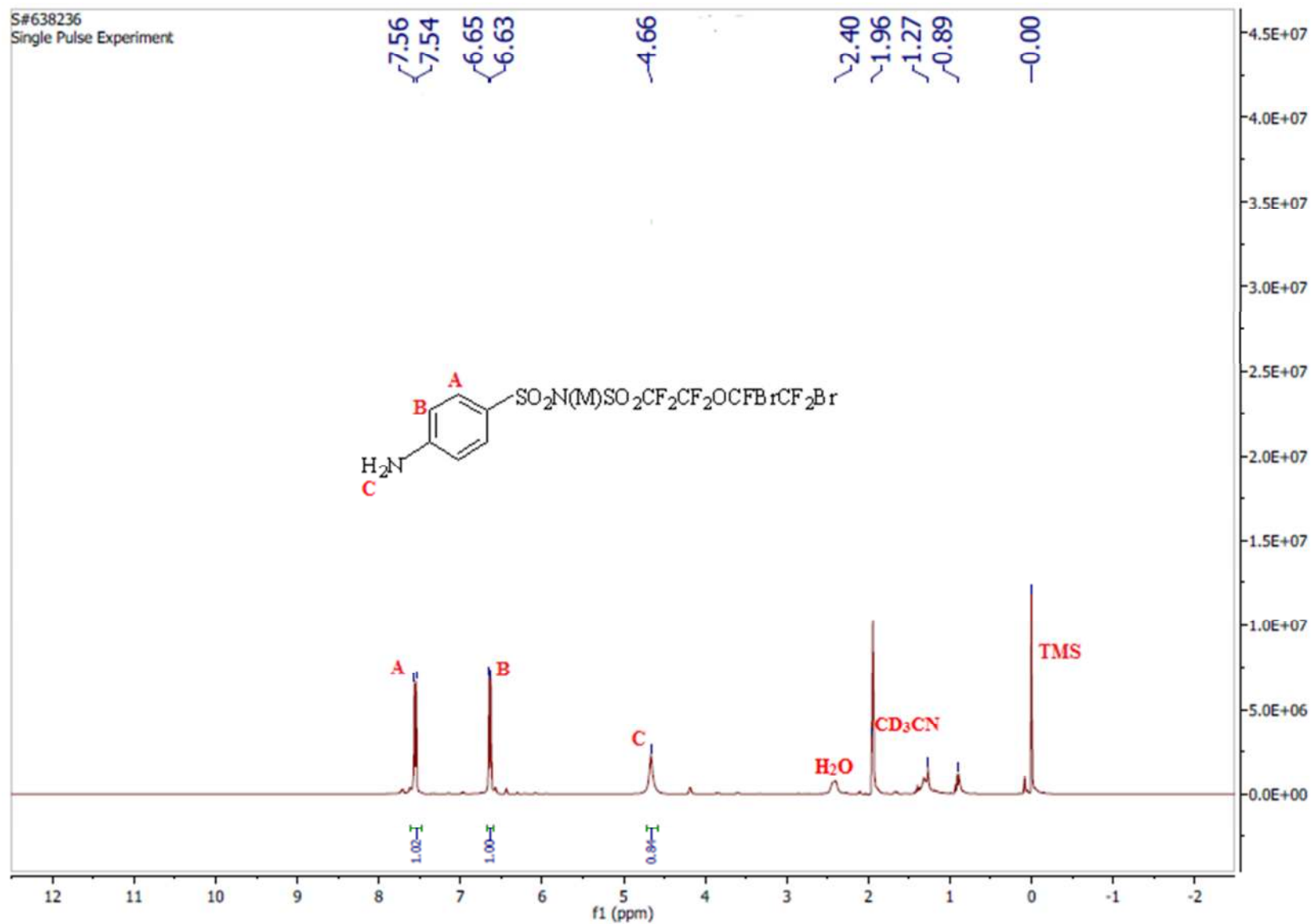
APPENDIX D3: ¹HNMR spectrum of compound **5a**, 400MHz, Acetone, d₆



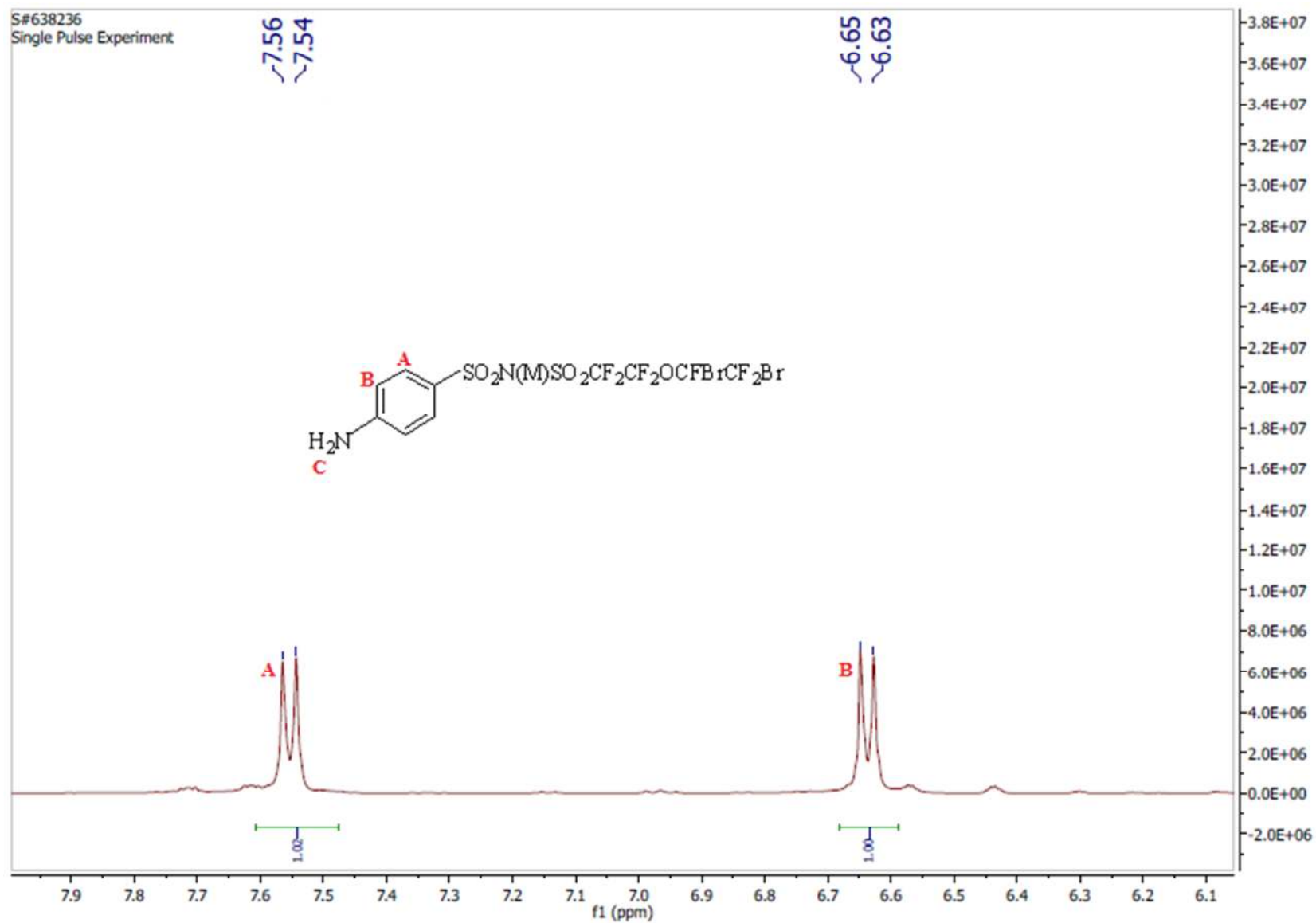
APPENDIX D4: Expanded ^1H NMR spectrum of compound **5a**, 400MHz, Acetone, d_6



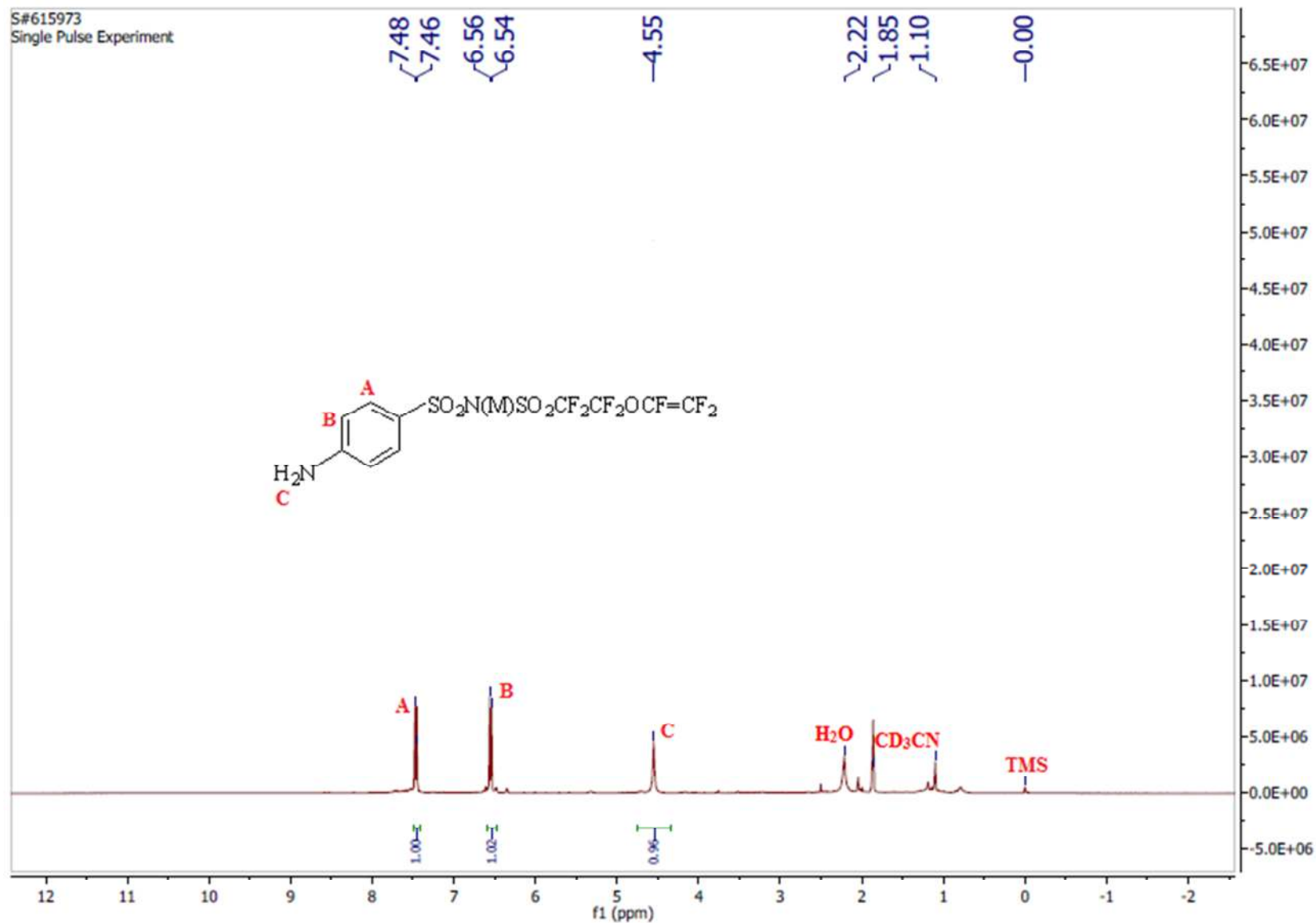
APPENDIX D5: ¹H NMR spectrum of compound **6a**, 400MHz, CD₃CN



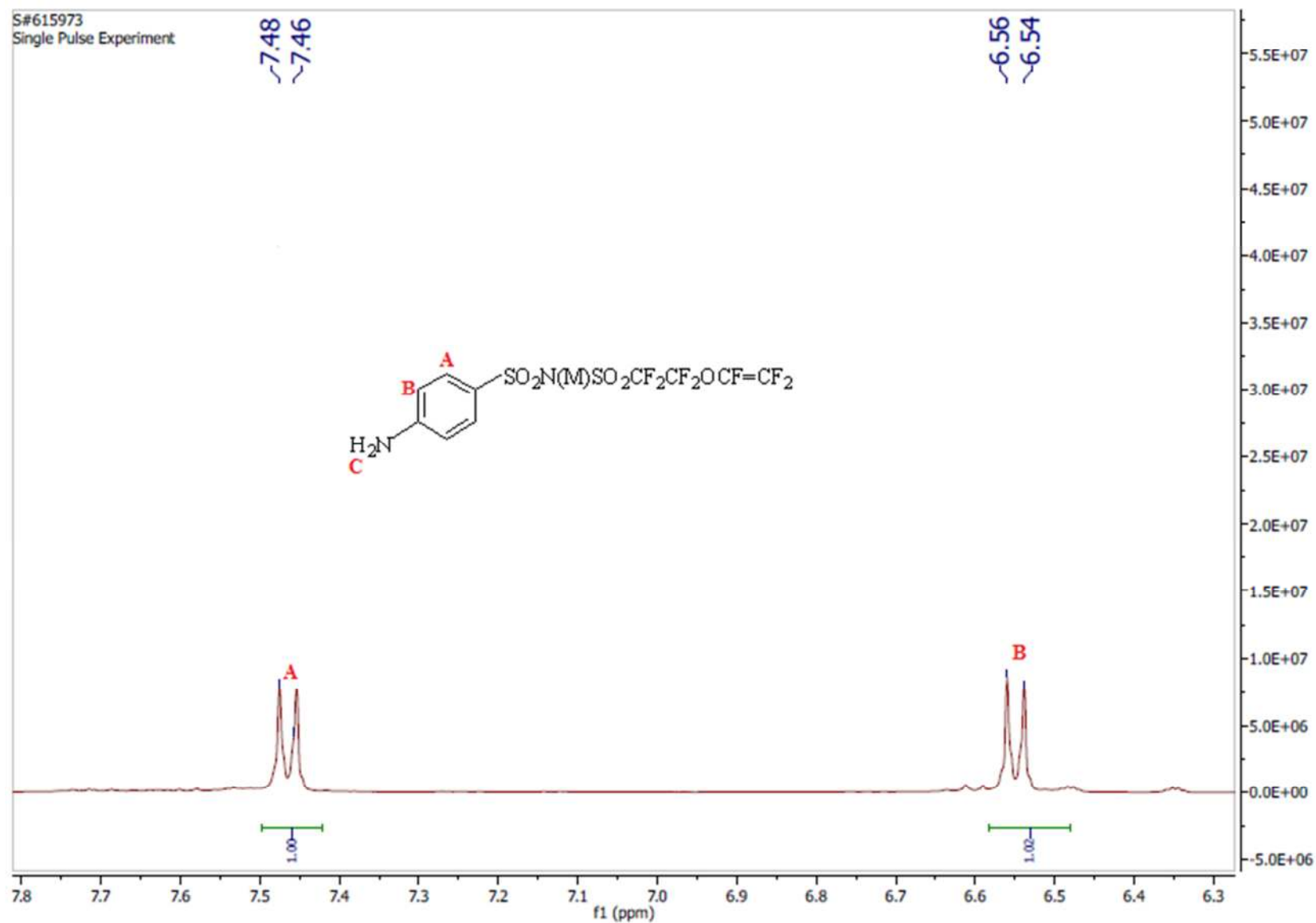
APPENDIX D6: Expanded ^1H NMR spectrum of compound **6a**, 400MHz, CD_3CN



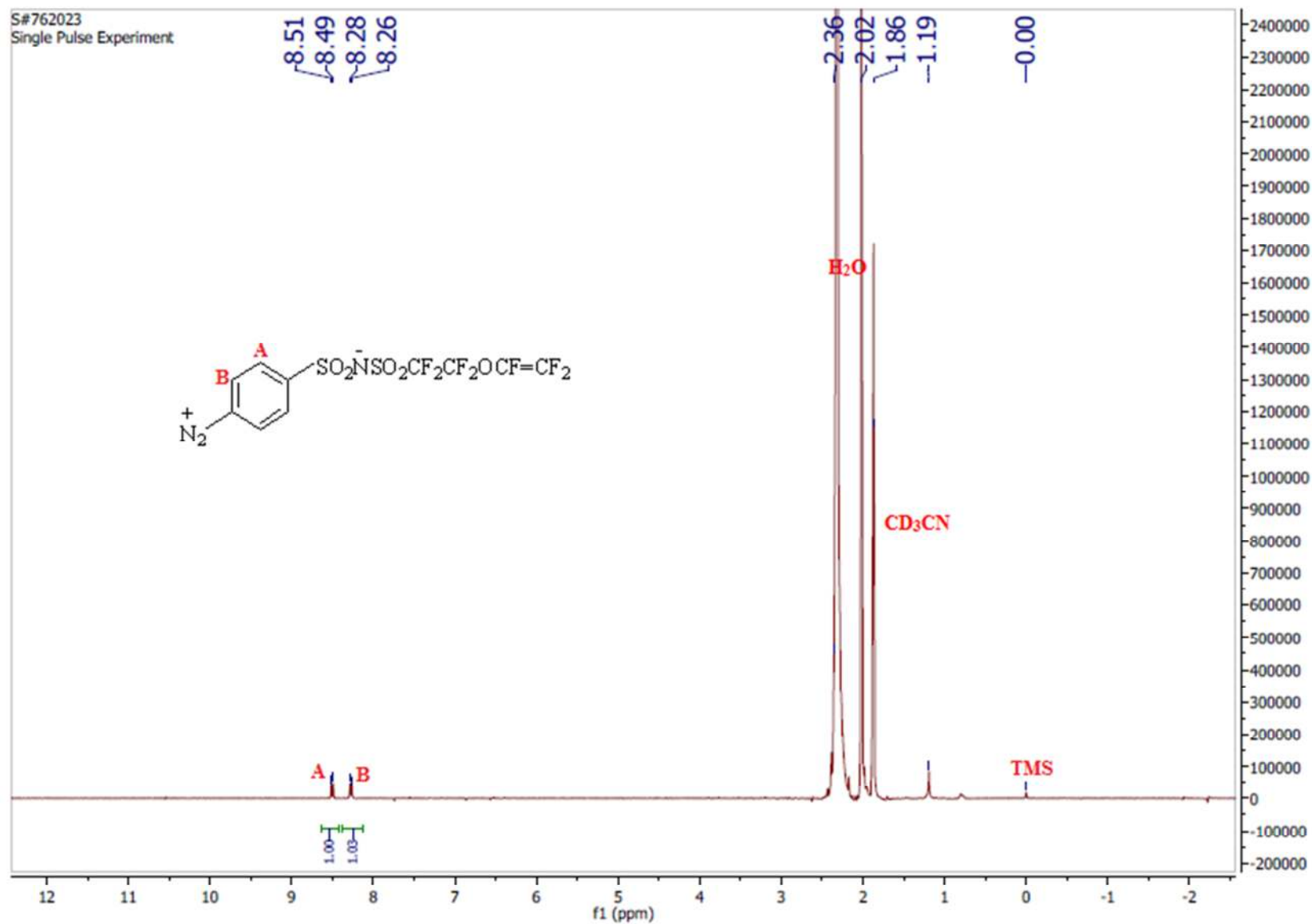
APPENDIX D7: ¹H NMR spectrum of compound **7a**, 400MHz, CD₃CN



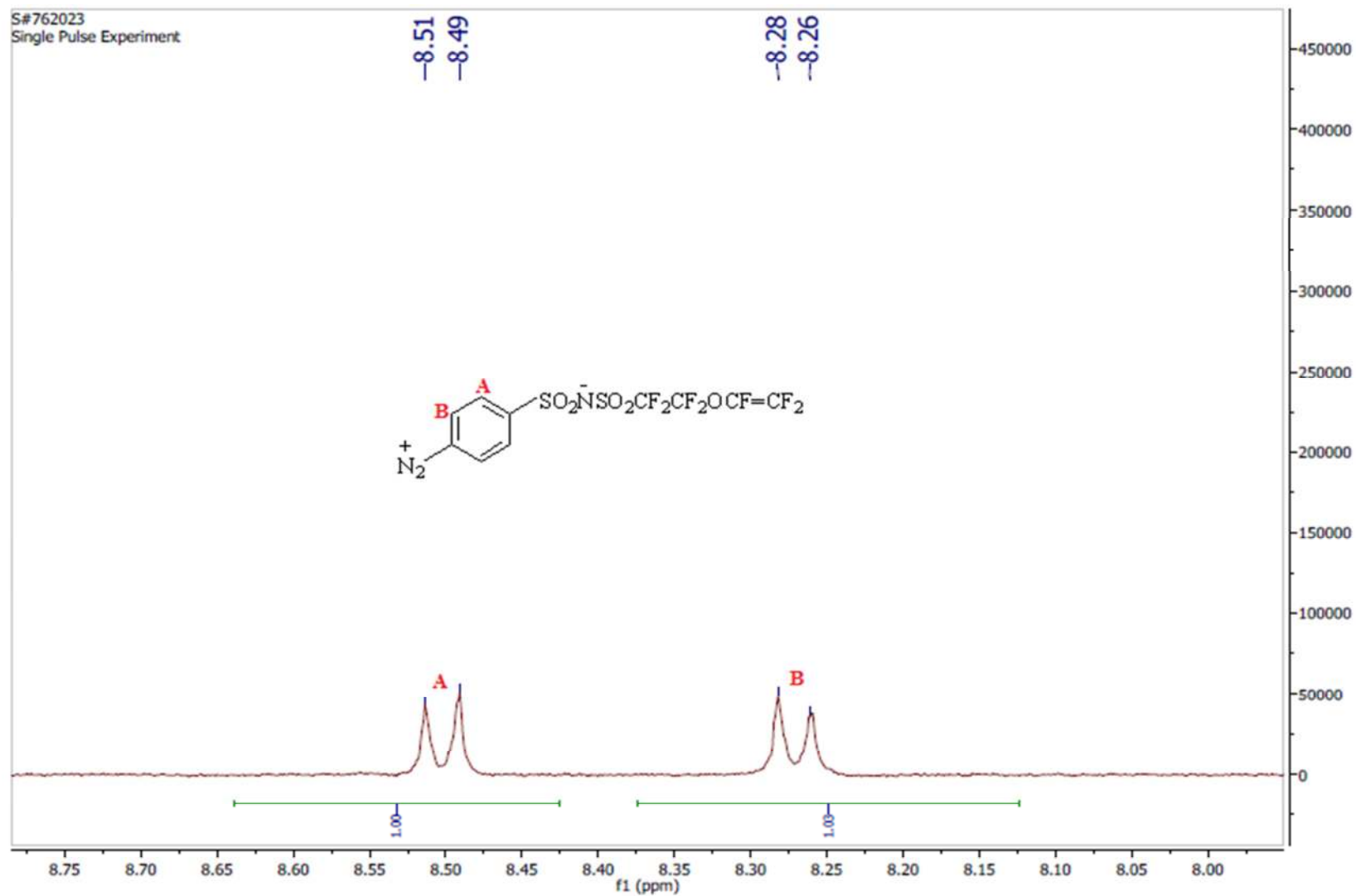
APPENDIX D8: Expanded ^1H NMR spectrum of compound **7a**, 400MHz, CD_3CN



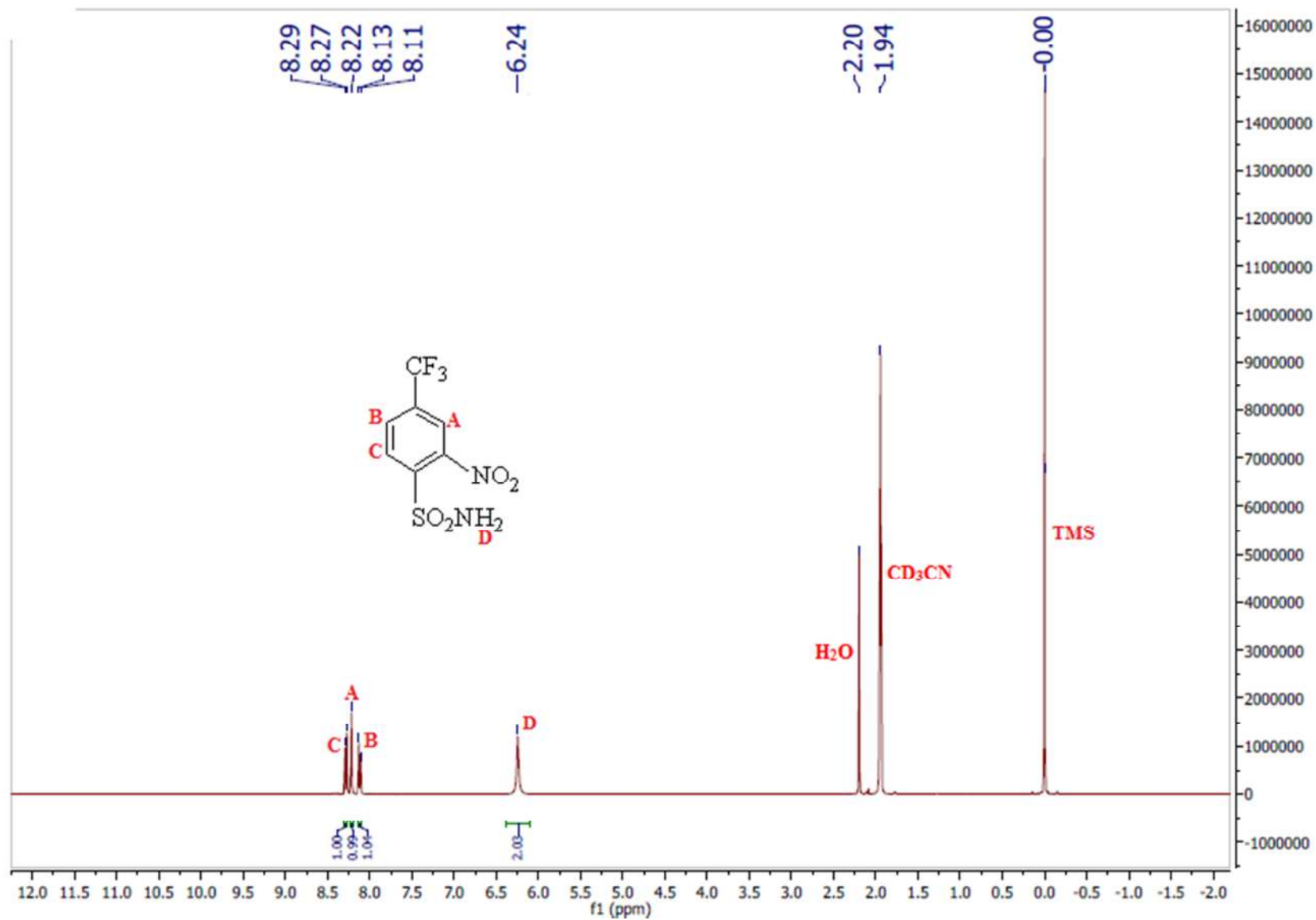
APPENDIX D9: ¹H NMR spectrum of compound **8a**, 400MHz, CD₃CN



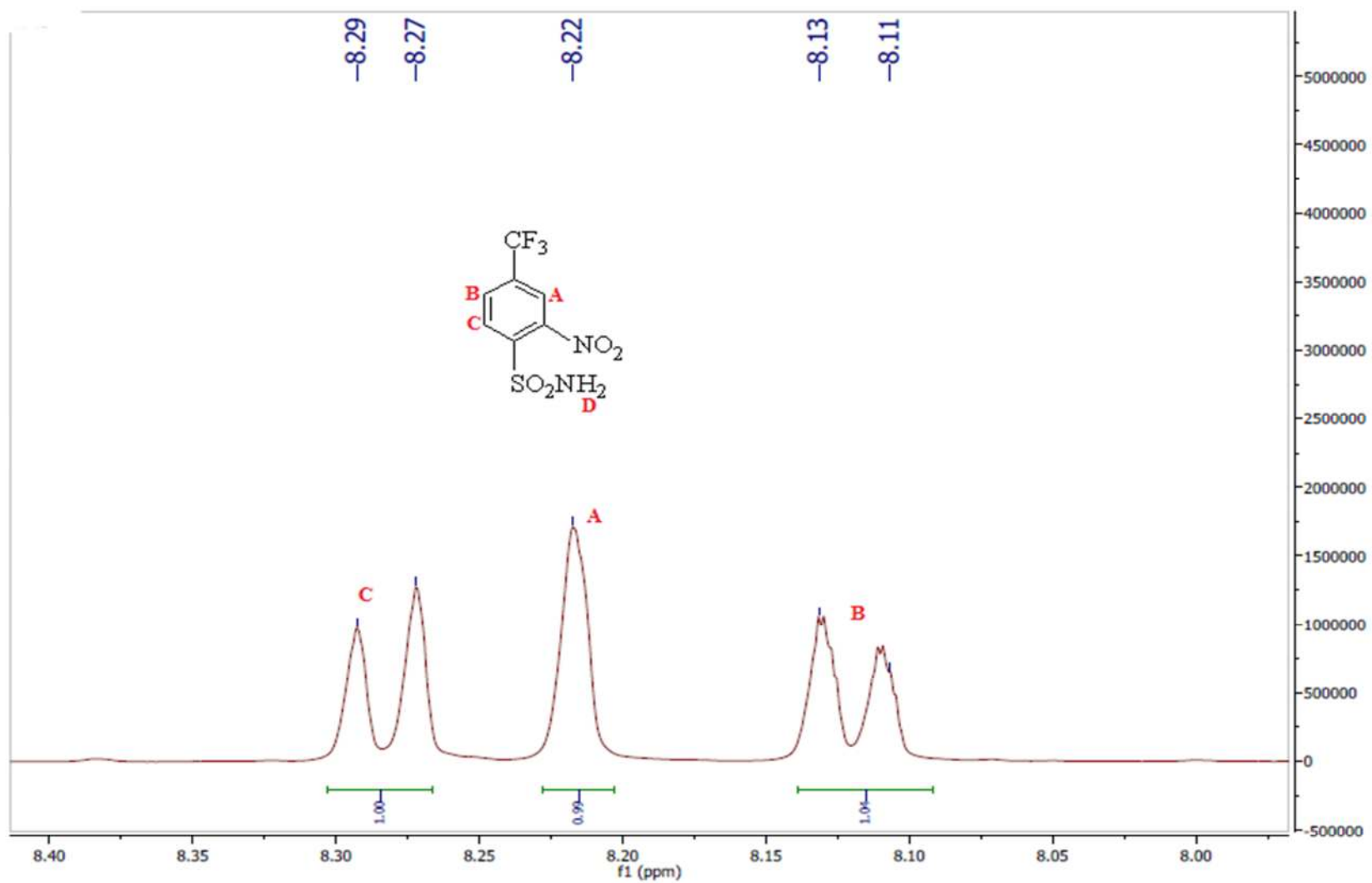
APPENDIX D10: Expanded ^1H NMR spectrum of compound **8a**, 400MHz, CD_3CN



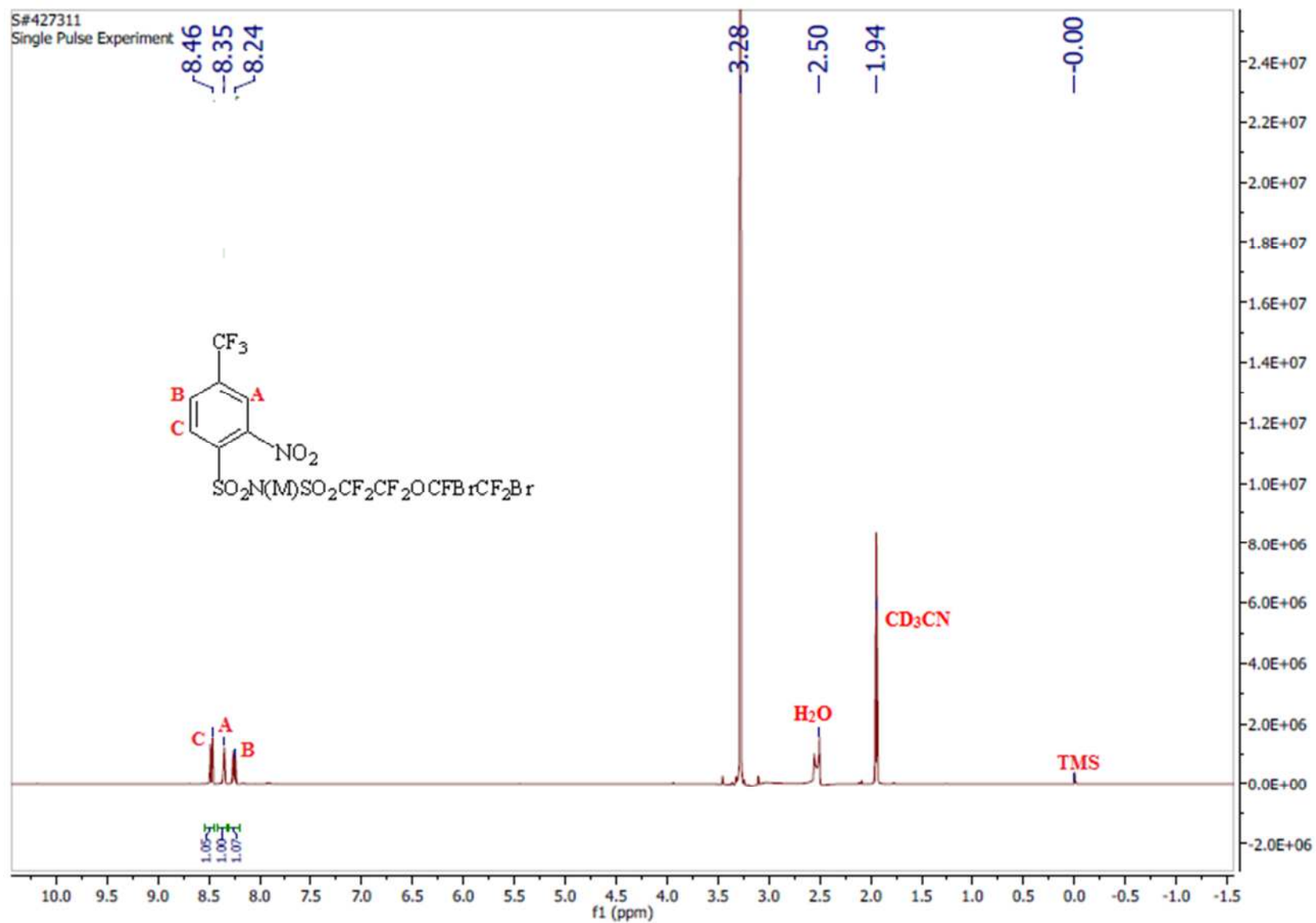
APPENDIX E1: ^1H NMR spectrum of compound **2b**, 400MHz, CD_3CN



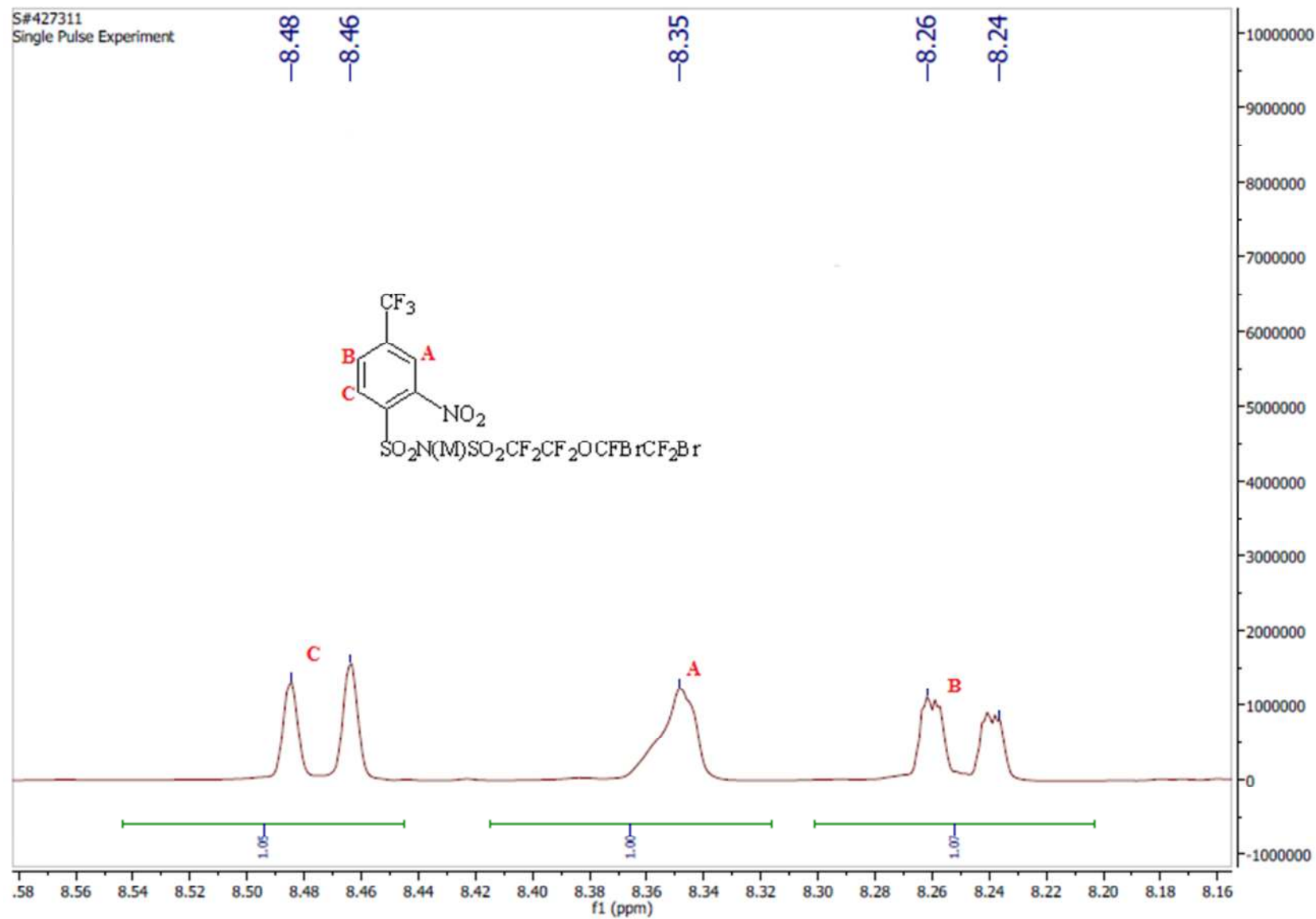
APPENDIX E2: Expanded ^1H NMR spectrum of compound **2b**, 400MHz, CD_3CN



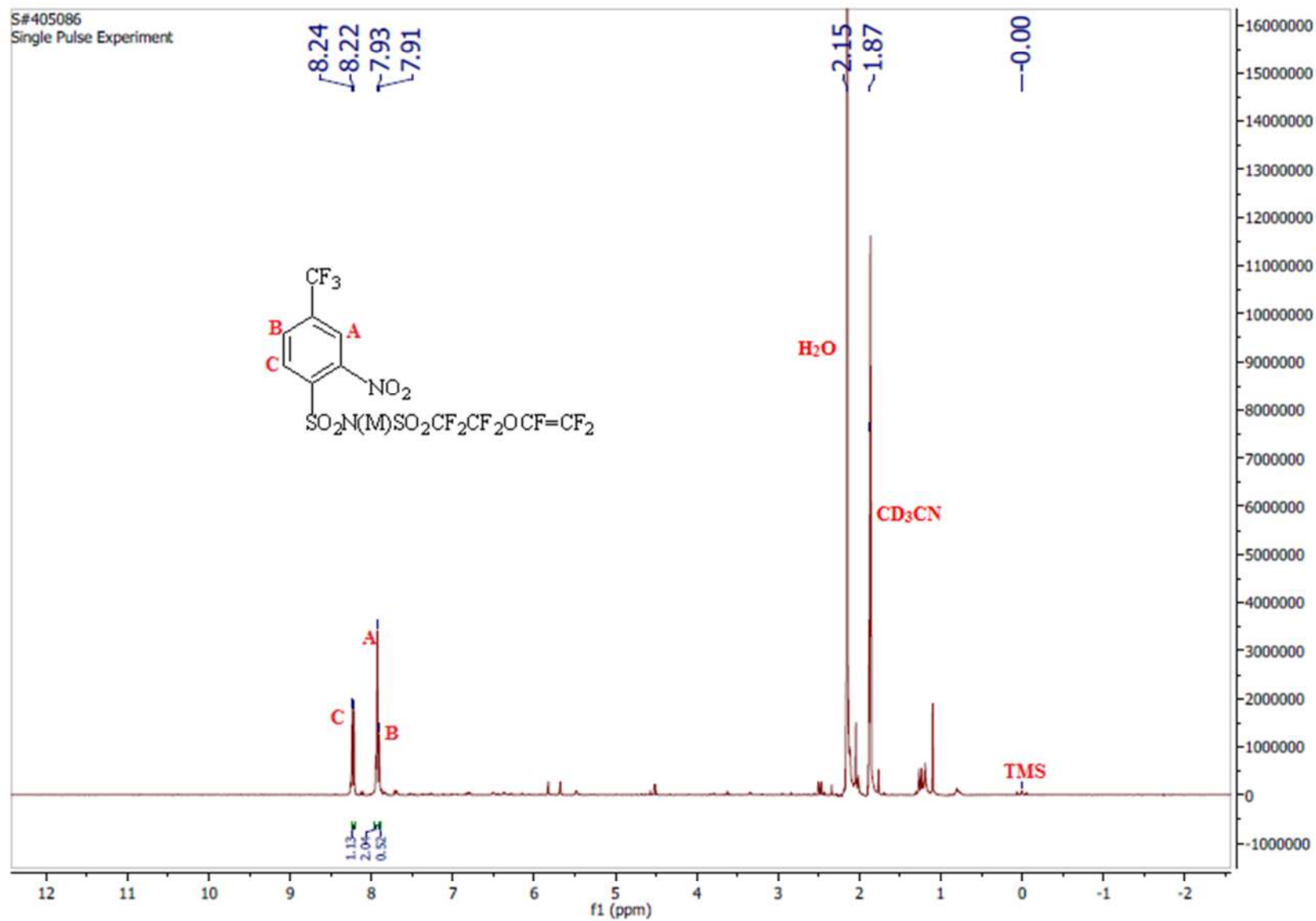
APPENDIX E3: ^{19}F NMR spectrum of compound **5b**, 400MHz, CD_3CN



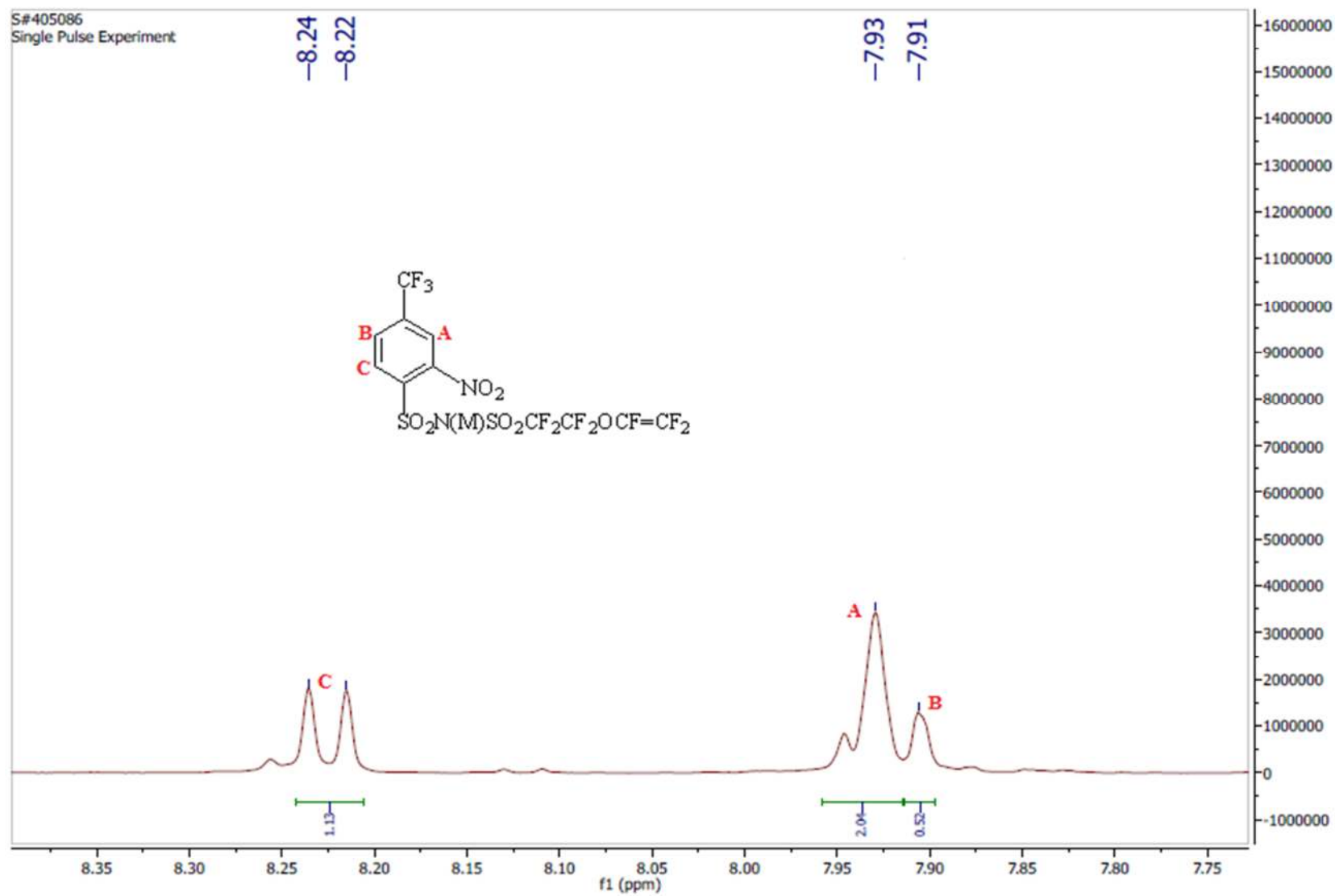
APPENDIX E4: Expanded ^{19}F NMR spectrum of compound **5b**, 400MHz, CD_3CN



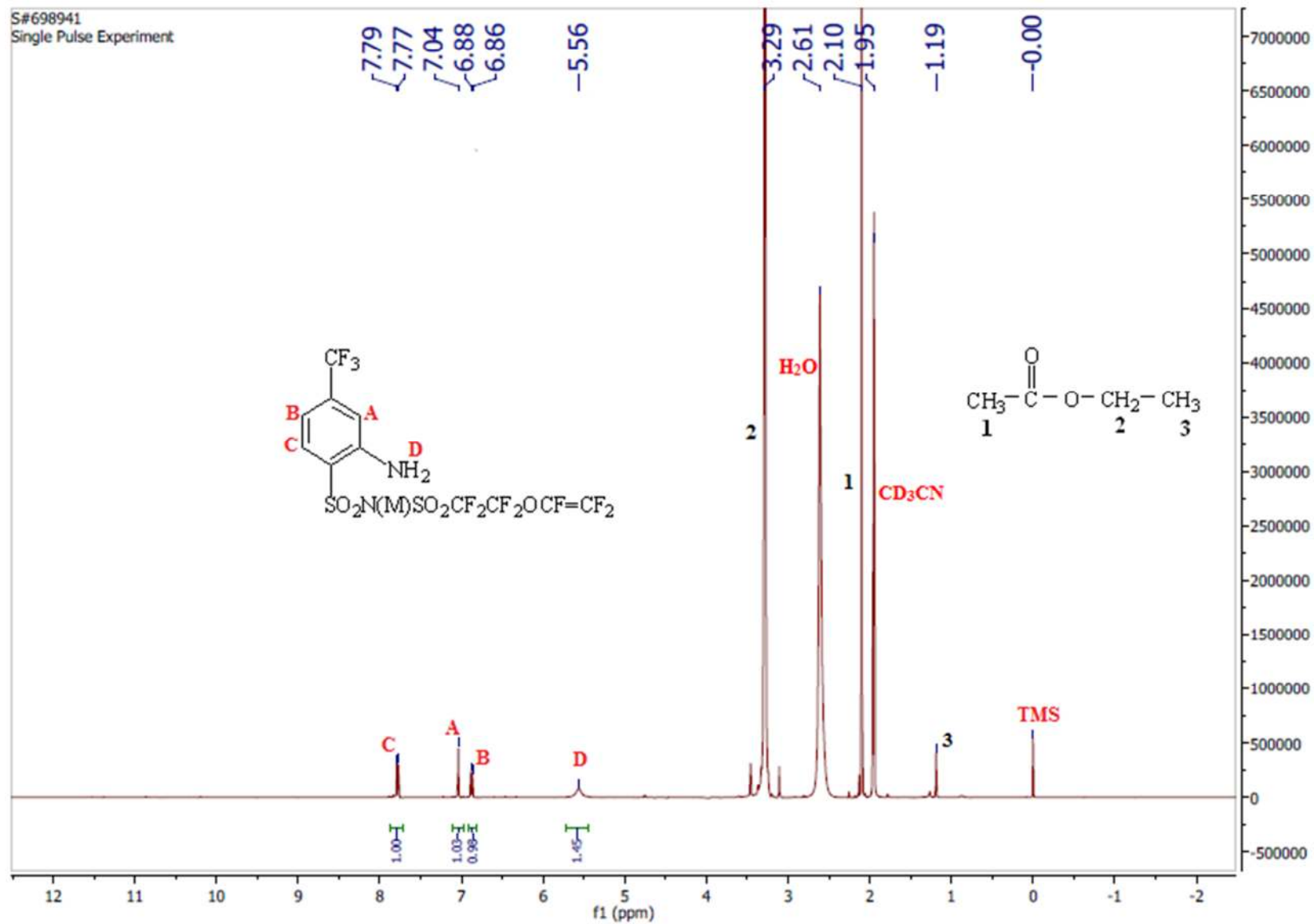
APPENDIX E5: ¹HNMR spectrum of compound **6b**, 400MHz, CD₃CN



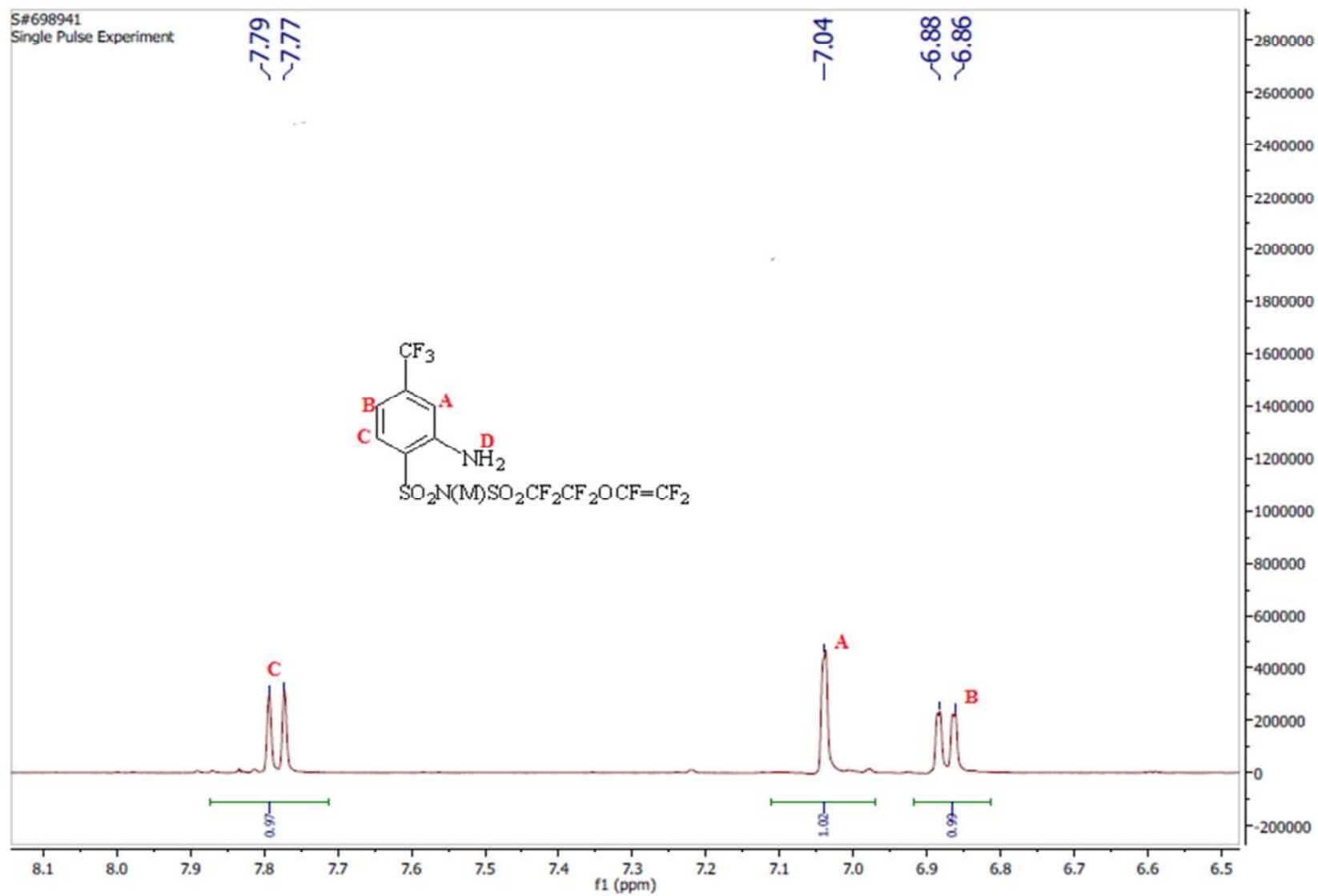
APPENDIX E6: Expanded ^1H NMR spectrum of compound **6b**, 400MHz, CD_3CN



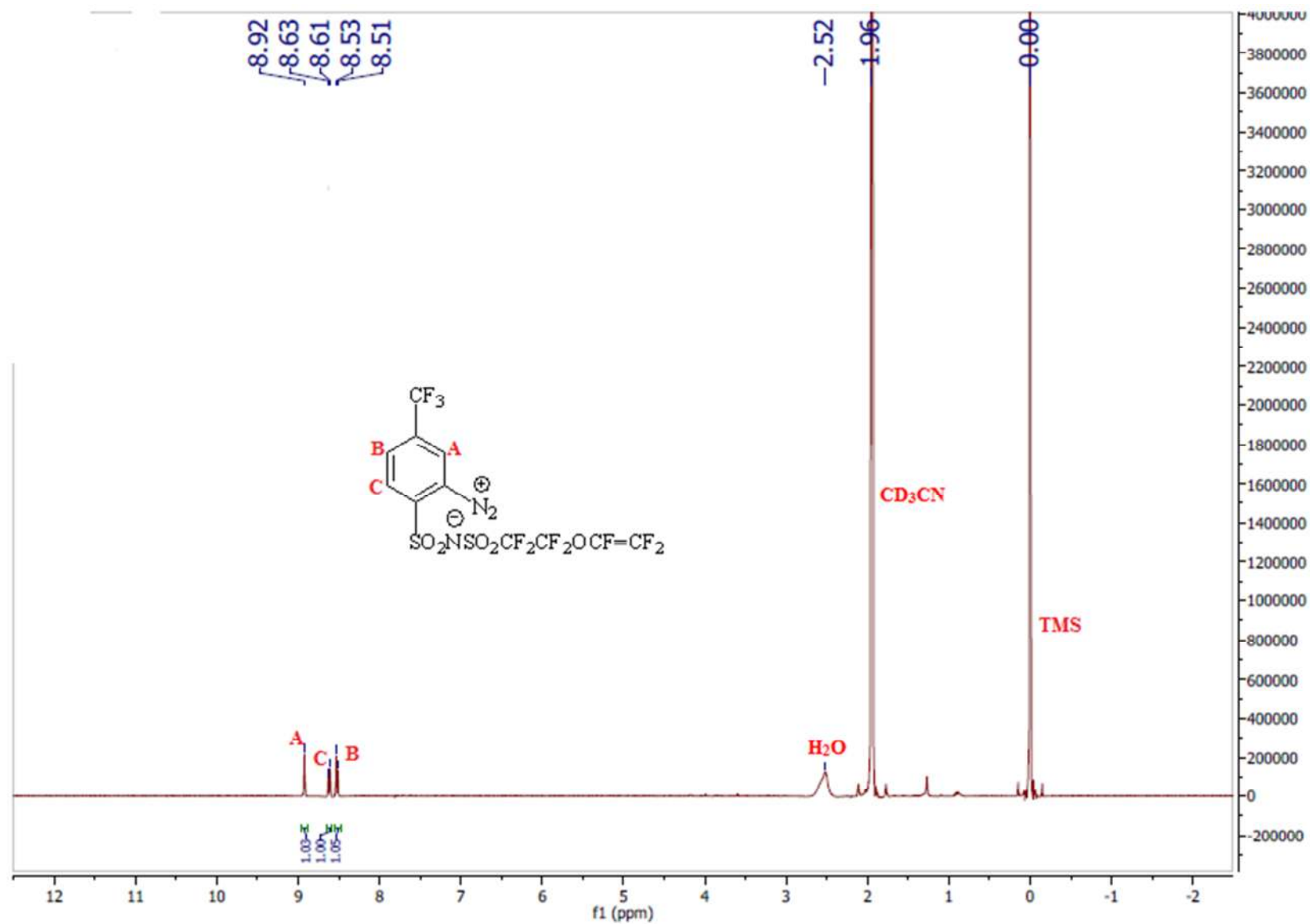
APPENDIX E7: ¹H NMR spectrum of compound **7b**, 400MHz, CD₃CN



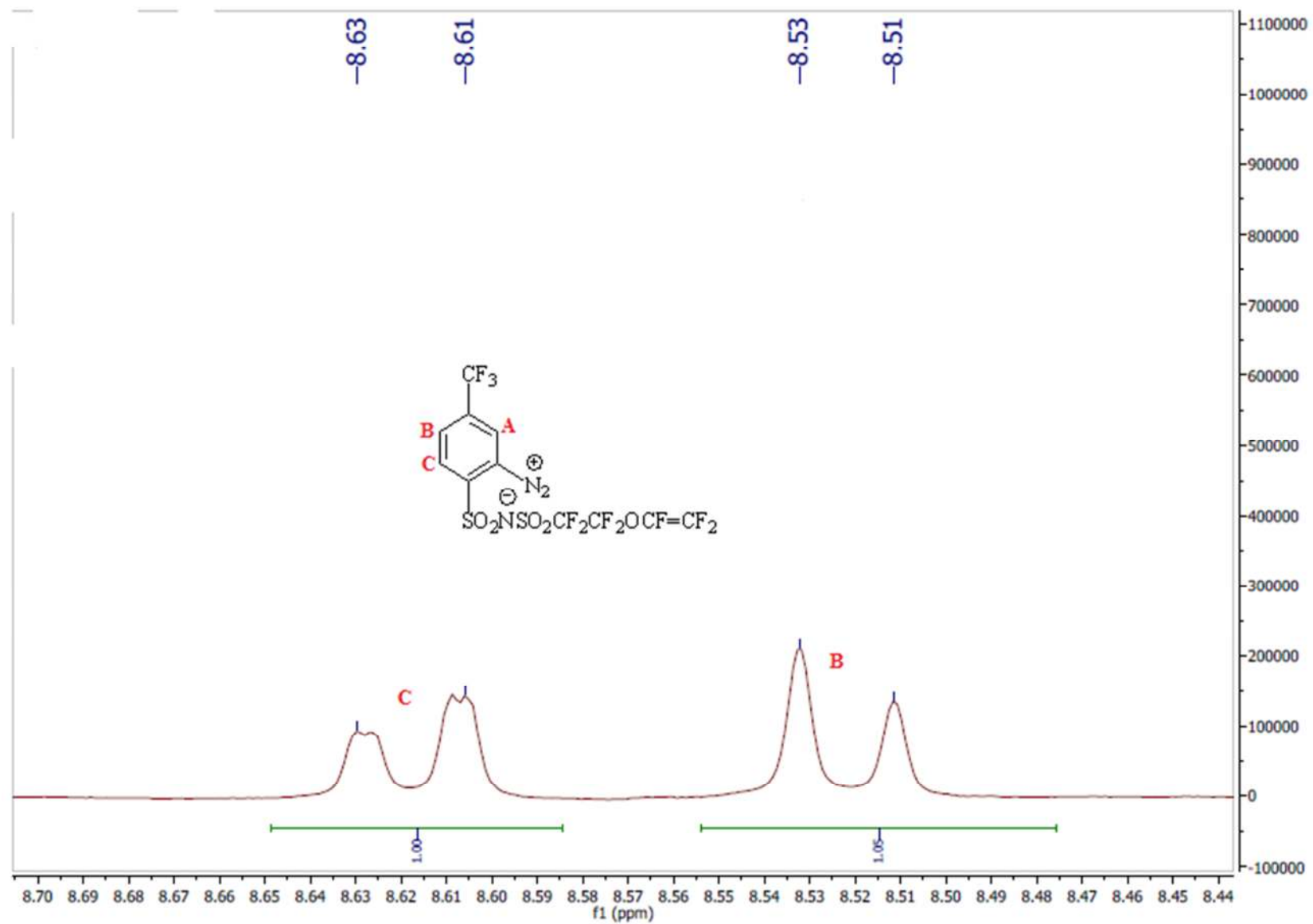
APPENDIX E8: Expanded ^1H NMR spectrum of compound **7b**, 400MHz, CD_3CN



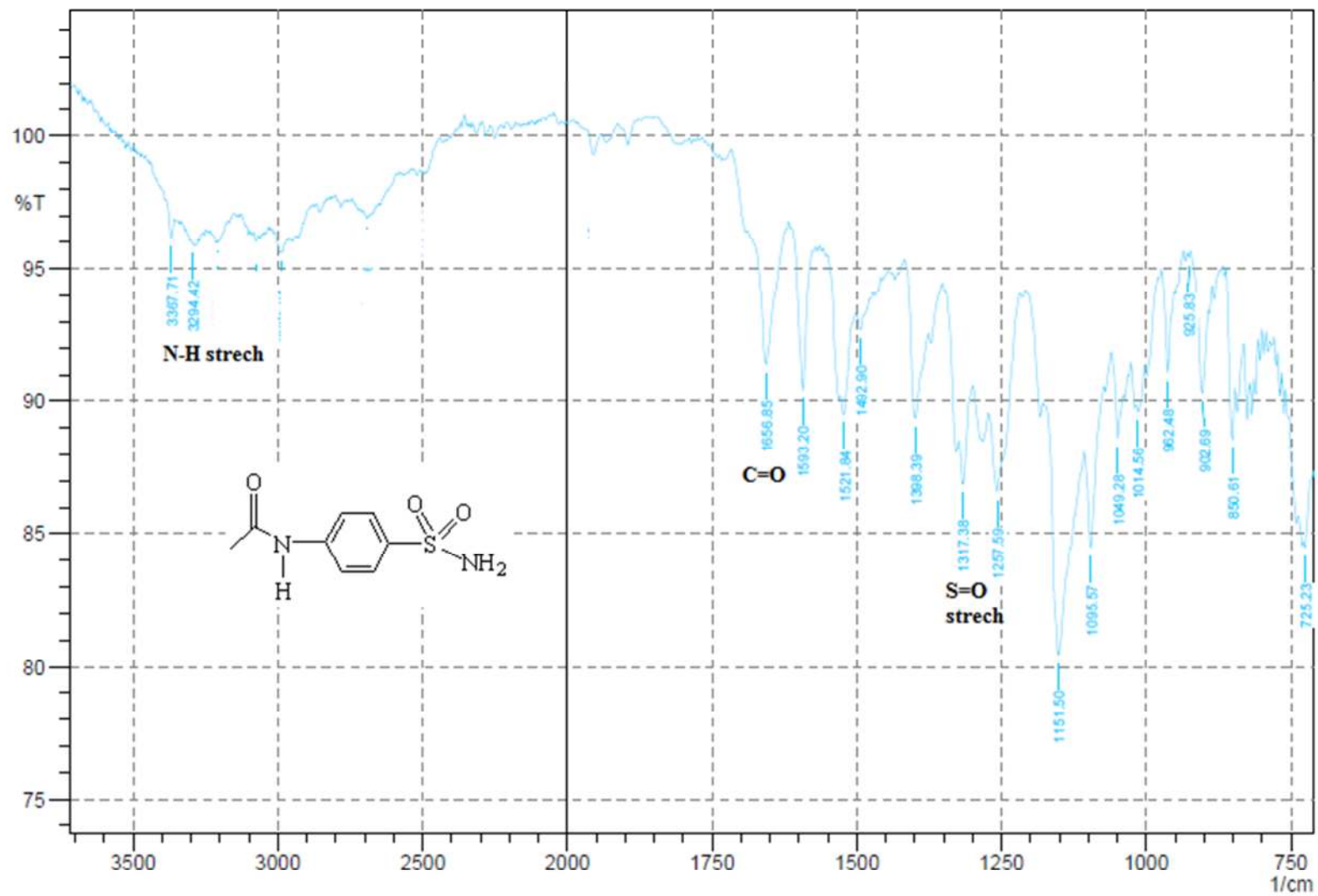
APPENDIX E9: ^1H NMR spectrum of compound **8b**, 400MHz, CD_3CN



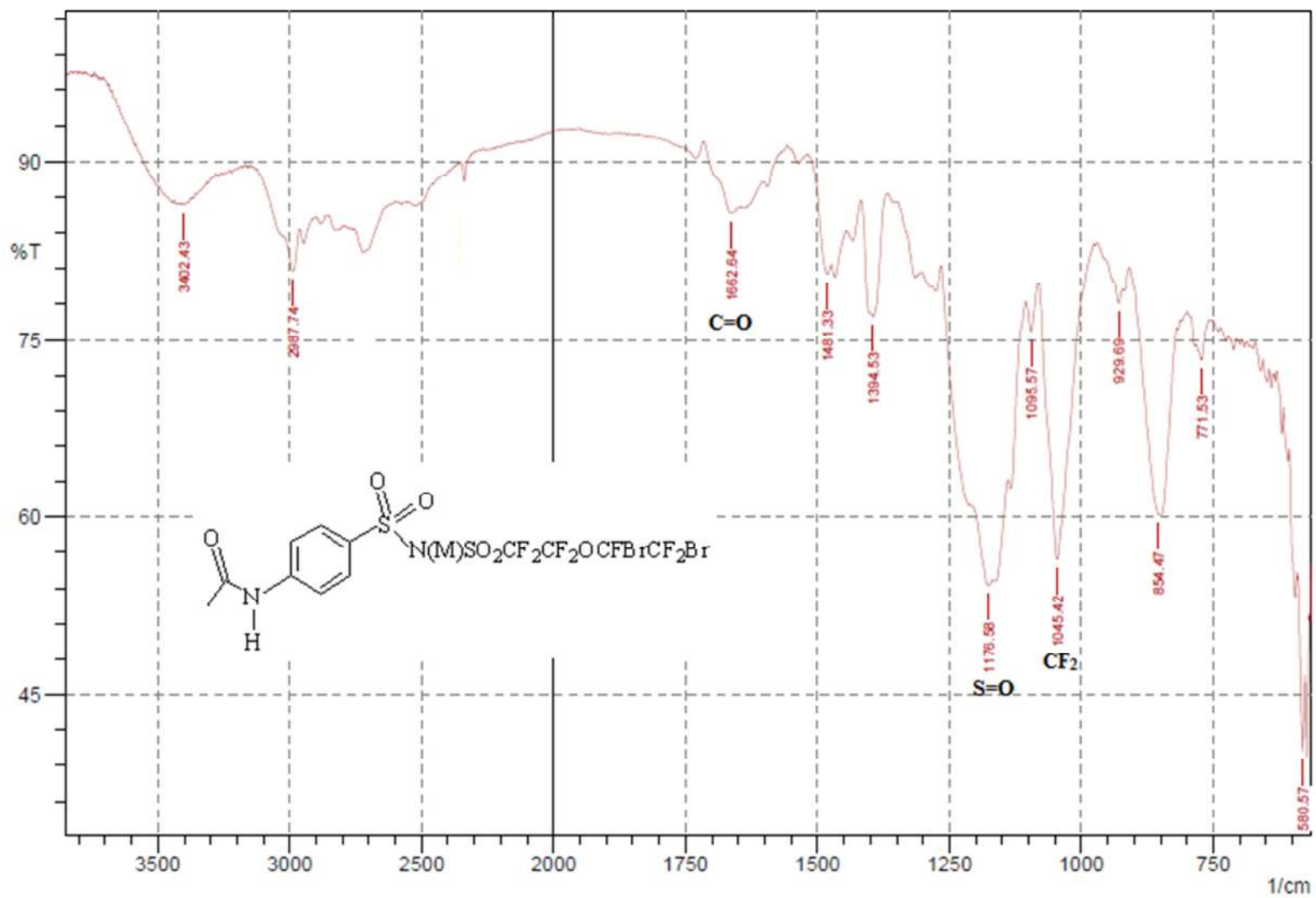
APPENDIX E10: Expanded ^1H NMR spectrum of compound **8b**, 400MHz, CD_3CN



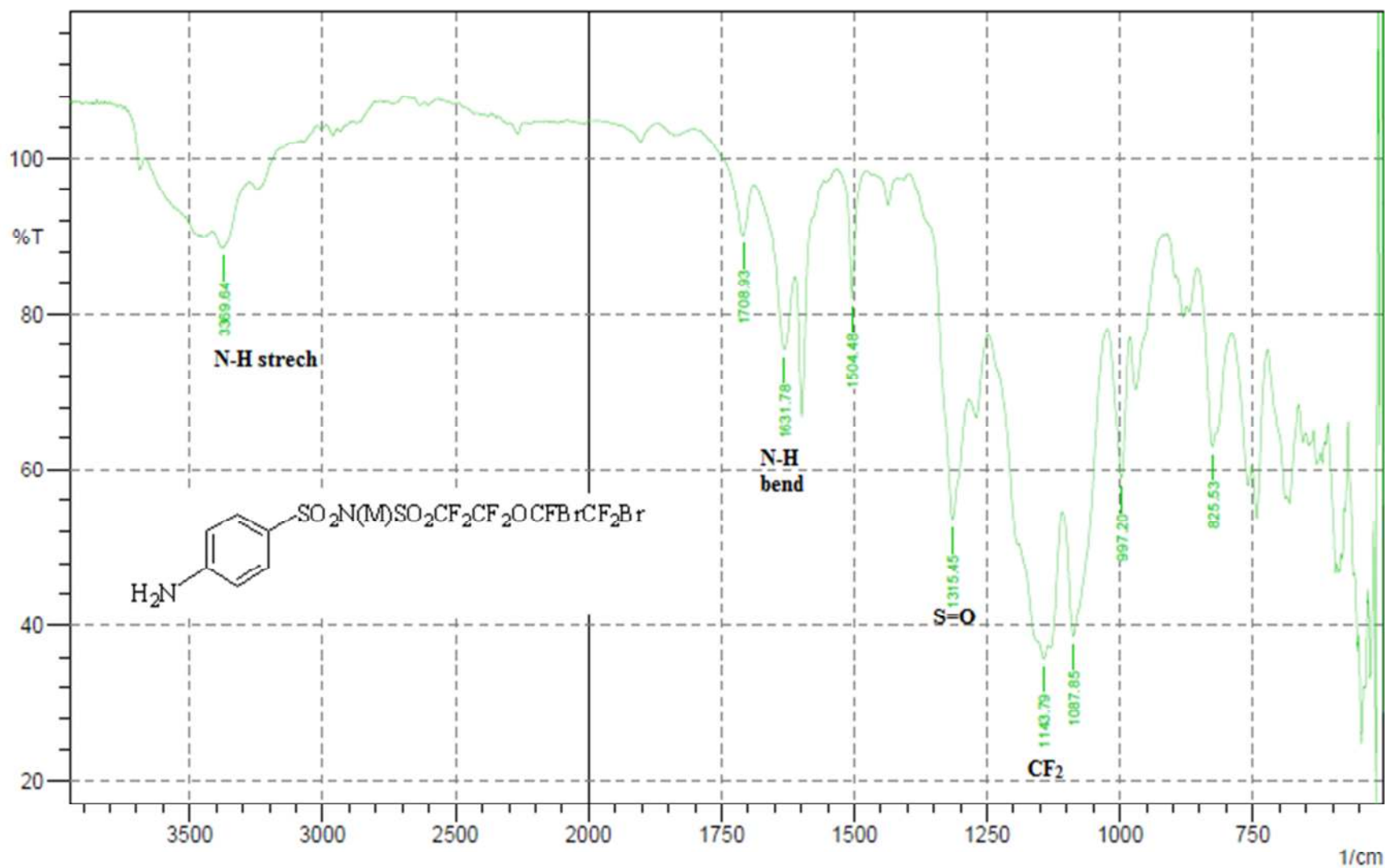
APPENDIX F1: FT-IR Spectrum of Compound 2a



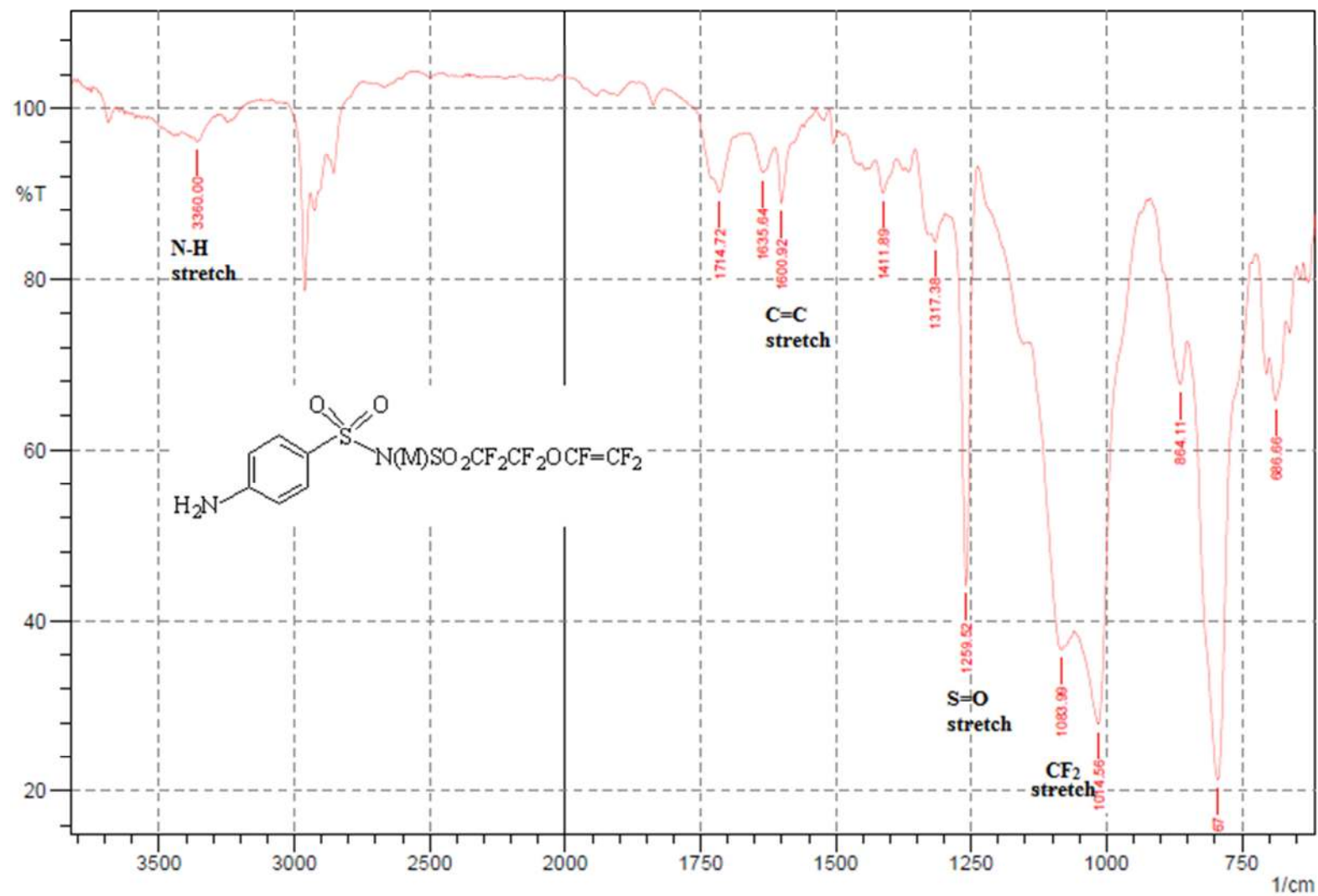
APPENDIX F2: FT-IR Spectrum of Compound 5a



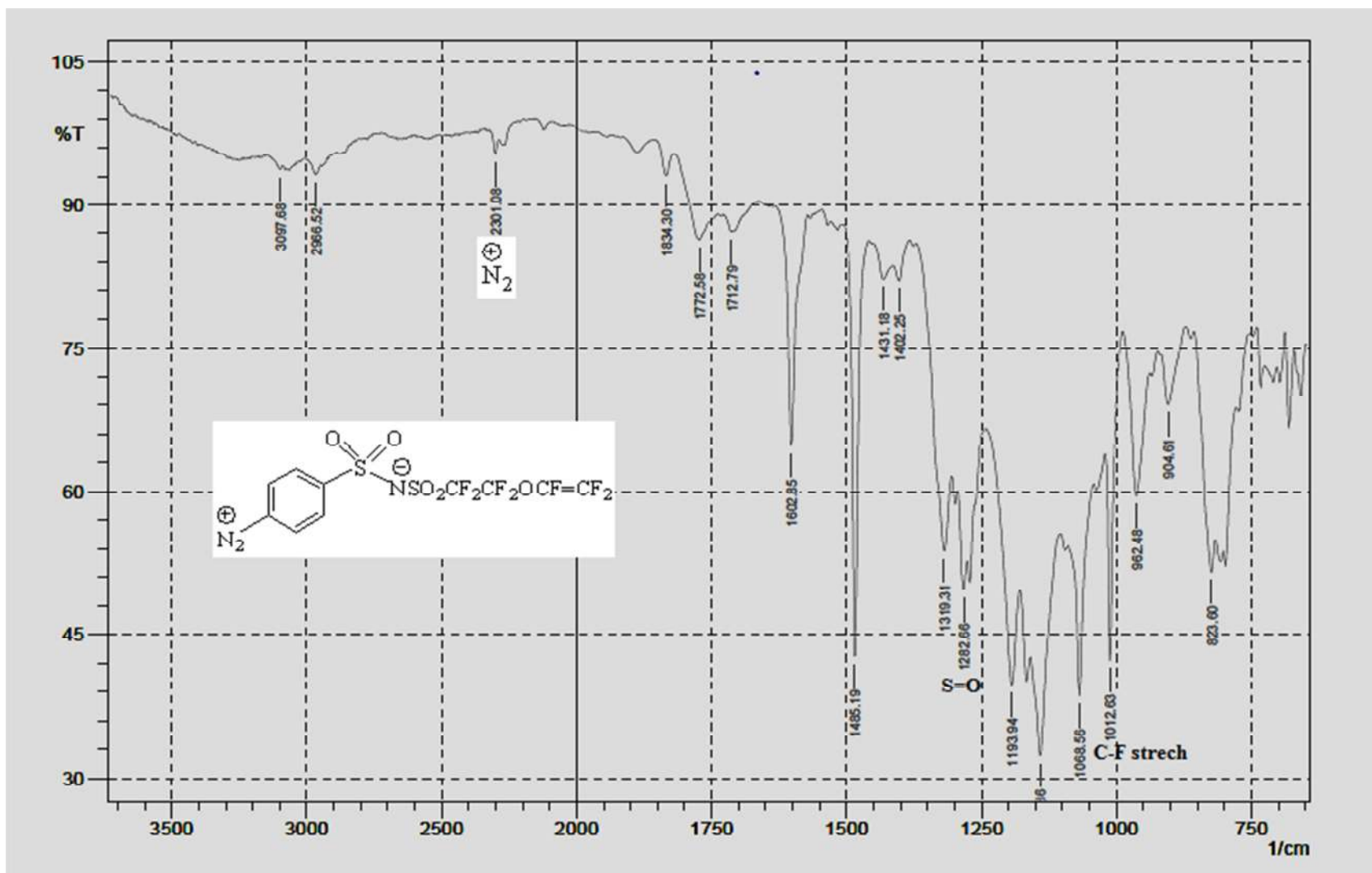
APPENDIX F3: FT-IR Spectrum of Compound 6a



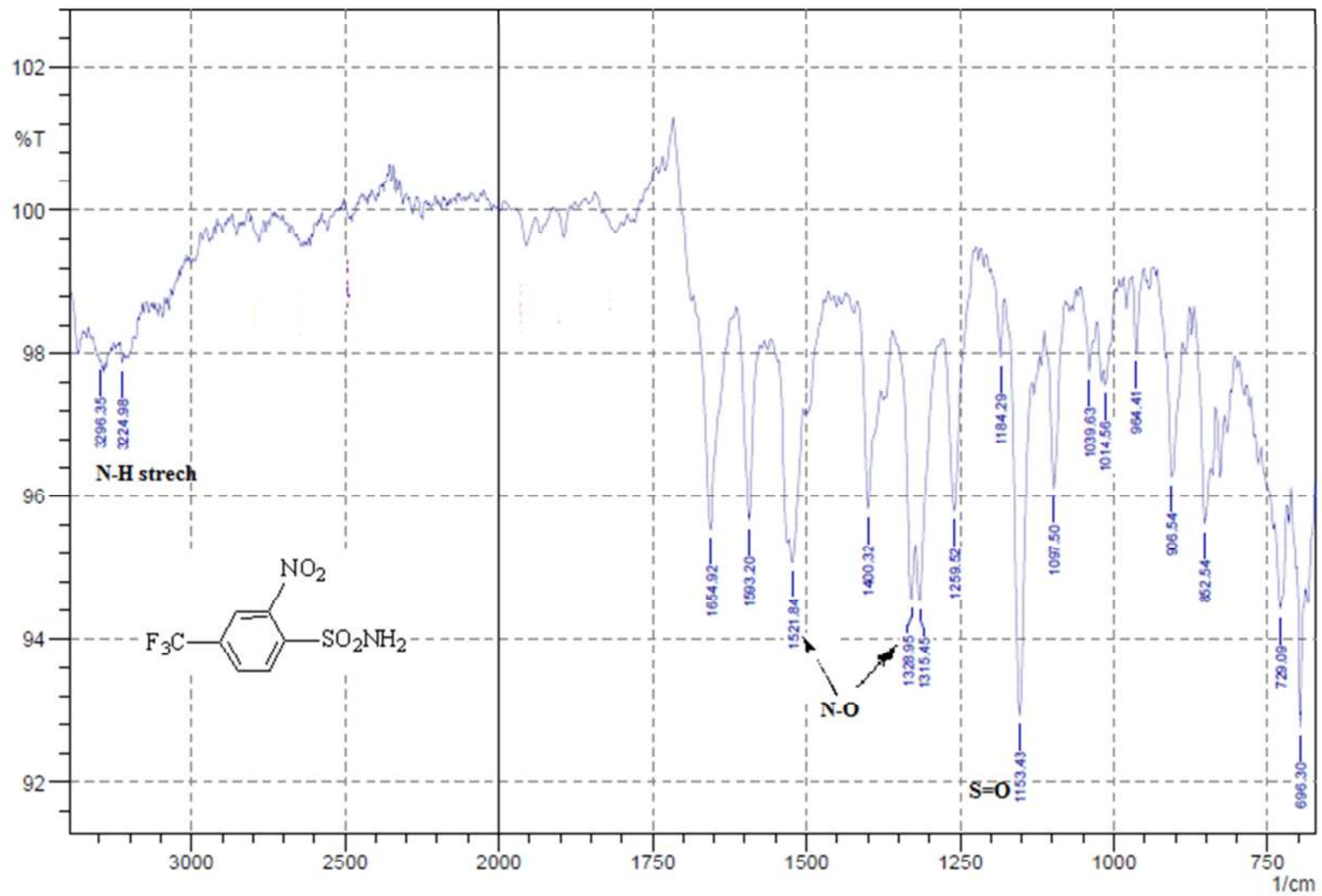
APPENDIX F4: FT-IR Spectrum of Compound 7a



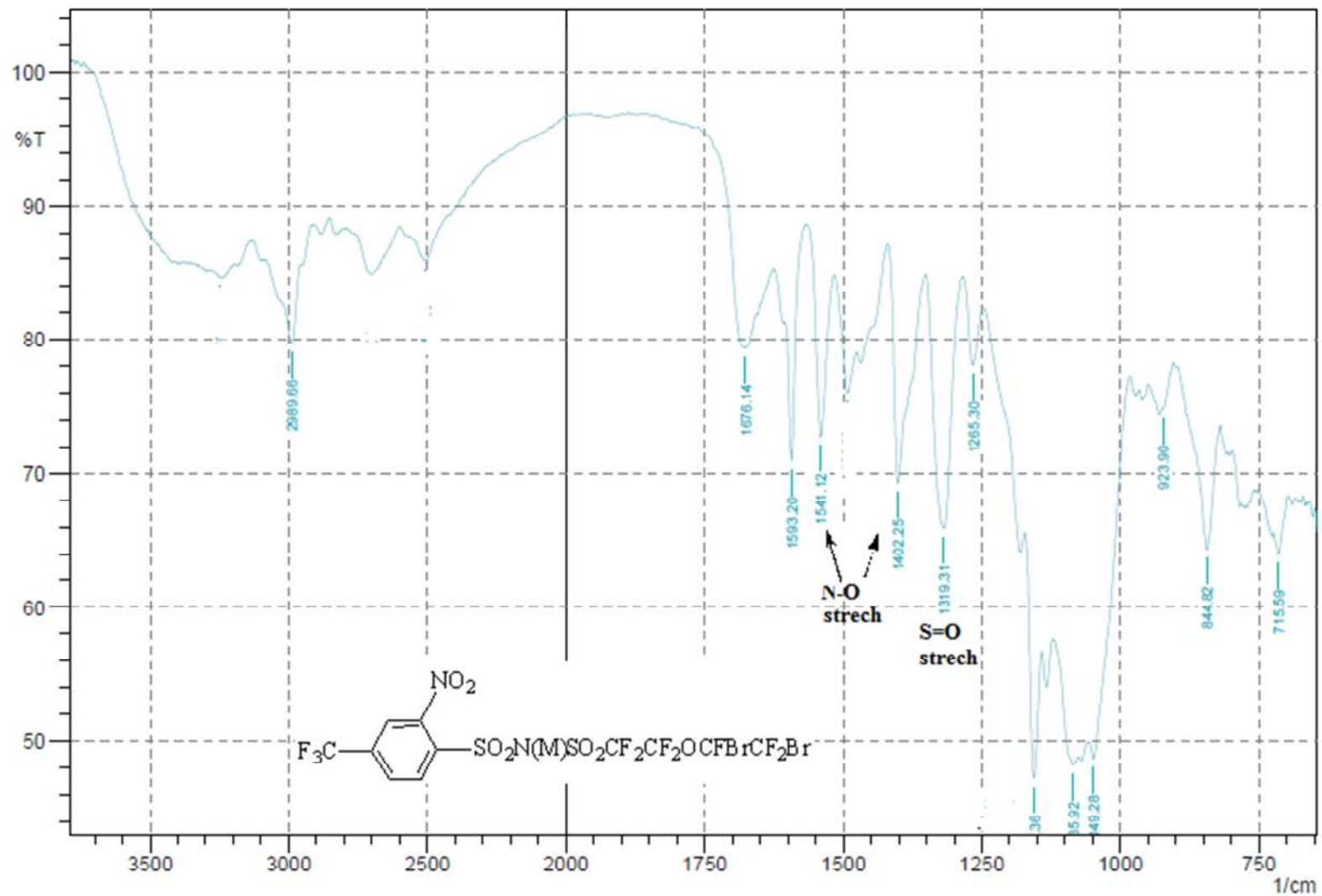
APPENDIX F5: FT-IR Spectrum of Compound **8a**



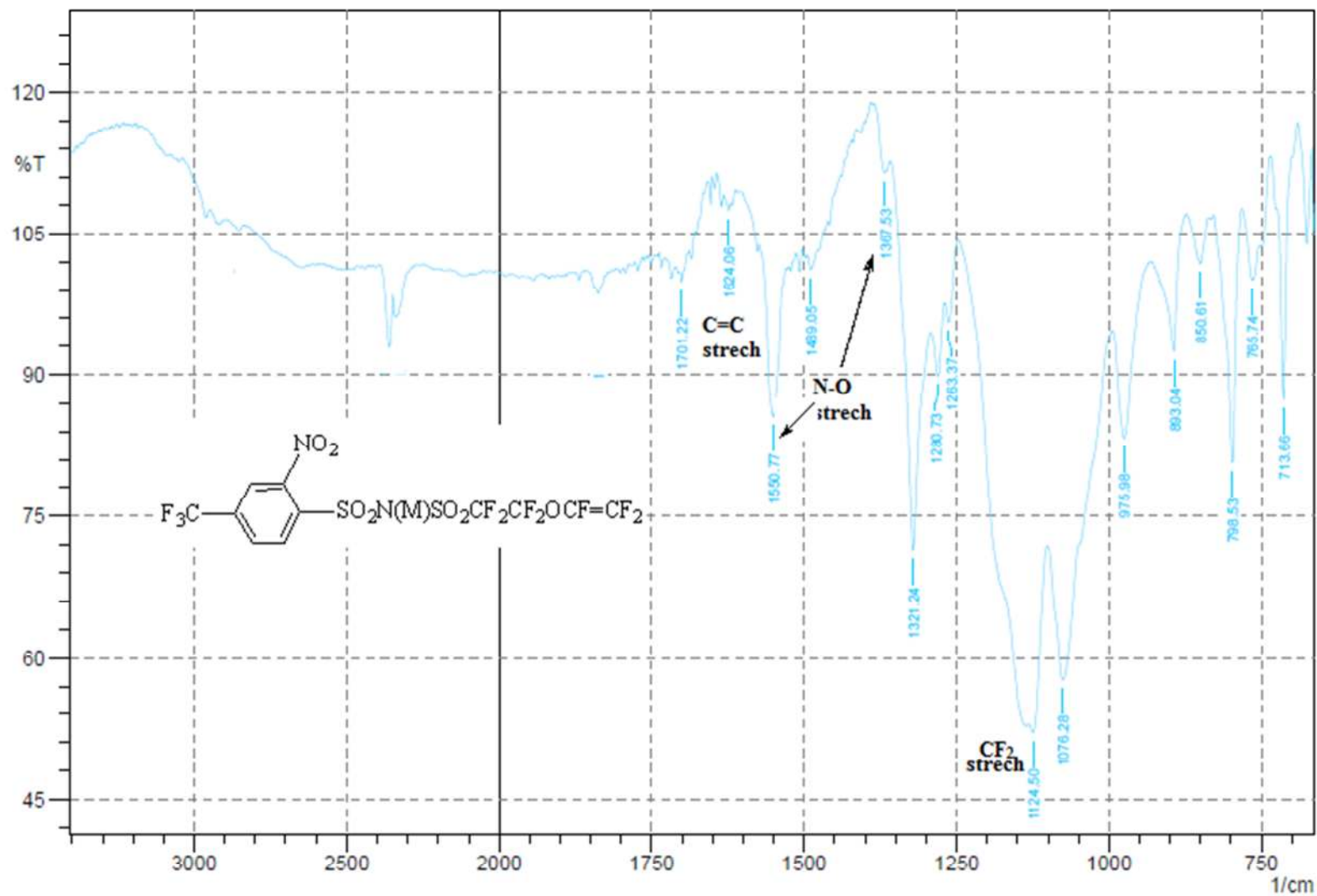
APPENDIX G1: FT-IR Spectrum of Compound 2b



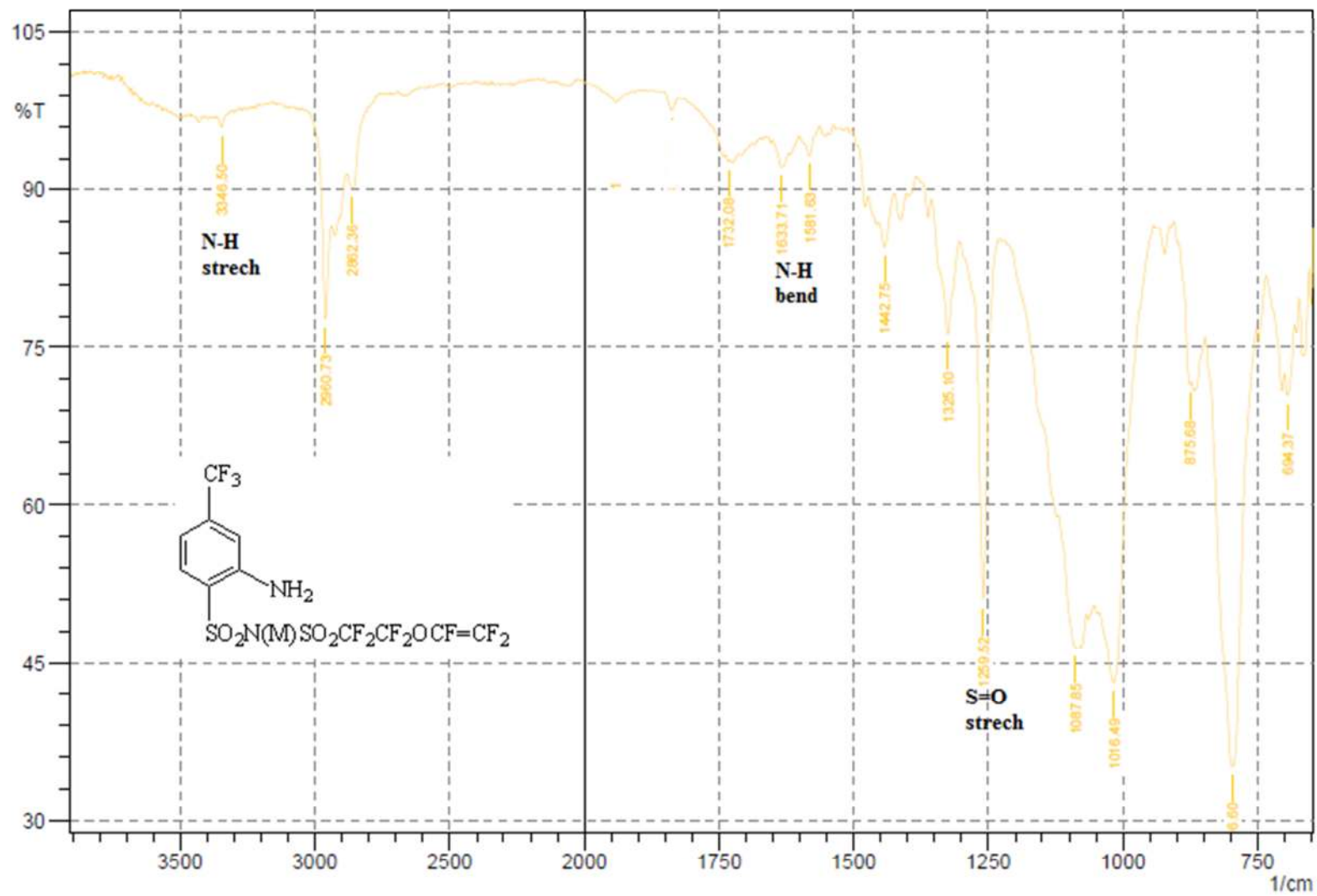
APPENDIX G2: FT-IR Spectrum of Compound **5b**



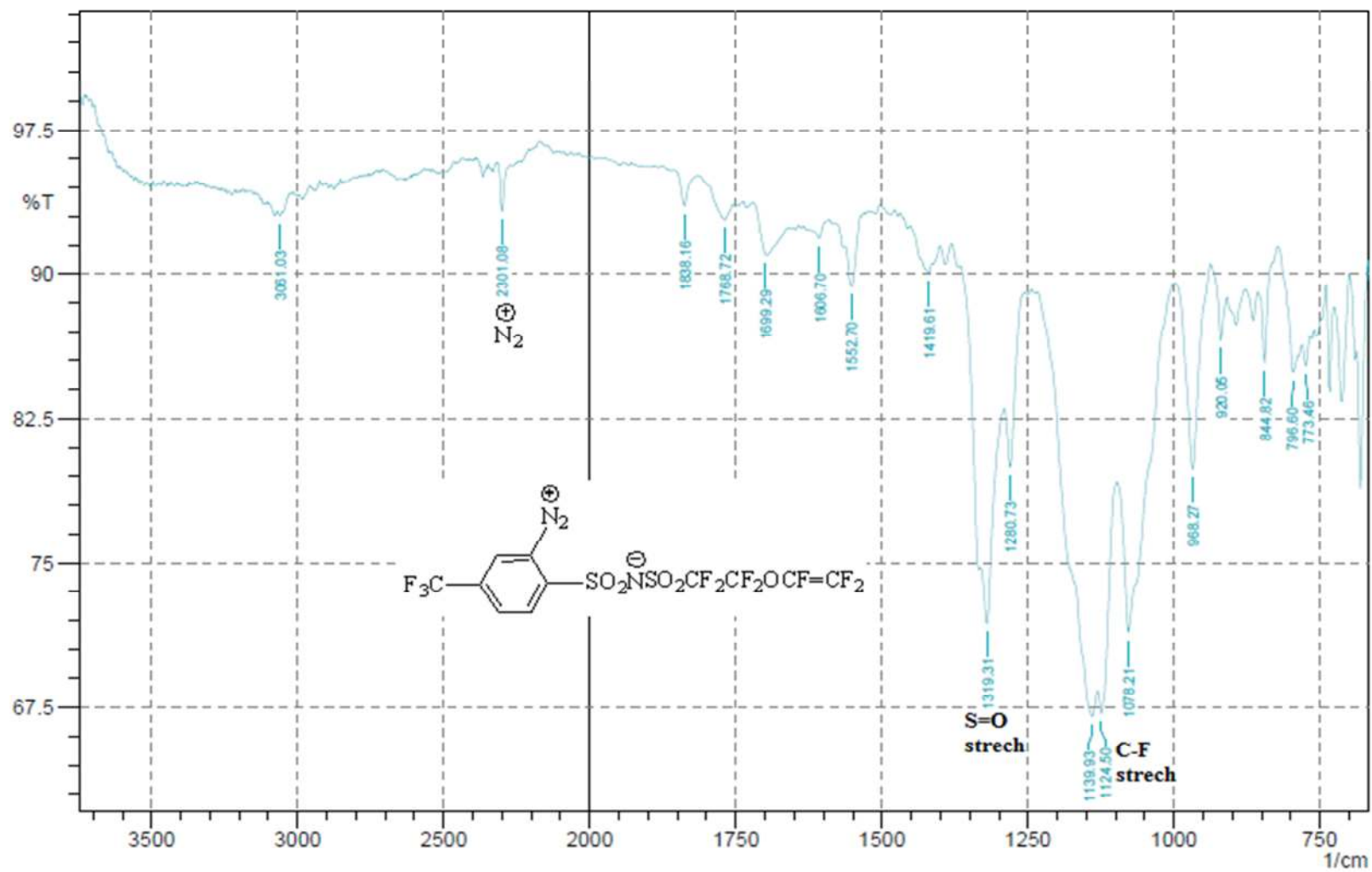
APPENDIX G3: FT-IR Spectrum of Compound **6b**



APPENDIX G4: FT-IR Spectrum of Compound **7b**



APPENDIX G5: FT-IR Spectrum of Compound **8b**



VITA

FAISAL IBRAHIM

- Education: M.S. Chemistry, East Tennessee State University, Johnson City, Tennessee, USA, 2016
- B.S. Applied Chemistry (First Class Honors), University for Development Studies, Tamale, Ghana, 2009
- Professional Experience: Graduate Teaching Assistant, East Tennessee State University, College of Arts and Sciences, 2014 – 2016
- Assistant Director IIB, Ministry of Local Government and Rural Development, Ejura, Ghana, 2013
- Quality Assurance Chemist, Kinapharma Limited, Accra, Ghana, 2010-2013
- Teaching Assistant, University for Development Studies, Faculty of Applied Sciences, 2009-2010
- Presentations: F.Ibrahim, H. Mei, “Synthesis of Diazonium (Perfluoroalkyl) Benzenesulfonimide Monomer for Proton Exchange Membrane (PEM) Fuel Cells”, Appalachian Student Research Forum, Johnson City, TN, April 7, 2016
- F.Ibrahim, H. Mei, “Synthesis of Diazonium (Perfluoroalkyl) Benzenesulfonimide Monomer for Proton Exchange Membrane (PEM) Fuel Cells”, 2015 Joint Southeastern

/Southwest Regional Meeting of American Chemical

Society, Memphis TN, November 4-7, 2015.

F.Ibrahim, H. Mei, “Synthesis of Diazonium (Perfluoroalkyl)

Benzenesulfonimide Monomer for Proton Exchange

Membrane (PEM) Fuel Cells”, Appalachian Student Research

Forum, Johnson City, TN, April 8, 2015

Award:

First Place, Natural Science Poster Presentation (Group B) at the

2016 Appalachian Student Research Forum, Johnson City,

TN, USA, April 2016.